Host and Viral Determinants of Respiratory Reovirus Infection

A DISSERTATION
SUBMITTED TO THE FACULTY OF THE GRADUATE SCHOOL
OF THE UNIVERSITY OF MINNESOTA
BY

Rachel M. Nygaard

IN PARTIAL FULFILLMENT OF THE REQUIREMENTS
FOR THE DEGREE OF
DOCTOR OF PHILOSOPHY

Leslie A. Schiff, Ph.D., Advisor

April 2012

ACKNOWLEDGEMENTS

I dedicate this thesis to my son and my mother. Mom, I miss you every day and wish you were still here to see this milestone. Thank you for instilling me with the drive to succeed, even in the face of seemingly insurmountable odds. Zeb, I would have never had the courage to undertake such an endeavor without you to motivate and inspire me. You bring so much joy to my life. I hope that through this process you have learned what hard work and perseverance can do for your life. I love you.

It would not have been possible to complete my doctoral thesis without the help and support of many people around me. To my partner, Josh, thank you for your love, support, and calming influence. I would like to thank my father, his partner Cathy and my sister for their support and comic relief. Thank you to my 'adoptive' families over the years. Ed and Sandra Elliott fostered a work ethic in me that has served me well throughout this process. Fernando Teson and Maria Martinez, thank you for your unyielding love and support (Maria, I kept my eye on the prize).

This thesis would not have been possible without the help, support and patience of my advisor, Dr. Leslie Schiff. She provided an environment where I could thrive; gave me support and knowledge that I will take with me for life. She

taught me what it means to be a strong, intelligent woman and I thank her for believing in me. I am also extremely lucky to have had the added guidance from Leslie's husband, Dr. Steve Rice. Thank you both for your friendship and advice throughout the years.

One of the best parts about the Schiff-Rice lab were the people who I worked with every day. Linse, I absolutely don't know how I would have survived without you. You have been a guide, sounding board, friend and awesome travel partner throughout this process, thank you. I would like to also thank Megan and Lindsey for help with all the laboratory upkeep and late nights dissecting mice (Megan, I am always available for sniper patrol!). Thanks to my fellow graduate students, Wade, Pete and Lenka, for all your advise, support and help.

The members of my dissertation committee, Wade Breshnahan, Dave Masopust and Peter Bitterman, have all generously given their time and expertise to better my work. I thank them for their contribution and their support. I also thank my fellow graduate students in the MICaB program, faculty and staff which have made my experience in graduate school so positive. I also acknowledge my funding sources, especially the DOVE fellowship. Finally, I am very grateful for the reovirus 'family' for their friendship and collaboration.

ABSTRACT

Many viruses enter hosts by invading mucosal surfaces. Mammalian reoviruses gain access to the host by the gastrointestinal and respiratory tracts. Determinants of reovirus infection of the gastrointestinal tract are well-understood, however the host and viral determinants of respiratory reovirus infection are unknown. The work within this thesis characterizes the host and viral determinants of respiratory reovirus infection and systemic dissemination. To accomplish this, we developed a murine model of respiratory reovirus infection. Using this model, we showed that endogenous respiratory and inflammatory proteases can promote reovirus infection *in vitro* and that pre-existing inflammation augments *in vivo* infection in the murine respiratory tract. Through this work, we identified two laboratory isolates of T3D, $T3D^C$ and $T3D^F$, that differ in their capacity to replicate in the respiratory tract and spread systemically, and we used these viruses to describe genetic polymorphisms that regulate reovirus replication and dissemination. The data presented in this thesis illustrate that reovirus infection of the respiratory tract and systemic dissemination are influenced by multiple factors including virion composition, resistance or sensitivity to protease-mediated inactivation and respiratory inflammation.

TABLE OF CONTENTS

LIST OF TABLES

LIST OF FIGURES

LIST OF ABBREVIATIONS

BALF	Bronchial alveolar lavage fluid
BHK-T7	Baby hamster kidney cells expressing T7 RNA polymerase
Cat	Cathepsin
CHT	Chymotrypsin
CNS	Central nervous system
COPD	Chronic obstructive pulmonary disease
CPE	Cytopathic effect
DC	Dearing-Cashdollar
DF	Dearing-Fields
ds	Double-stranded
GMEM	Glasgow's modification of eagle's medium
h	Hour/hours
HA	Hemaglutinin
HAT	Human airway trypsin-like protease
IFN	Interferon
ISVP	Intermediate subvirion particles
JAM-A	Junctional adhesion molecule – A
KO	Knock-out
L929	Immortalized mouse fibroblast L929 cell line
LPS	Lipopolysaccharide
MEF	Mouse embryo fibroblast
MEM	Minimal essential medium
min	Minute
MOI	Multiplicity of infection
mRNA	Messenger RNA
NE	Neutrophil elastase
NIH3T3	NIH 3T3 mouse embryonic fibroblast cells
PAGE	Polyacrylamide gel electrophoresis
PBS	Phosphate buffered saline
PFU	Plaque forming unit
PMN	Polymorphonuclear cells
PMSF	Phenylmethanesulfonyl fluoride
RT-PCR	Reverse transcriptase polymerase chain reaction
SCID	Severe combined immunodeficiency
SEM	Standard error of the mean
SD	Standard deviation
SDS	Sodium dodecyl sulfate
sec	second
SMEM	Spinner modified eagle's medium
T1L	Reovirus serotype 1 Lang
T3D	Reovirus serotype 3 Dearing
$T3D^C$	Reovirus serotype 3 Dearing-Cashdollar
$T3D^F$	Reovirus serotype 3 Dearing-Fields

TMPRSS2	Transmembrane protease serine 2
TNB	Tris-NaCl-blocking buffer
VDB	Virion dialysis buffer

CHAPTER 1

Introduction

I. **Introduction to mammalian reovirus**

Mammalian orthoreoviruses (reoviruses) are the prototypic members of the *Reoviridae* family that includes the pathogenic rotaviruses. Reovirus was first isolated from a child in 1951; in subsequent years, reovirus has been isolated from both healthy children and children with respiratory and gastrointestinal illnesses. In 1959, Sabin suggested these viruses be classified as reoviruses (respiratory enteric orphan viruses) based on the routes of transmission and the generally asymptomatic nature of infection (191, 195). While reovirus infections are generally asymptomatic or result in mild upper respiratory or gastrointestinal disease, there have been cases of reovirus-associated acute respiratory disease and necrotizing encephalitis in humans (43, 44, 170).

The generally nonpathogenic nature of reoviruses in human infection, coupled with their preferential replication in transformed cells has led to their development as an oncolytic agent. An isolate of type 3 Dearing (T3D) is currently undergoing stage III clinical trials to treat prostate, breast and small cell lung cancers (92, 111, 114, 133, 182). The oncolytic potential of reovirus was initially linked to activation of the Ras oncogene; NIH3T3 cells were susceptible to reovirus infection only after transformation with activated Ras (143, 203, 211).

The hypothesis that Ras transformation conferred cellular susceptibility to reovirus infection (211) assumed that active cellular PKR, and the resulting host shut-off, was detrimental to reovirus infection. However, work from our lab revealed that reovirus replicates to higher titers in cells that express and can activate PKR (209). Alain and colleagues further challenged the model in which Ras transformation mediated reovirus susceptibility, reporting that untransformed NIH3T3 cells are permissive to infection with *in vitro* uncoated particles (1). Their results demonstrated that NIH3T3 cells restrict reovirus infection at the step of uncoating, not protein synthesis (1). These studies, together with work by Golden et al. which demonstrated that many cell types are permissive to reovirus infection when infection is initiated by uncoated particles, suggest that protease-mediated virion disassembly is a critical step for reovirus oncolysis (85). Understanding the role of specific proteases in reovirus oncolysis could positively affect human health because it would allow oncolytic reoviruses to be paired with tumor targets based on the tumor protease profile.

Studies of reovirus biology have contributed to the fundamental understanding of both molecular biology and virology. Early studies in reovirus biology and RNA synthesis (25, 208) led to the discovery of the 5'cap on mRNAs (156) and consensus sequences for translation initiation (122). Animal models of reovirus infection were among the first to examine the genetic basis for viral pathogenesis and led to the identification of specific gene products that regulate

tropism, pathogenicity and dissemination (98, 219, 228, 229). The importance of understanding reovirus pathogenesis is twofold. By identifying viral determinants that regulate dissemination, one could improve the safety and efficacy of reovirus as a cancer therapeutic. In addition, new knowledge about the tissue-specific activity of proteases in the host may lead to development of therapeutic agents that will target other (more pathogenic) viruses that require proteolytic activation. For example, clinical studies suggest that influenza virus symptoms may be lessened after aerosolized treatment with protease inhibitors such as aprotinin (171, 243-245).

In my dissertation research, I investigated the host and viral determinants of respiratory reovirus infection and systemic dissemination. To accomplish this, I developed a murine model of respiratory reovirus infection. Using this model, I identified respiratory proteases that can mediate reovirus disassembly and promote infection in cell culture. I also characterized the impact of an inflammatory state on respiratory reovirus infection. Using the recently developed reovirus reverse genetics system, I identified viral determinants that regulate reovirus pathogenesis in the respiratory tract.

II. **Reovirus biology**

Reoviruses are classified by serotype and strain. There are three reovirus serotypes, which can be differentiated by anti-reovirus antisera that recognize the

viral cell attachment protein, σ1. The three serotypes are each represented by a prototype strain isolated from a human host: T1 Lang (T1L), type 2 Jones (T2J), and type 3 Dearing (T3D). Studies in this thesis take advantage of two different laboratory isolates of reovirus T3D – Dearing-Fields ($T3D^F$) and Dearing-Cashdollar ($T3D^C$). Reovirus strains can differ significantly in viral replication and pathology. The earliest studies examining reovirus pathogenesis exploited the segmented nature of the reovirus genome and generated reassortant viruses, which allowed viral gene segments that segregate with various biological and biochemical phenotypes to be identified. (69, 71). Recently, Kobayashi et al. developed a plasmid-based reverse genetics system for reovirus (119, 120). This system has enabled investigators to specifically test hypotheses about the genetic regulation of reovirus replication, systemic dissemination and pathology.

Reoviruses are nonenveloped, icosahedral viruses that contain a genome of 10 double-stranded (ds) RNA gene segments encased in two concentric protein shells. The 10 reovirus genome segments, three large (L1, L2, L3), three medium (M1, M2, M3), and four small (S1, S2, S3, S4), encode 12 viral proteins. The reovirus proteins are also categorized by size: large (λ), medium (μ) and small (σ), although the protein and gene numbers do not always correlate. Eight of the 12 proteins are structural (λ1, λ2, λ3, μ1, μ2, σ1, σ2 and σ3) and the remaining four (μNS, μNSC, σNS and σ1s) are nonstructural (reviewed in (195). Important for my thesis work are the reovirus S1 gene, which encodes the cell

attachment protein σ1 and non-structural protein σ1s, the S4 gene, which encodes the outermost capsid protein σ3, and the M2 gene, which encodes the penetration protein μ1 (reviewed in 195).

Four distinct particle types have been identified during reovirus infection: the virion, the ISVP, the ISVP* and the core (60, 210). The environmentally stable virion contains all eight structural proteins surrounding the 10 segments of genomic dsRNA (195). The defining feature of virions is the presence of an intact outer capsid consisting of the σ3 and μ1 proteins (60, 210). The σ3 protein forms a heterohexamer with μ1, the viral protein responsible for membrane penetration (129). The interaction of σ3 with μ1 prevents the premature exposure of hydrophobic residues within μ1 and therefore aids in the proper timing of membrane penetration (164, 197, 241). Trimers of the viral attachment protein, σ1, protrude from the pentamers of λ2 at the icosahedral vertices (124).

In cell culture, reovirus initiates infection when the cell attachment protein, σ1 binds to widely expressed cellular receptors, sialic acid and/or junctional adhesion molecule A (JAM-A) (31, 74, 81, 88). Upon attachment, β1 integrin mediates particle uptake into endocytic vesicles (139). Virions are associated with clathrin- and caveolin- coated endocytic vesicles (26, 64). In endosomes, particles undergo protease-mediated disassembly (63). However, after gastrointestinal infection, virion uncoating occurs extracellularly by pancreatic

serine proteases (3, 10). Either extracellular or intracellular proteolysis of reovirus virions renders them capable of membrane penetration (136, 217). It was hypothesized that ISVPs (because they are uncoated) bypassed the requirement for receptor-mediated endocytosis and could penetrate the cell membrane directly, but recent work from our lab demonstrates that ISVPs utilize caveolar endocytosis to enter cells (unpublished observation).

The conversion from virion to ISVP is characterized by proteolytic removal of the outer capsid protein σ3. σ3 proteolysis exposes and primes μ1 for membrane penetration and enables the cell attachment protein σ1 to extend from the particle surface (24, 109). An important characteristic of ISVPs is the capacity to infect cells in the absence of active cellular proteases (26, 85). ISVPs undergo further conformational changes, generating a particle type referred to as an ISVP*, which is believed to mediate membrane penetration (35, 241). In the ISVP*, conformational changes in μ1 and λ2 result in the loss of the cell attachment protein σ1 (34). Autocatalytic N-terminal cleavage in μ1 releases a small myristoylated fragment, μ1N, from the viral particle (35, 103, 241). Free-myristoylated μ1N is sufficient to cause membrane pore formation (35, 103, 241). Once an ISVP* penetrates the cellular membrane, it is converted into a core particle through a process that is not well understood.

Core particles are differentiated from ISVP*s by the absence of the membrane penetration protein μ1 and further conformational changes in λ2 (149). λ1 and σ2 form the shell of the core particle with 12 turret-like structures of λ2 that provide capping functions and create a channel to pass viral mRNA synthesized by λ3, the RNA-dependent RNA polymerase (42, 76-78). The core synthesizes mRNAs that are released from the particle interior into the cytoplasm.

III: Proteases that mediate reovirus disassembly

In vitro:

A wide range of proteases can mediate reovirus disassembly *in vitro*. Rates of virion disassembly differ depending upon treatment conditions and the type of protease. Within minutes of treatment, chymotrypsin (CHT) cleaves the reovirus outer capsid proteins σ3 and μ1 (24). After 1 h of treatment with cathepsin (Cat) L or neutrophil elastase (NE), no virion-associated σ3 is present and μ1 is cleaved into its characteristic μ1C and δ fragments (63, 86). The inflammatory protease Cat S mediates virion disassembly by 6 h of treatment, while the majority of σ3 remains virion associated after 4 h of treatment with the endosomal cysteine protease Cat B (63, 84). The aspartyl protease, Cat D, has been reported not to mediate reovirus disassembly, however, this failure to mediate cleavage is reovirus strain specific (121). Recent work from our lab and

others has shown that some reovirus strains can utilize Cat D for virion disassembly (unpublished observation) (233).

Cell culture:

In tissue culture, a variety of host proteases can also mediate the conversion of virions to ISVPs (4, 10, 55, 63, 108, 197, 212, 231). Proteases involved in reovirus disassembly in murine L929 fibroblasts have been extensively studied. Inhibition of the acid-dependent cysteine proteases, Cats L and B, completely abrogates viral growth in L929 cells. While active Cat L and B are required for reovirus to reach peak titers in L929 cells (63), these proteases do not promote replication equally. Infection of Cat L-deficient L929 cells or L929 cells treated with Cat L inhibitor resulted in inefficient virion disassembly and low viral yields (63). Viral growth was only modestly inhibited in L cells treated with an inhibitor of Cat B (63).

Early studies suggested that reovirus disassembly in cells required cysteine proteases and low pH (4, 212). However, it was unclear if the low pH was required to activate the acid-dependent cysteine proteases required for infection in L929 cells or if the low pH was essential for conformational change in virion proteins. More recent work from our lab reveals that virion disassembly can be mediated at neutral pH (84, 86). Two acid-independent proteases, Cat S and neutrophil elastase (NE), promote reovirus disassembly and infection in cell

culture (84, 86). These results demonstrate that acidic pH is not required for reovirus disassembly.

Gastrointestinal infection:

In reovirus infections of the gastrointestinal tract, uncoating occurs extracellularly and is mediated by pancreatic serine proteases CHT and trypsin (20). The importance of extracellular uncoating was revealed in a study that demonstrated that pretreatment of mice with the serine protease inhibitors aprotinin and chymostatin blocked infection by reovirus virions, but not infection by ISVPs (10). Extracellular uncoating in the gastrointestinal tract occurs within 5 minutes of peroral inoculation and is thought to be critical because virion disassembly promotes the extension of the cell attachment protein, σ1, which is necessary for attachment to intestinal M cells (3, 237). It is believed that after σ1 binds to the cellular receptors JAM-A and/or sialic acid (31, 38, 74, 81, 88, 172), virions are transported basolaterally where they access adjoining epithelial cells (237). Prior to my thesis work, the role of specific proteases in respiratory infection had yet to be examined.

While virion disassembly occurs extracellularly to establish reovirus infection in the gastrointestinal tract (10, 20), progeny virions are believed to be uncoated by endosomal Cats in secondary sites of infection (108). Endosomal Cats L and B are expressed in all major organs and mediate tissue-specific

activities (6, 7, 94, 158, 169, 189). In contrast, expression of Cat S is largely limited to cells and tissues of the immune system (61, 117, 131, 132, 176-178, 187, 200, 201).

The role of specific proteases in systemic reovirus dissemination from the enteric tract has been examined using both genetic and pharmacological approaches (108). Studies of gastrointestinal reovirus infection in single protease knockout (KO) mice demonstrated that each endosomal Cats L, B and S impact reovirus replication and dissemination (108). Peak organ titers were decreased in Cat L KO, Cat B KO or Cat S KO mice. Interestingly, the presence or absence of endosomal Cats did not significantly impact reovirus viremia, as infectious virus could be recovered in the blood of all mice at all times investigated. This suggests that viral replication in the intestine does not significantly impact reovirus access to the blood.

IV: Viral infection of the respiratory tract

Numerous animal models have been developed to study acute respiratory distress syndrome (ARDS), however few duplicate all phases of disease progression (147). ARDS involves three phases: acute (days 1-7), fibroproliferative (days 7-21) and resolution (days >21) (54, 101, 215, 224). London and colleagues developed a murine model of ARDS that recapitulates each phase (135). In this model, 4 – 5 week-old CBA/J mice were inoculated

intranasally with 10^7 PFU of T1L reovirus virions. This resulted in 60% of the animals dying between days 6-10. By 5 dpi, patchy pneumonia developed with infiltration of PMNs and a significant increase of protein concentration in bronchial alveolar lavage fluid (BALF). By day 9, hyaline membranes began to form and fibrotic lesions continued to develop through day 14; resolution began around day 14 (135).

Morin et al. established a reovirus-induced pneumonia model in the rat (153). After intratracheal inoculation of reovirus T1L, rats exhibit notable respiratory distress (153). Reovirus T1L-induced pneumonia in the rat is characterized by extensive epithelial damage, type II alveolar epithelial cell hyperplasia and an influx of leukocytes (153). Reovirus replication occurs in type 1 alveolar cells and reovirus particles are also detected in alvelolar macrophages (153). One might predict that access to alveolar macrophages would promote hematogenous dissemination, however, Morin and colleagues did not examine dissemination from the respiratory tract.

These studies in the murine and rat models of respiratory infection largely focused on the host response and resolution of lung injury and did not consider the role of host proteases in respiratory reovirus infection. Unlike the enteric tract, which contains abundant active proteases, the respiratory tract retains a balance of proteases and protease inhibitors to support an optimal environment for

oxygen exchange (80, 151). Upon insult or injury, the balance between proteases and their inhibitors can be tipped due to the inflammatory response (79, 80, 151). Although the role of the inflammatory response is to provide protection to the tissue, uncontrolled inflammation can result in significant injury and lead to pulmonary dysfunction (49, 57, 127, 137, 184, 225). Disruption in the protease:antiprotease balance in the respiratory tract contributes to chronic obstructive pulmonary disease (COPD) and asthma (51, 107, 173, 184, 242). In adult asthmatics, 76% of patients requiring hospitalization for acute asthma had evidence of an ongoing viral respiratory infection (226). The specific role of viral infection in the exacerbation of COPD is currently unknown (107, 173). With an estimated 64 million people with COPD worldwide, a well-developed model to examine the impact of viral infection, inflammation and airway remodeling could have significant clinical benefits.

Proteases clearly play an important role in many pathogenic viral infections, including those of the respiratory tract (14, 16, 27-29, 83, 99, 204, 206, 207). For example, most influenza virus infections remain localized to the respiratory tract, despite the fact that the virus interacts with broadly-expressed cellular receptors (48). One factor that limits influenza virus infection is the requirement for host proteases that activate the fusion protein, hemagglutinin (HA), for membrane penetration (96, 227). Host proteases that are resident in the respiratory tract, including tryptase clara, human airway trypsin-like protease

(HAT) and TMPRSS2, can cleave influenza's HA protein enabling it to initiate membrane fusion (15, 17, 28, 29, 33, 165, 243). Whereas most influenza viruses are activated by secreted or membrane-associated proteases in the respiratory tract, highly pathogenic strains, such as the avian H5N1, express HA molecules that can be cleaved by furin during virion maturation (112). These viruses have the potential to disseminate systemically in chickens (40, 96, 227). Similarly, the SARS coronavirus fusion protein requires activation by host proteases. Activation of SARS coronavirus has been linked to both membrane associated and endosomal proteases: Cat L, HAT, TMPRSS2 and TMPRSS4 (14, 16, 83, 99, 204, 206, 207). These studies helped to focus our research on respiratory proteases that might mediate reovirus disassembly in the respiratory tract.

V: Host response to reovirus infection

Mice deficient in components of the immune system have been used to understand the roles of humoral and cellular immunity in reovirus pathogenesis. While both the innate and the adaptive immunity are involved in reovirus clearance, studies in severe combined immunodeficiency (SCID) mice revealed that antigen-specific lymphocytes are important for viral clearance after oral inoculation (214). Reovirus infection dramatically increases CD4+, CD8+ and CD4/CD8 double-positive T-cell populations in the respiratory and gastrointestinal tracts (18, 66). The cytokine profile of reovirus specific CD4+ T-cells revealed a predominantly TH1 response (66). Neonatal mice treated with

anti-CD4 or anti-CD8 antibodies developed severe hepatobiliary pathology and increased reovirus titers, but adoptive transfer of preimmune CD4+ or CD8+ T-cells protects against lethal infection (223). These results suggest that both CD4+ and CD8+ T cells contribute to reovirus clearance in murine infection models. In addition, humoral immunity is also an important component in host clearance of reovirus infection. Secretory IgA, directed against the cell attachment protein σ1, is protective *in vivo* through inhibition of viral entry (100, 205). These results show that the host depends on many aspects of the immune response to mediate efficient reovirus clearance.

VI: Systemic reovirus dissemination

Systemic dissemination of reovirus infection after peroral inoculation has been extensively studied in the murine model (3, 10, 20, 22, 73, 152, 155). Inoculation of adult mice results in a limited local infection, however inoculation of SCID or neonatal mice results in systemic disease (82, 126), indicating that a mature immune system can efficiently limit systemic dissemination and pathogenesis. Studies in neonatal mice reveal differences in the capacity of different reovirus strains to replicate in and spread from the enteric tract. In newborn mice, one type 3 strain (clone 9) spread from the intestinal tract into mononuclear cells and through neurons to the brainstem (155). In contrast, reovirus T1L followed a hematogenous pathway to spread to secondary sites (155). After transport across M cells, T1L was sequentially detected in Peyer's

patches, mesenteric lymph nodes, blood and the spleen (110). After reovirus spreads to secondary sites from the enteric tract, apoptotic cell death is induced in both the central nervous system (CNS) (12, 46, 97, 186) and heart (53, 97, 150, 168). In my thesis work, I sought to characterize reovirus dissemination from the respiratory tract.

VII: Role of the reovirus S1 gene in strain specific differences in reovirus infection of the gastrointestinal tract

As discussed above, reovirus strains differ in capacity to replicate *in vivo*. After intragastric inoculation of 10^8 PFU, titers of some type 3 strains rapidly decrease while titers of type 1 strains increase in the gastrointestinal tract (110). The difference in capacity to replicate in the intestine was associated with the reovirus S1 gene. After intragastric inoculation of S1 gene reassortant viruses 1HA3 (a T1L virus with a T3D S1 gene) or 3HA1 (a T3D virus with a T1L S1 gene), titers in the gastrointestinal tract were equivalent at 6 and 24 h post-inoculation, however, by 48 hours, titers of 3HA1 decreased while the titer of 1HA3 increased (110). This result revealed that the S1 gene is a major determinant for viral replication in the gastrointestinal tract.

The S1 gene encodes two proteins: the cell attachment protein σ1 and a nonstructural protein, σ1s, in overlapping reading frames. Biochemical studies have correlated protease sensitivity of the cell attachment protein, σ1, with the

failure of some reovirus strains to replicate in the gastrointestinal tract (55, 160). Since some type 3 strains do not replicate to high titers in the gastrointestinal tract (19, 110), Nibert et al. proposed that the cell attachment protein may be cleaved by the abundant pancreatic serine proteases present in the gastrointestinal tract (160). In support of this model, some type 3 reovirus strains lost infectivity in the presence of the proteases CHT and trypsin *in vitro* (160). The loss of infectivity after protease treatment was correlated with a degradation of the cell attachment protein, σ1 (37, 160). Protease-mediated instability of the σ1 protein was associated with a polymorphism in the neck of the protein at amino acid 249 (37). Interesting recent work has revealed that the S1 gene encoded non-structural protein, σ1s, while not required for replication in cell culture, modestly enhances viral replication in the gastrointestinal tract, through mechanisms that are not understood (22).

Reovirus strains also differ in capacity to disseminate systemically after oral inoculation and this has been linked to the S1 gene as well. T1L spreads efficiently to secondary sites while T3D does not (110). However, failure to reach high viral loads in the gastrointestinal tract may impact capacity of T3D to spread to the spleen. Kauffman et al. examined the genetic determinants that impact the capacity of reovirus to spread to the spleen (110). After oral inoculation with reassortant viruses 3HA1 and 1HA3, titers in the draining lymph nodes were similar, but only 3HA1 spread to the spleen (110). These results indicate that the

reovirus S1 gene is the primary determinant of the capacity to disseminate systemically after oral inoculation.

VII: Strain specific differences in reovirus infection of the respiratory tract

Prior to my thesis work, there was some evidence to suggest that reovirus strains also differ in capacity to replicate in the respiratory tract. Morin and colleagues compared T1L and T3D infection in rat lungs (67, 153). After intratracheal inoculation, reovirus strain T1L replicated to higher titers than strain T3D (153). T3D infection induced pneumonia that differed slightly compared to T1L induced pneumonia, as T3D infection and resulting pneumonia included a greater infiltration of PMNs (67, 153). BALF from T1L infected rats contained 24% PMNs while BALF from T3D infected rats consisted of 66% PMNs (67). Serotype specific induction of pulmonary PMN infiltration correlates with significant differences in cytokine induction. After respiratory infection, T3D has been reported to induce more IFN, TNF-α and MIP-2 than T1L (67).

Morin et al. also examined the genetic basis for the serotype specific differences in reovirus replication in the respiratory tract and determined that they segregate with the S1 gene (153). Viral load after inoculation with the reassortant virus 3HA1 reached levels similar to titers recovered after T1L inoculation, while inoculation with 1HA3 resulted in lung titers similar to T3D (153). The S1 gene also appears to contribute to the difference in PMN recruitment, as reassortant

virus 3HA1 recruited 46% PMNs whereas 1HA3-infected animals had more PMNs in the BALF (58%) (153). These results argue that the S1 gene is the primary determinant for replication in the respiratory tract and induction of pulmonary neutropenia.

VIII. The goals of this study

One of the research goals of the Schiff laboratory was to gain insight into the host and viral determinants for respiratory reovirus infection and systemic dissemination. Prior to the work in this thesis, nothing was known about the proteases that mediate virion uncoating when infection is initiated in the respiratory tract. I set out to investigate the role of endogenous respiratory proteases in reovirus infection. Through this work, I discovered that reovirus titers were enhanced upon respiratory inflammation, and this observation led us to investigate the role of inflammation in reovirus replication and systemic dissemination. In the course of these studies, I identified strain specific differences in reovirus pathogenesis after respiratory inoculation. I used a reverse genetic approach to identify genetic determinants of reovirus replication in the respiratory tract and systemic dissemination from the lungs. Preliminary biochemical experiments suggest a molecular mechanism that might contribute to this difference in pathogenesis.

CHAPTER 2

Materials and Methods

Mammalian cells. Murine L929 cells were maintained as suspension cultures in SMEM supplemented to contain 5% heat-inactivated fetal calf serum (Hyclone Laboratories, Logan, UT), 2 mM glutamine, 50 units/ml penicillin G, and 50 μg/ml streptomycin sulfate. Vero cells were maintained in DMEM supplemented to contain 5% heat-inactivated fetal calf serum (Hyclone Laboratories, Logan, UT), 2 mM glutamine, 50 units/ml penicillin G, and 50 μg/ml streptomycin sulfate. Baby hamster kidney cells expressing T7 RNA polymerase (BHK-T7 cells) (30) were maintained as monolayer cultures in GMEM supplemented to contain 10% heat-inactivated fetal calf serum (Hyclone Laboratories, Logan, UT), 2 mM L-glutamine, 2% MEM amino acids solution 50x (Invitrogen), 50 units/ml penicillin G, and 50 μg/ml streptomycin sulfate. Alternating passages of BHK-T7 cells were made using medium supplemented to contain 1 mg/ml geneticin (Gibco).

Viruses. Reovirus strains Dearing (T3D) and Lang (T1L) are prototypic laboratory strains. Two isolates of strain Dearing, Dearing-Cashdollar ($T3D^C$) and Dearing-Fields ($T3D^F$) were used in these studies. Dr. B. Fields provided the Schiff laboratory with $T3D^F$ and T1L reassortant viruses (3HA1 and 1HA3) that had been isolated from L929 cells coinfected with strains $T3D^F$ and T1L (229). Dr. J. Parker graciously provided us with third passage lysate stocks of $T3D^C$.

Viral titers were determined by plaque assay on L929 cells (222). The elecrophoretic mobility of viral dsRNA gene segments was verified on 10% polyacrylamide gels and detected by silver staining (8).

Generation of recombinant viruses. Baby hamster kidney cells that stably express T7 RNA polymerase (BHK-T7) (30) were cotransfected with nine plasmid constructs representing cloned gene segments from the $T3D^F$ genome (23, 119): pT7-L1T3D (2 μg), pT7-L2T3D (2 μg), pT7-L3T3D (2 μg), pT7-M1T3D (1.75 μg), pT7-M2T3D (1.75 μg), pT7-M3T3D (1.75 μg), pT7-S2T3D (1.5 μg), pT7-S3T3D (1.5 μg), pT7-S4T3D (1.5 μg) (119, 120) in combination with 2 μg of pT7-S1T3D^F, pT7- S1T3D^F/T3D^{C}S1-77, pT7- S1T3D^F/T3D^{C}S1-1234, or pT7-S1T3D^F/T3D^{C}S1. The S1 gene recombinant plasmids (pT7- S1T3D^F/T3D^{C}S1-77, pT7- S1T3D^F/T3D^{C}S1-1234, or pT7-S1T3D^F/T3D^{C}S1) were generated by altering pT7-S1T3D^F using the Quickchange site-directed mutagenesis system (Stratagene) and forward primers: 5'-cgagtgataatggagcgtcactgtcaaaagggcttgaatcaaggg-3' (rsT3D^F/T3D^{C}S1-77), 5'-agggttgtcgtcgggtggtgcccctcagtatatgagtaagaa-3' (rsT3D^F/T3D^{C}S1-1234); reverse primers: 5'-cccttgattcaagccctttgacagtgacgctccattatcactcg-3' (rsT3D^F/T3D^{C}S1-77), 5'-ttcttactcatatactgaggggcaccacccgacgacaaccct-3' (rsT3D^F/T3D^{C}S1-1234). The pT7-S1T3D^F/T3D^{C}S1 plasmid was altered by Quickchange site-directed mutagenesis to generate pT7-S1T3D^F/T3D^{C}S1 σ1s-null. The S1 gene recombinant plasmids (pT7- S1rsT3D^F/T3D^{C}S1-77, pT7- S1rsT3D^F/T3D^{C}S1-

1234, or pT7-S1rsT3D^F/T3D^{C}S1) were generated by altering pT7-S1T3D using Quickchange (Stratagene) site-directed mutagenesis and forward primers: 5'-Attaacgagtgataacggagcgtcactgtcaaaaggg-3' (rsT3D^F/T3D^{C}S1-77 σ1S-null and rsT3D^F/T3D^{C}S1 σ1S-null), 5'- Attaacgagtgataacggagtatcactgtcaaaaggg-3' (rsT3D^F σ1S-null and rsT3D^F/T3D^{C}S1-1234 σ1S-null); reverse primers: 5'-ccctttgacagtgacgctccgttatcactcgttaat -3' (rsT3D^F/T3D^{C}S1-77 σ1S-null and rsT3D^F/T3D^{C}S1 σ1S-null), 5'- ccctttgacagtgatactccgttatcactcgttaat-3' (rsT3D^F σ1S-null and rsT3D^F/T3D^{C}S1-1234 σ1S-null). S1 and L1 gene sequences of viruses recovered by reverse genetics were confirmed using viral RNA extracted from purified virions and Onestep RT-PCR (Qiagen) with S1 or L1 specific primers (119).

Generation of third passage reovirus stocks. Reovirus stocks were prepared in L929 cells. Well-isolated viral plaques were picked and disrupted in gel saline (0.14 M $NaCl_2$, 0.27 mM $CaCl_2$-$2H_2O$, 0.84 mM $MgCl_2$-$6H_2O$, 0.2 M H_3BO_3, 0.13 mM $Na_2B_4O_7$-$10H_2O$, and 3 g/L gelatin at a pH of 7.4). L929 cells that had been plated the previous day were infected with the virus/agar/gel saline mixture. Samples were incubated at 37^{o}C for with gentle agitation to allow particles to adsorb, and SMEM medium was added after 1 h. Samples were incubated at 37^{o}C until $\geq$ 90% of the cells demonstrated cytopathic effect (CPE). The plates were subjected to three cycles of freeze-thawing and the resulting lysates were placed into sterile dram vials and stored at 4^{o}C. Generally 0.5 ml of this passage

1 stock was used to generate passage 2 stocks following the adsorption and incubation protocol described above. Second passage stocks were titered by standard plaque assay to quantify plaque forming units (PFU)/ml and a sufficient quantity of passage 2 stock to result in a multiplicity of infection (MOI) of 0.5 PFU/cell was used to generate passage 3 stocks. The third passage stocks were titered by standard plaque assay and the genotype was confirmed by sodium dodecyl sulfate (SDS)-polyacrylamide gel electrophoresis (PAGE) and silver staining of the dsRNA gene segments and genetic sequencing of specific genes.

Purification of reovirus virions. Purified virions were generated by pelleting 2 x 10^8 L929 cells by low speed centrifugation (145 g for 10 min). Cells were infected at a MOI of 2 PFU/cell in a final volume of 10 ml with third passage or high titer second passage cell-lysate stocks. The samples were incubated in a 35^{o}C H_2O bath for 1.5 to 2 h with gentle swirling every 15 min to allow particles to adsorb. After adsorption, medium was added so that the cells were at a final concentration of 5 x 10^5 cells/ml. The infected cells were then stirred in a 35^{o}C H_2O bath until 25-35% of the cells were dead – determined by failure to exclude 0.4% trypan blue. Infected cells were pelleted by low speed centrifugation and frozen for 2 h to overnight at -80^{o}C. Pellets were resuspended in 7 ml HO buffer (250 mM NaCl, 10 mM Tris [pH 7.4]), and transferred to a 30 ml Corex tube. Cells were disrupted by two 30-second sonication pulses at 30% power with a Sonifier cell disrupter. The disrupted cells were placed on ice and 1/100th of the

volume of 10% deoxycholic acid was added. The mixture was incubated on ice for 30 min, with gentle swirling every 10 min. One half of the total volume of trichlorotrifluoroethane (freon) was added to the sample and it was sonicated until it emulsified. Another half volume of freon was added and the sample was sonicated again. The sample was centrifuged at 7000 g for 25 min at 4^{o}C. The aqueous phase, which contains the virions, was removed with sterile plastic pipet and placed in a sterile corex tube and the freon/centrifugation step was repeated. The second aqueous phase was layered onto a 1.25-1.45 g/cc CsCl gradient and centrifuged overnight at 88700 g and 4^{o}C using a SW41 rotor (Beckman, Fullerton, CA). After centrifugation, the visible band of virions was collected by puncturing the bottom of the centrifugation tube and collecting the drops corresponding to the band in a sterile dram vial. Purified virions were dialyzed at 4^{o}C for 2 days in 2 L of 1x virion dialysis buffer (VDB) (0.15 M NaCl, 10 mM $MgCl_2$, 10 mM Tris at a pH of 7.5) in Spectra/Por molecularporous membrane tubing with a molecular weight cut off of 12,000-14,000 daltons (Spectrum Laboratories, Inc., Rancho Dominguez, CA). The titer of the purified virions was determined by standard plaque assay, particle concentration was determined using a spectrophotometer and the assumption that 1 OD_{260} = 2.1 x 10^{12} particles/ml and the genotype was confirmed by SDS-PAGE and silver staining and/or sequencing.

Generation of intermediate subvirion particles. Intermediate subvirion particles (ISVPs) were prepared by diluting purified virions in cold 1x VDB to a concentration of 1 x 10^{12} particles/ml and treating with 200 mg/ml chymotrypsin (CHT). Virions of T3D were incubated in a 27^{o}C H_20 bath for 7.5 min, whereas virions of the other strains were incubated at 32^{o}C for 30 min. Tubes were removed from the H_2O bath, placed on ice and phenylmethanesulfonyl fluoride (PMSF) was added to a final concentration of 1 mM. ISVPS were stored at 4^{o}C.

Protease treatment of reovirus virions. Purified virions (5 x10^{10} particles/ml) with 50 μg/mL purified chymase (Calbiochem), 25 μg/mL purified Cat G, 21 μg/mL of purified HAT (R&D Systems), 200 μg/ml chymotrypsin (Sigma) or 25 μg/ml neutrophil elastase (Calbiochem) in 20μL VDB at 37°C. Mock-treated samples were incubated in VDB for the longest time point. Digestions were terminated with PMSF (Sigma) at a final concentration of 2mM, benzamidine at a final concentration of 5 mM, or PMSF (2mM) and neutrophil elastase inhibitor (Calbiochem) (200 μM). Protein sample buffer (0.125 M Tris [pH 8.0], 1% SDS, 0.01% bromphenol blue, 10% sucrose and 5% β-mercaptoethanol) was added to each reaction mixture and samples were resolved on SDS-12% polyacrylamide gels. The protein gels were stained with Coomassie Brilliant Blue in order to visualize viral proteins.

Isolating reovirus dsRNA gene segments. To isolate virion dsRNA, L929 cells were plated at a density of 2 x 10^6 cells in 60-mm tissue culture plates to result in confluent monolayers after overnight incubation at 37^{o}C. Medium was removed and cells were infected with 100 ul of virus stock. After 1 h of adsorption at 37^{o}C, 5 ml of SMEM was added to each plate and cells were placed in a 37^{o}C incubator. Cells were monitored daily and frozen at –80^{o}C when $\geq$ 90% of the monolayer displayed cytopathic effects. The monolayers were then thawed and each infected cell lysate was transferred into a 13-ml Sarstedt tube (Sarstedt Aktiengesellschaft & Co., Germany). 0.3 ml of 5% ethylphenyl-polyethylene glycol (Nonidet P40, NP-40) (USB, Cleveland, OH) in NP-40 buffer (10 mM Tris [pH 7.4], 0.14 M NaCl, 3.15 mM $MgCl_2{\cdot}6H_2O$) was added to each tube, gently vortexed and incubated on ice for 30 min. The samples were centrifuged at 600 g for 10 min at 4^{o}C. The supernatant was gently poured to a new Sarstedt tube that contained 0.3 ml 10% SDS and proteinase K was added so that its final concentration was 100 mg/ml. The samples were gently vortexed and incubated in a 37^{o}C water bath for 1 h. After the incubation, 2 ml equilabrated phenol and 2 ml chloroform was added to each sample. Samples were vigorously vortexed for 30-60 sec until a stable emulsion formed and then centrifuged at 1500 g for 15 min at room temperature. The aqueous phase was transferred to a new Sarstedt tube and 0.1 aqueous volume of 3 M sodium acetate and 2.5 volumes of cold 100% EtOH were added. After mixing, samples were incubated overnight at –20^{o}C or for 1-2 h at –80^{o}C. To collect the precipitated nucleic acid, samples were

centrifuged at 9700 g for 10 min at 4^{o}C and the supernatant was discarded. Pellets were flash frozen in a dry ice/EtOH bath and dried under vacuum. The pellets were resuspended in 0.1 ml H_2O or TE and stored at –20^{o}C.

Standard reovirus plaque assay. On day 1, L929 cells were plated in 6-well plates at a concentration of 1 x 10^6 cells/well in 3 ml total volume and incubated overnight at 37^{o}C. On day 2, medium was removed from the wells and cells were infected with 0.1 ml dilutions of virus in cold gel saline. Plates were rocked every 15 min for 1-1.5 h at room temperature or 1 h at 37^{o}C, after which a 3 ml overlay (1% agar, 1X199, 2.5% heat-inactivated fetal calf serum, 2 mM glutamine, 100 units/ml penicillin G sodium and 100 mg/ml streptomycin sulfate) was added to each well. The overlay was allowed to solidify for ~15 min at room temperature and plates were returned to a 37^{o}C incubator. On day 5, 2 ml of overlay was added to each well as described for day 2. On day 8, 2 ml of overlay was added to each well, except that 2.5% fetal calf serum was omitted from the overlay and neutral red was included at a final concentration of 0.05%. On day 9, plaques were counted and viral titers determined.

Chymotrypsin reovirus plaque assay. Rapid chymotrypsin plaque assays were occasionally used to determine viral titer prior to an experiment. Day 1 of the CHT plaque assay is identical to the standard plaque assay described above. After medium was removed from the wells on day 2, each well was rinsed with 2

ml PBS + 2 mM $MgCl_2$. Cells were infected as described above. After adsorption, the inoculum was removed by aspiration and cells were overlaid with 5 ml of 1% agar, 1X199, 2 mM glutamine, 100 units/ml penicillin G sodium, 100 mg/ml streptomycin sulfate, 0.25 mg/ml amphotericin B and 10 mg/ml CHT. The plates were incubated at 37°C for 2 to 5 days until plaques could be counted and viral titers determined.

Viral replication assays. Virus was adsorbed to cells at 4°C for 1.5 h. For all experiments shown in this thesis, cells were infected at an MOI of 5. In some experiments, cells were pretreated for 3 h with protease inhibitor E-64. After adsorption, cells were pelleted by low-speed centrifugation and resuspended in fresh medium (with or without E-64). Virus and cells were added to dram vials (2 x 10^5 cells/vial) containing 1 ml of chilled medium. Triplicate samples were prepared for each time point. Time zero samples were frozen immediately at -70°C. The remaining samples were incubated at 37°C for various intervals and subjected to three cycles of freezing and thawing. Viral titers were determined by plaque assay using L929 cells (75). Viral yields were calculated according to the following formula: $\log_{10}$ yield at $t_x = \log_{10}(PFU/ml)t_x - \log_{10}(PFU/ml)t_0$, where t_x is the time post-infection and t_0 is the time immediately post-adsorption.

Transfection of vero cells with protease expression plasmids. Vero cell cultures were plated in 1 mL of DMEM medium onto 1mm coverslips in the wells of a 12-well plate. The cells were allowed to adhear overnight. Medium was removed 1 h prior to transfection and replaced with incomplete DMEM. 30 h prior to infection, cells were transfected with FLAG-tagged protease-expression plasmids (pCAGGS-HAT, pCAGGS-TMPRSS2, or pcDNA22) (11, 28) by Lipofectamine 2000 reagent (Invitrogen) according to product instructions. HAT and TMPRSS2 expression plasmids were generous gifts of Dr. Mikhail Matrosovich and ICP22 expression plasmid was a generous gift of Dr. Steve Rice. Transfected cells were infected with reovirus strain T1L virions or CHT-ISVPs (MOI 10 PFU/cell). At 18 h post-infection, cells were fixed with 4% parafromaldehyde for 20 min and permeabilized with 0.5% Triton X100 for 10 min. After permeablization, cells were washed in PBS 2 x 10 min. Cells were then incubated with diluted antibody, anti-σNS or anti-FLAG (Sigma-Aldrich), for 1 h at 37°C. The polyclonal antibody to reovirus nonstructural protein σNS was a generous gift of Dr. Terry Dermody. After incubation with primary antibody, cells were washed 3 x 5 min each in PBS, incubated with secondary antibody (Sigma-Aldrich) for 30 min, washed 3 x 5 min and counterstained with Hoechst (Invitrogen). Slides were mounted with mounting medium (Sigma-Aldrich) and placed at 4^{o}C overnight.

Animals and inoculation protocol. Four to five week-old female CBA/J mice were lightly anesthetized with isoflurane and inoculated with 30 μl onto the nares (approximately 15 μl each nare) and depressing the diaphragm (134). Three week-old CBA/J mice were lightly anesthetized with isoflurane and infected by peroral inoculation. Organs were resected at various intervals post-inoculation, and viral titers in organ homogenates were determined by plaque assay using L929 cells (222). BALF was obtained by intubating mice with small-gauge needle with 1cc syringe with 0.9cc sterile saline. Saline was carefully injected into animal's lungs and then aspirated slowly. Animal housing and infection and euthanasia procedures were performed in accordance with and approved by University of Minnesota Institutional Animal Care and Use Committee.

Titration of infectious virions from animal organs. Freshly harvested lungs, spleens, gut, and lymph nodes (mediastinal, cervical and thoracic) were resected and suspended in 1 ml gel saline. Blood was obtained by heart puncture and suspended in 1 ml gel saline. Lungs, spleen and gut were homogenized with a high shear tissue homogenizer (Omni) for 30 seconds using a soft tissue microprobe tip (Omni). Lymph nodes and blood were sonicated for two 30 s pulses. Homogenized samples underwent 3 freeze-thaw cycles, and the amount of infectious virus in each organ was determined by standard plaque assay on L929 cells.

Serine protease inhibitor treatment *in vivo.* Four week-old CBA/J mice were treated intranasally with 20 µl of saline or aprotinin (250 U) (Sigma-Aldrich) in 20 µl total volume one day, 20 min prior and 1 day post-inoculation. Mice were inoculated with 1 x 10^7 PFU of T1L. Organs were resected and blood was obtained by heart puncture. Organ titers were detected by plaque assay on L929 cells.

Induction of a respiratory inflammatory response. Four week-old CBA/J mice were untreated or treated intranasally with 1.5 mg LPS, 1.7 x 10^9 UV-inactivated T3D virions or saline 24 h prior to intranasal infection with 1 x 10^7 PFU reovirus strain T1L virions. Eight hours post-inoculation, BALF was harvested from infected mice.

Cytospin analysis of BALF. BALF was obtained from mice as described above. Slides and filters were placed in slots with the filters facing the center of the cytospin. 100ul of sample was added to the wells of the cytospin. Slides were spun at 450 g for 20 min and filters were removed. Slides were dried overnight prior to staining. Neutrophils and monocytes in the BALF were quantified after hemotoxylin and eosin staining.

Cytokine expression profile. Four week-old CBA/J mice were treated intranasally with virions, ISVPs, UV-inactivated ISVPs or saline. Two days post-

treatment, lungs were resected and cytokine expression was detected using the Proteome Profiler Array panel A (R&D Systems) according to the published protocol and Image J analysis.

Histology. Lungs were inflated *in situ* with 4% paraformaldehyde by intratracheal intubation using a tuburculin syringe. After insertion of the syringe and fluid, the trachea was clamped and the lungs were removed. The lungs were suspended in 4% paraformaldehyde for four h. The 4% paraformaldehyde was changed at least 1 x to remove excess blood, and lungs were placed in tissue cassettes and stored in 70% ethanol prior to processing and embedding in paraffin. 5 μm sections of embedded tissues were mounted on glass slides.

Slide staining. Slides were warmed in a 60^{o}C oven for 1 h before being passed through a series of xylene (2 x 5 min), graded ethanols (2 x 5 min absolute ethanol, 1 min each 90%, 80%, 70% and 60% ethanol) and water (2 x 5 min) to remove paraffin and hydrate the tissue sections. Slides were kept wet to ensure that tissues did not dehydrate. Moist slides were placed in a 1x Rodent Decloaker (BIOCare) at 90-95^{o}C for 30 min and then allowed to cool at room temperature for 30 min. Slides were transferred to glass rack and rinsed under running DI water until soap was removed. Tissue samples were encircled with a PAP pen and peroxidaze solution was added to each tissue sample for 2 min. Slides were then washed in DI water and blocked for 30 min with Tris-NaCl-

blocking buffer (TNB) (0.1M Tris-Cl, 150 mM NaCL, pH 7.5) and 10% Sniper (BIOCare) or Rodent Block M (BIOCare) to limit nonspecific binding. Dilutions of primary antibody diluted in TNB were added to samples and slides were incubated at either room temperature for 1-2 h or 4^{o}C overnight. After primary antibody, slides were washed in PBS or TBST (2 x 5 min). Viral antigen was detected using a horseradish peroxidase linked secondary antibody. After secondary antibody, slides were washed in DI water for 5 min and Vector DAB (BIOCare) was added for approximately 5 min. Slides were then counterstained with hematoxcylin (time varied by age of stain) or hemotoxylin and eosin and washed in warm water 2 x 5 min. Slides were then dehydrated (1 x 1 min 70%, 80%, 90% ethanol and 2 x 5 min absolute ethanol), cleared (2 x 5 min xylene) and mounted (Permount). Mounted slides were placed at 4^{o}C overnight and stored at room temperature.

Statistical Analysis. For those experiments in which viral titers were determined in an organ or blood, the Mann-Whitney test was used to calculate two-tailed P values. This test is appropriate for experimental data that display a non-Gaussian distribution. When all values are less than the limit of detection, a Mann-Whitney test P value cannot be calculated. Student T test was applied to experiments in cell culture. ANOVA test was used to calculate P values in cytokine profile experiment. Statistical analyses were performed using Prism software (GraphPad Software, Inc.).

CHAPTER 3
Development and Characterization of a Murine Model of Respiratory Infection

I. Introduction

Mammalian reoviruses have been used as a model system to characterize viral pathogenesis *(70, 72, 110, 152, 154, 163, 237)*. Establishment of reovirus infection in the gastrointestinal tract depends upon host proteases CHT and trypsin (10, 20), which cleave the outer capsid proteins σ3 and μ1. Particle disassembly promotes the extension of the cell attachment protein σ1 (3, 75, 230, 236, 237), which is required to enable reovirus attachment to intestinal M cells for entry (3, 10, 228). The murine model of gastrointestinal infection in newborn mice was used to identify viral determinants that regulate local and systemic reovirus infection (22, 55, 89, 108, 110, 190, 228, 237). Reovirus strains differ in their capacity to establish local infection (110), a characteristic that segregates with the S1 gene. The S1 gene encodes two proteins: the cell attachment protein σ1 and a non-structural protein, σ1s, in overlapping reading frames. The σ1 protein has been implicated as a major determinant of serotype-specific differences in reovirus replication in the gastrointestinal tract (37, 72, 110, 229). These differences are linked to a sequence polymorphism in the $T3D^F$ σ1 protein that increases sensitivity to cleavage by pancreatic serine proteases (37, 160). Interesting recent work has revealed that the S1 gene encoded non-structural protein, σ1s, while not required for replication in cell culture, plays a

role in hematogenous dissemination after peroral or intramuscular inoculation (21, 22).

Reoviruses also infect by the respiratory tract and have been used as a murine model to characterize ARDS (134, 135). However, studies examining the viral determinants and mechanisms that regulate reovirus replication and systemic dissemination after respiratory infection are limited. Reovirus strains differ in their capacity to replicate in rat lungs and studies using reassortant viruses show that the S1 gene regulates this difference (67, 153). The S1 gene also impacts the recruitment of neutrophils into the lungs. In the lungs, type 1 reoviruses (T1L) replicate to higher titers but recruit fewer neutrophils than type 3 reoviruses ($T3D^F$) (67, 153). Compared to the gastrointestinal tract, the respiratory tract is relatively protease neutral in the absence of infection or pathology. It is unknown if the limited replication of $T3D^F$ in the lungs is due to cleavage of σ1 by respiratory proteases. This chapter presents the results of studies designed to develop and characterize a murine model of respiratory infection and investigate the role of the S1 gene in viral replication in the lungs and systemic dissemination.

II. Results

Prior to my thesis work, our lab had no experience with animal models of reovirus pathogenesis. During the course of my work, I established a murine

model of respiratory reovirus infection based upon the ARDS model of respiratory reovirus infection. To determine if there were differences between our murine model of reovirus infection and the established ARDS model (135), we compared viral replication and gross pathology after intranasal inoculation to results obtained in the published ARDS model of respiratory reovirus infection. We infected 4-week old CBA/J mice with 10^7 PFU of T1L virus by intranasal inoculation and analyzed viral titers in resected organs at various times post-inoculation (Fig. 3.1A). We recovered between 10^5 and 10^7 PFU of virus in the lungs between 0.1 and 1 day post-inoculation. By day 2, we recovered approximately 10^{10} PFU of T1L, which reflects 3 logs of growth over the inoculating dose. While titers recovered at early times post-inoculation were more than 2 logs lower than titers in the ARDS model at similar times post-inoculation, peak titers were similar. In our infected animals, peak titers in the lungs were achieved at day 2 post-inoculation and clearance began by day 3 post-inoculation, indicating that viral clearance occurs much earlier in our model. Together, these results reveal that there are some differences between our model of respiratory reovirus infection and the published ARDS model.

Experimental animals were also monitored for signs of clinical disease. The ARDS model is characterized by a significant morbidity and mortality, with greater than 60% of mice moribund by day 10 post-inoculation (135). In sharp contrast, mice in our model were as physically active as sham-infected (saline

Fig. 3.1. Characterization of a murine model reovirus infection. CBA/J mice (4 weeks-old) were inoculated intranasally with 1 x 10^7 PFU T1L virions. Organs were resected at indicated times post-inoculation. (A) Viral titers in the lungs were determined by plaque assay on L929 cells. Results are expressed as a mean of viral titers for 6 to 12 mice per time point. Error bars indicate standard errors of the means (SEM). (B-K) Four week-old CBA/J mice were infected as described for panel A. (B-H) Gross pathology of lungs (B) 0.5, (C) 1, (D) 2, (E) 5, (F) 7, (G) 14 days post-inoculation or (H) 2 days post-inoculation of saline control. (I-K) At (I) 0.5, (J) 1, and (K) 2 days post-inoculation with T1L virions, lungs were isolated, sectioned and stained with antiserum directed against the reovirus nonstructural protein μNS. Viral antigen was detected using a horseradish peroxidase-linked secondary antibody and diaminobenzidine, and slides were counterstained with hematoxylin. Representative sections are shown. Specificity of the staining was determined from control slides, which included infected lung sections incubated with pre-immune serum and uninfected lung sections incubated with μNS-specific antiserum (data not shown).

Fig. 3.1

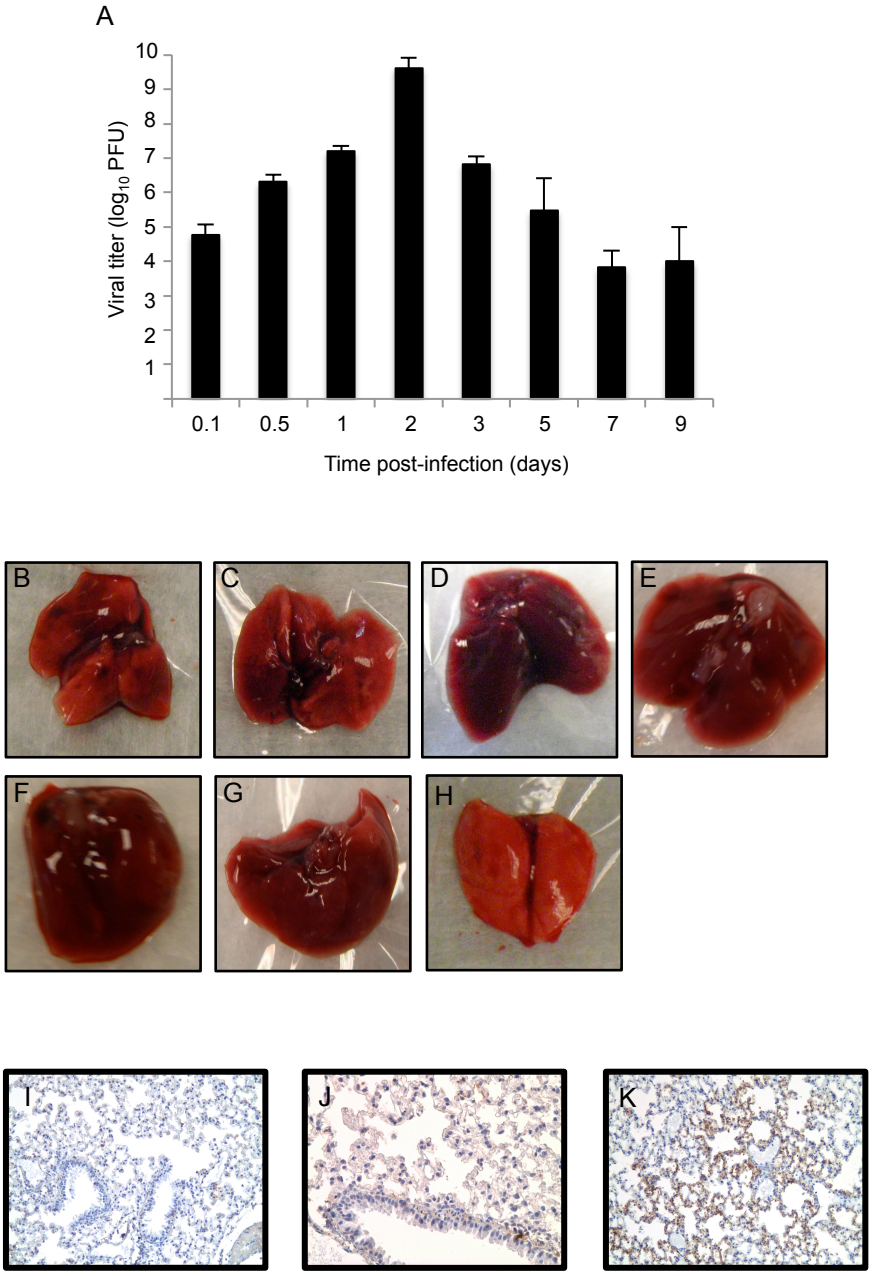
A
Viral titer (log_{10} PFU)
10
9
8
7
6
5
4
3
2
1
0.1
0.5
1
2
3
5
7
9
Time post-infection (days)
B
C
D
E
F
G
H
I
J
K

control) animals, and no net loss of weight was noted. We observed animals out to 14 days post-inoculation and never observed either morbidity or mortality. While we did not detect overt signs of clinical disease in our model of respiratory infection, gross observation of the lungs of reovirus-infected mice demonstrated dramatic increased areas of hemorrhage compared to saline controls (Fig. 3.1H). Gross pathology revealed spotty areas of hemorrhage at 0.5 and 1 day post-inoculation (Fig. 3.1B, C); lungs contained numerous hemorrhages by days 2-7 (Fig. 3.1D-F). At 14 days post-inoculation, we observed fewer lung hemorrhages, suggesting the tissues were undergoing repair (Fig. 3.1G). We observed viral replication in type 1 alvelolar cells and alveolar monocytes (Fig. 3.1I-K). Immunohistochemistry revealed evidence of new viral replication (μNS staining) by day 2 post-inoculation in reovirus-infected mice (Fig. 3.1K). Although the pathological consequences of infection were similar in our model of reovirus infection and the rat model (153), our murine model of respiratory reovirus infection results in significantly less viral induced pathology than the murine ARDS model of infection.

Studies in the rat model suggested that the S1 gene is a major determinant of viral replication in the respiratory tract (153). We sought to determine if the S1 gene also regulates replication in the lungs in our murine model of respiratory infection. We infected mice intranasally with the single-gene reassortant viruses, 1HA3 and 3HA1. Reassortant virus 1HA3, which has a T1L

Fig. 3.2. Role of reovirus S1 gene in respiratory replication and dissemination in a murine model. CBA/J mice (4 weeks-old) were inoculated intranasally with 1 x 10^7 PFU 3HA1 or 1HA3 virions. Organs were resected at indicated times post-inoculation. Viral titers in the (A) lungs and (B) spleen were determined by plaque assay on L929 cells. Results are expressed as viral titer for each mouse examined.

Fig. 3.2

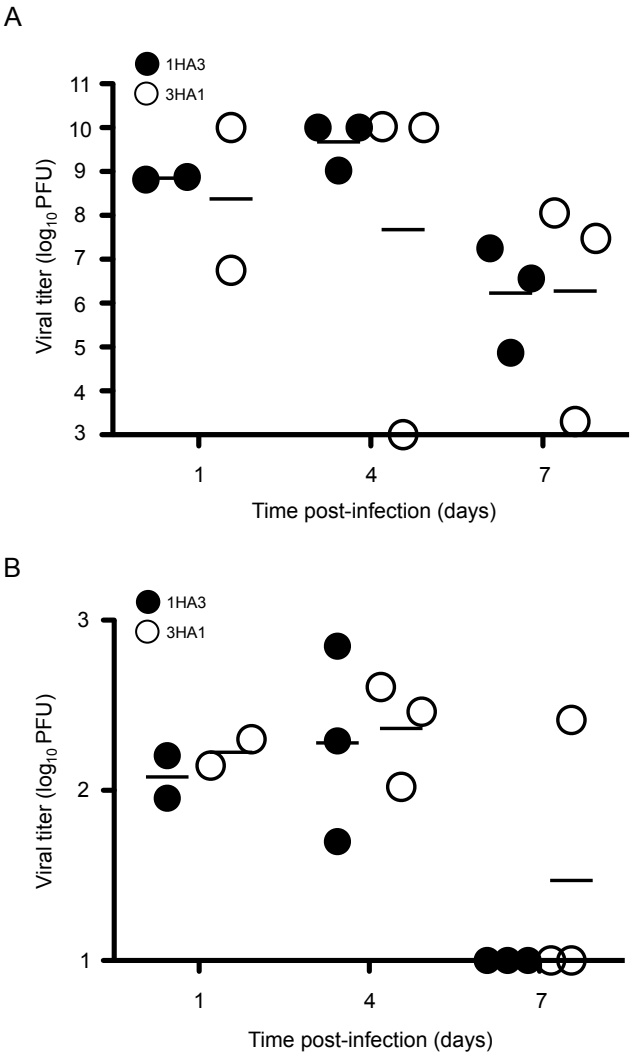
A
1HA3
3HA1
Viral titer (log_{10} PFU)
11
10
9
8
7
6
5
4
3
1
4
7
Time post-infection (days)
B
1HA3
3HA1
Viral titer (log_{10} PFU)
3
2
1
1
4
7
Time post-infection (days)

background with the S1 gene of T3D, replicated to similar titers in the lungs as reassortant virus 3HA1, which has a T3D background with the S1 gene of T1L (Fig. 3.2A). We recovered over 10^8 PFU of virus at day 1 and almost 10^{10} PFU by day 4 after inoculation with either virus (Fig. 3.2A). The rate of viral clearance after inoculation with either 3HA1 or 1HA3 also appeared to be equivalent at day 7 post-inoculation. Although Morin et al. did not examine reovirus spread after respiratory viral infection in the rat model, we quantified viral dissemination after inoculation with 3HA1 and 1HA3 and found no significant difference between viral loads in the spleen (Fig. 3.2B). Both 1HA3 and 3HA1 were recovered in the spleen at days 1 and 4 post-inoculation (Fig. 3.2B). Virus appeared to clear by day 7 post-inoculation in all mice inoculated with 1HA3 and in 2 of 3 mice inoculated with 3HA1 (Fig. 3.2B). These results suggest that the S1 genes in reassortant viruses 1HA3 and 3HA1 do not regulate reovirus replication in or dissemination from the murine respiratory tract.

Given that these same reassortant viruses had been used to associate the S1 gene with pathogenesis in the murine gastrointestinal tract and the respiratory tract of rats (110, 153), we considered that our failure to detect an S1 gene effect on respiratory replication could be due to other genetic changes that had occurred in our stocks (110, 153). To confirm our findings, we used plasmid-based reverse genetics (119, 120) to engineer a recombinant virus with 9 gene segments from $T3D^F$ and the S1 gene from T1L (Fig. 3.3A). We first asked

Fig. 3.3. Analysis of viral replication in the gastrointestinal tract and systemic dissemination of murine reoviruses generated by reverse genetics. (A) Reverse genetics system adapted from Kobayashi and colleagues (119). Cloned cDNAs representing each of the 10 full-length reovirus RNA gene segments are flanked by the bacteriophage T7 RNA polymerase promoter (T7P) and hepatitis delta virus (HDV) ribozyme (Rib). The ten reovirus cDNA constructs are transfected into BHK cells expressing T7 RNA polymerase. Transfected cells are incubated for up to 5 days and lysed by freeze-thaw. Viable viruses rescued from cloned cDNAs were isolated, purified, and titered on murine L929 cells. (B,C) CBA/J mice (3 weeks-old) were inoculated intragastrically with 1 x 10^8 PFU of T1L, $T3D^F$ or rs3HA1 virions. Organs were resected at indicated times post-inoculation. Viral titers in the (B) intestine and (C) spleen were determined by plaque assay on L929 cells. Results are expressed as viral titer for each mouse examined.

Fig. 3.3

A

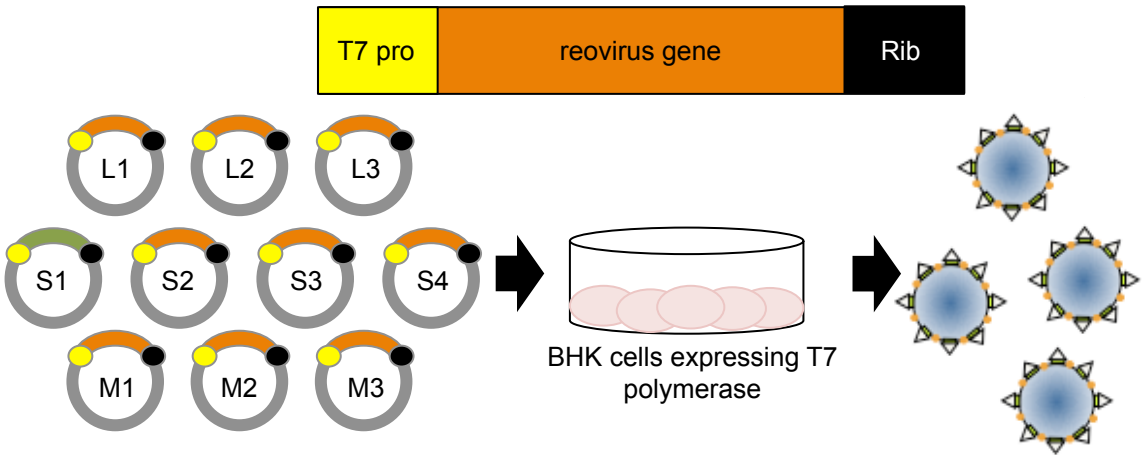
T7 pro
reovirus gene
Rib
L1
L2
L3
S1
S2
S3
S4
M1
M2
M3
BHK cells expressing T7 polymerase

B

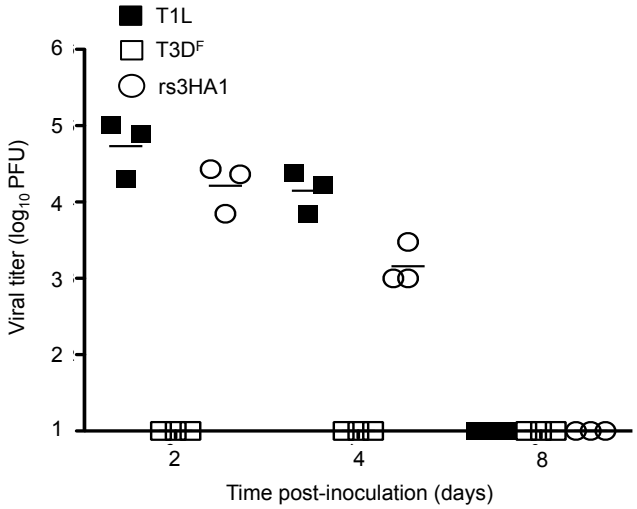
T1L
T3D^F
rs3HA1
Viral titer (log10 PFU)
Time post-inoculation (days)

C

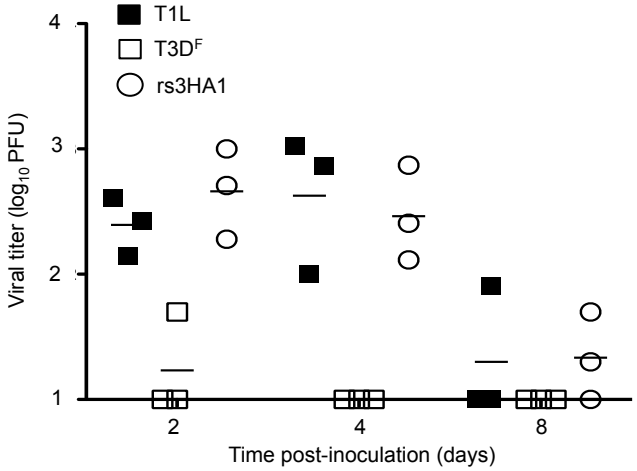
T1L
T3D^F
rs3HA1
Viral titer (log10 PFU)
Time post-inoculation (days)

whether this virus (rs3HA1), like T1L and the reassortant 3HA1, had the capacity to replicate in the gastrointestinal tract. We inoculated young mice intragastrically with 10^8 PFU of T1L, $T3D^F$ or rs3HA1 and quantified viral load in the gastrointestinal tract and spleen. As expected, we recovered high titers of T1L at day 2 and 4 post-inoculation, but $T3D^F$ was not recovered in the gastrointestinal tract (Fig. 3.3B). Inoculation with rs3HA1 resulted in 5 logs of growth by 2 days post-inoculation (Fig. 3.3B). Titers of rs3HA1 in the gastrointestinal tract were modestly lower than T1L titers at day 4 post-inoculation and both viruses were cleared from the gastrointestinal tract by day 8 post-inoculation (Fig. 3.3B). We also quantified systemic dissemination after intragastric inoculation. We found that reovirus strain $T3D^F$ failed to spread systemically while T1L and rs3HA1 spread efficiently (Fig. 3.3C). We recovered more than 10^2 PFU of virus in the spleen after inoculation with either T1L or rs3HA1 (Fig. 3.3C). These results demonstrate that the engineered rs3HA1 has phenotypes that are similar to the well-characterized reassortant virus 3HA1 after intragastric inoculation.

We then used this engineered virus to determine if the T1L S1 gene contributes to viral replication in our model of respiratory reovirus infection. We inoculated mice intranasally with T1L, $T3D^F$ or rs3HA1 and assessed viral loads in the lungs. At 1 day post-inoculation, mice inoculated with reovirus strain T1L had viral loads a log greater than mice inoculated with $T3D^F$ (Fig. 3.4A). The engineered virus rs3HA1 was recovered at titers similar to $T3D^F$ at 1 day post-

Fig. 3.4. Analysis of strain specific differences in reovirus capacity to replicate and disseminate after respiratory infection. CBA/J mice (4 weeks-old) were inoculated intranasally with 1 x 10^7 PFU of T1L, $T3D^F$ or rs3HA1 virions. Organs were resected at indicated times post-inoculation. Viral titers in the (A) lungs and (B) spleen were determined by plaque assay on L929 cells. Results are expressed as viral titer for each mouse examined.

Fig. 3.4

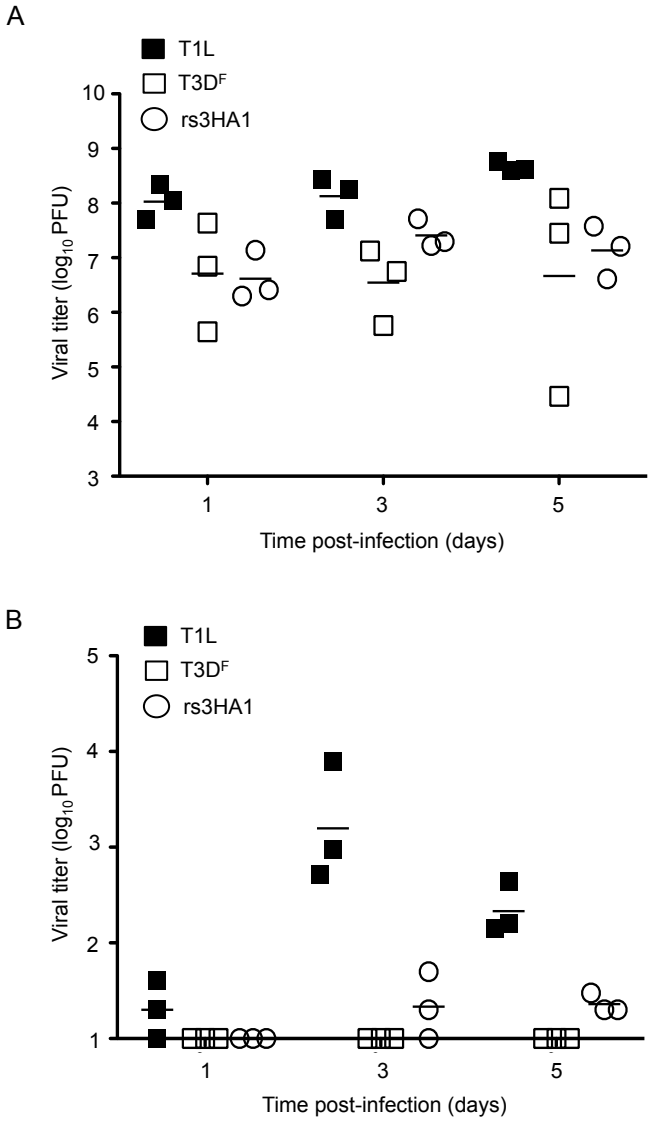
A
T1L
T3D^F
rs3HA1
Viral titer (log10 PFU)
10
9
8
7
6
5
4
3
1
3
5
Time post-infection (days)
B
T1L
T3D^F
rs3HA1
Viral titer (log10 PFU)
5
4
3
2
1
1
3
5
Time post-infection (days)

inoculation, however by day 3, rs3HA1 was recovered at modestly higher titers than $T3D^F$ in the lungs (Fig. 3.4A). Peak titers in the lungs also differed between the strains, T1L reached 10^9 PFU while both $T3D^F$ and rs3HA1 peak titers were 2 logs lower than T1L (Fig. 3.4A). While this result contrasts with findings from the rat model (153), it is consistent with our earlier finding (Fig. 3.2) that the S1 gene does not significantly impact viral replication in the murine respiratory tract.

Prior to my thesis work, no one had examined the genetic regulation of systemic dissemination after respiratory reovirus infection. Using S1 gene mono-reassortant viruses, we found no significant difference in systemic dissemination after intranasal inoculation. To confirm that the T1L S1 gene does not significantly enhance systemic reovirus dissemination, we assessed the capacity of reovirus strains T1L, $T3D^F$ and rs3HA1 to spread from the murine respiratory tract. One day post-inoculation, we recovered infectious virus in the spleen from mice inoculated with T1L and by day 3 post-inoculation T1L titers in the spleen reached a peak titer of 10^3 PFU (Fig. 3.4B). Virus was not recovered in the spleen at any time point after intranasal inoculation with $T3D^F$ (Fig. 3.4B). These results indicate that, while T1L efficiently disseminates systemically after intranasal inoculation, $T3D^F$ does not gain access to routes for systemic dissemination. We recovered rs3HA1 in 2 out of 3 mice at day 3 post-inoculation and 3 out of 3 mice at day 5 post-inoculation (Fig. 3.4B). However, the titers of rs3HA1 in the spleen were significantly lower than titers of T1L. These results

indicate that the S1 gene enhances reovirus dissemination from the respiratory tract, but that other genes contribute to dissemination and replication in secondary organs.

III. Discussion

Experiments described in this chapter characterize the murine respiratory model of reovirus infection developed during my thesis work. This model differs in several ways from the published ARDS model of respiratory reovirus infection. In our model, we observe neither mortality nor significant morbidity after intranasal inoculation with 10^7 PFU of T1L. The rate of viral replication is less rapid and virus is cleared from the lungs more rapidly. We did observe significant gross pathology (Fig. 3.1B-H) and histological evidence (Fig. 3.1I-K) of patchy edema, characteristic of viral pneumonia and cellular infiltration. These differences may stem from slight modifications in the inoculation protocol and/or sequence polymorphisms in viral stocks. In addition, our anesthesia protocol differs from the protocol utilized by London and colleagues (REF). We anesthetized mice by isoflurane treatment, which is a more shallow form of anesthesia than intraperitoneal injection of ketamine/acepromazine , but results in recovery that is more rapid. This may cause more swallowing of inoculum, which would result in a decrease in the inoculating dose in the lungs. Sequence polymorphisms can also result in significant differences in reovirus-mediated pathology. While it is known that the sequences of a number of the genes of

reovirus stocks differ between laboratories, we do not know if any of these changes contribute to differences observed in our model of respiratory reovirus infection.

The role of the S1 gene in viral replication and systemic dissemination is well-established from studies of reovirus infection of the gastrointestinal tract in mice (19, 21, 22, 110). We sought to characterize the role of the S1 gene in replication and systemic dissemination in our murine model of respiratory reovirus infection. In a pilot study, we found no difference in viral load in the lungs or spleens in mice inoculated with reassortant viruses, 3HA1 and 1HA3 (Fig. 3.2A). Since reassortant viruses 3HA1 and 1HA3 were generated with temperature-sensitive mutagenized stocks, and have significant genetic polymorphisms compared to the T3D and T1L viruses being used today, we used the reverse genetics system to engineer a virus with 9 $T3D^F$ gene segments and a T1L S1 gene, rs3HA1 (119) (Fig. 3.3A). As a control, we inoculated mice intragastrically and quantified titers of this engineered virus in the intestine and spleen. Consistent with studies that demonstrated that the reassortant virus 3HA1, like T1L, is resistant to protease-mediated inactivation and can replicate in and spread systemically from the gastrointestinal tract (110, 160). We found that rs3HA1 replicated to similar high titers as T1L in the gastrointestinal tract and disseminates systemically (Fig. 3.3B,C). This confirms that the T1L S1 gene

promotes replication and dissemination after peroral inoculation of newly weaned mice.

After intranasal inoculation in our murine model, we found that reovirus strains T1L and $T3D^F$ differ in their capacity to replicate in the murine respiratory tract (Fig. 3.4A). By immunohistochemistry we found evidence that both $T3D^F$ and T1L replicate in alveolar cells in the murine lungs, although expression of the nonstructural protein, μNS, was more abundant after inoculation with T1L (data not shown). Viral loads in the lungs after rs3HA1 inoculation were more similar to viral loads after $T3D^F$ infection (Fig. 3.4A). Thus, the T1L S1 gene does not appear to enhance viral titers in the murine lungs as significantly as in the rat lungs or murine gastrointestinal tract. This suggests that other reovirus genes may significantly influence viral replication in the murine respiratory tract. Interesting recent work revealed that the T1L M1 gene (μ2 protein) inhibits IFN-β signaling and significantly enhances viral replication of a recombinant T3D virus in cardiac myocytes and fibroblasts (102). In future studies, it would be interesting to investigate a possible contribution of the M1 gene to replication in the respiratory tract.

Our results demonstrate that $T3D^F$ cannot disseminate systemically after replication in the respiratory tract (Fig. 3.4B). A $T3D^F$ virus with a T1L S1 gene, rs3HA1, was capable of systemic dissemination as it was recovered in the spleen

in 5 of 9 mice examined after intranasal inoculation (Fig. 3.4B). However, titers recovered in the spleen after rs3HA1 inoculation was significantly lower than titers recovered after intranasal inoculation of T1L. This result suggests that the T1L S1 gene promotes viral dissemination, but other genes may play a significant role in reovirus capacity to disseminate or replicate at secondary sites. Results from studies described in this chapter form the foundation for more in depth studies in Chapters 4 and 5 of my thesis that characterize the molecular and genetic determinants of reovirus infection and systemic dissemination.

CHAPTER 4

Impact of Host Proteases on Reovirus Infection in the Respiratory Tract

I. Introduction

Mammalian orthoreovirus (reovirus) entry into cells is characterized by the step-wise disassembly of virions into two functional subvirion particles, a membrane penetration competent infectious subvirion particle (ISVP) and a transcriptionally active core (36). In cell culture, entry is initiated by attachment of the viral protein σ1 (123) to a cell surface carbohydrate (8, 38, 81) and junctional adhesion molecule A (9). Virions are then internalized by β1 integrin-mediated endocytosis (26, 64, 139, 140). Within the endocytic compartment, host proteases remove the outer capsid protein σ3, exposing the membrane penetration protein, μ1 (4, 56, 212). In murine fibroblasts, virion disassembly is mediated by the acid-dependent cysteine proteases, cathepsins (Cats) L and B (4, 5, 63). In immune cells, acid-independent proteases, including Cat S and neutrophil elastase, can promote virion uncoating (84, 86).

After oral inoculation of newborn mice, reovirus virions are rapidly uncoated in the enteric tract by the secreted pancreatic serine proteases chymotrypsin (CHT) and trypsin (10, 20). Extracellular uncoating is required for reovirus adherence to Peyer's patch M cells and subsequent entry into intestinal tissue (3). In humans and animals, reoviruses are also associated with pulmonary infections (13, 43,

135, 153), but little is known about the proteases that mediate virion uncoating when infection is initiated by this route. This chapter presents the results of studies designed to investigate the role of inflammatory and endogenous respiratory proteases in reovirus infection.

II. Results

Type II transmembrane serine proteases (TTSPs) expressed in the human airway have been shown to activate membrane fusion and promote cell entry of a number of respiratory pathogens, including influenza virus, human metapneumovirus and SARS coronavirus (15, 16, 28, 29, 33, 83, 202, 204, 206). To assess the capacity of a respiratory TTSP to promote reovirus uncoating, we incubated purified reovirus T1L virions with human airway trypsin-like protease (HAT) and analyzed the products by SDS-PAGE (Fig. 4.1A). After 6 hours (h) of treatment, only 2% of the outer capsid protein σ3 remained associated with virions, as determined by NIH Image J quantitation. The particles resembled ISVPs generated by pancreatic serine proteases (24) although HAT-treatment did not lead to significant cleavage of the underlying capsid protein μ1C, as does treatment with CHT. To assess the infectivity of the HAT-treated subviral particles (HAT-SVPs) and determine if they require additional intracellular proteolysis, we measured viral yields in cultures of L929 mouse fibroblasts that were untreated or treated with the broad-spectrum cysteine protease inhibitor E-64 for 3 h prior to infection. E-64 inhibits Cats L and B, which mediate virion

Fig. 4.1. Effect of type II transmembrane serine proteases on reovirus virions and infectivity. (A) Reovirus T1L virions (5×10^{10}) in VDB (150 mM NaCl, 10mM $MgCl_2$, 10 mM Tris [pH 7.5]) were incubated with 21 μg/mL of purified HAT (R&D Systems) for the indicated time. Reactions were stopped with 5 mM benzamidine. The mock sample (M) consisted of virions held in reaction buffer in the absence of protease for 23 h. Treated particles were analyzed by SDS-12% polyacrylamide gels and proteins were visualized by Coomassie staining. The positions of reovirus capsid proteins are labeled. (B) L929 cells were untreated (white bars) or pretreated for 3 h with 300 μM E-64 (black bars) and infected with T1L virions, CHT-ISVPs, or HAT-SVPs at a multiplicity of infection (MOI) of 5 plaque forming units (PFU)/cell. Infections were carried out in the presence or absence of E-64 and terminated at 1 day post-infection. Viral yields were determined by plaque assay on L929 cells. Values represent the mean (+/- SE) of triplicate samples. (C) Vero cell cultures were transfected with HAT, TMPRSS2, or HSV ICP22 expression plasmids 30 h prior to infection with reovirus T1L virions or CHT-ISVPs (MOI 10 PFU/cell). At 18 h post-infection, cells were fixed and permeabilized with 4% paraformaldehyde. Indirect immunofluorescence was used to detect expression of the reovirus nonstructural protein σNS and the presence of the FLAG-tagged protease or control protein. Cells were counterstained with Hoechst to facilitate quantification. Reovirus-infected and transfected cells were quantified by counting fluorescent cells in a minimum of three fields in each of 3 independent experiments. Between 85 and

150 cells were counted per field. Data are presented as the percent of cells expressing σNS relative to the number of FLAG-positive cells in the field.

Fig. 4.1

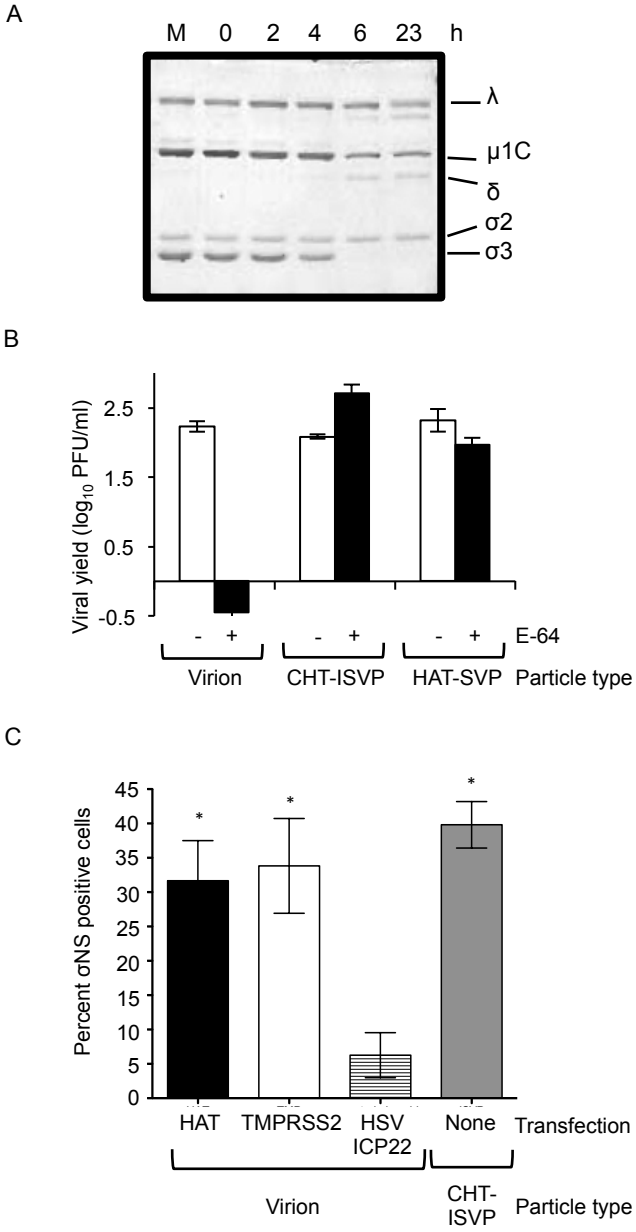
A
M 0 2 4 6 23 h
λ
μ1C
δ
σ2
σ3
B
Viral yield (log_{10} PFU/ml)
2.5
1.5
0.5
-0.5
- + - + - +
E-64
Virion
CHT-ISVP
HAT-SVP
Particle type
C
Percent σNS positive cells
45
40
35
30
25
20
15
10
5
0
*
*
*
HAT
TMPRSS2
HSV ICP22
None
Transfection
Virion
CHT-ISVP
Particle type

disassembly in L929 cells. As expected, E-64 treatment inhibited virion infection in L929 cells, whereas CHT-generated ISVPs (CHT-ISVPs), which lack the capsid protein σ3, replicated to high yields (Fig. 4.1B). Like CHT-ISVPs, HAT-generated subviral particles replicated to high yields in the presence and absence of the protease inhibitor. These results indicate that the respiratory protease HAT can productively uncoat reovirus virions.

We used an additional approach to test whether HAT and a second TTSP, TMPRSS2, could promote reovirus infection. Vero cells, which are permissive for reovirus infection but do not support efficient virion disassembly (85), were transfected with FLAG-tagged protease expression plasmids (28) or a similarly tagged control plasmid (11). Thirty h after transfection, the cultures were infected with reovirus virions. At 18 h post-infection, cells were fixed and analyzed for evidence of viral replication and expression of the FLAG antigen (Fig. 4.1C). In the transfected cultures, expression of either HAT or TMPRSS2 led to a significant increase in the number of reovirus-infected cells, whereas expression of the FLAG-tagged herpes simplex virus protein ICP22 from the control plasmid did not. In protease gene-transfected cultures, levels of infection were comparable to those in mock-transfected cultures that had been infected with CHT-ISVPs (Fig. 4.1C). When we compared infection by CHT-ISVPs in cultures expressing TTSPs and in control-transfected cultures, we found no significant difference in σNS expression in these samples (data not shown). Together, our

results reveal that endogenous respiratory TTSPs are capable of productively uncoating reovirus virions *in vitro* and of promoting infection in cell culture.

In vivo, HAT and TMPRSS2 are expressed on the membrane of bronchiolar epithelial cells (16, 41, 58, 145, 213) and have murine homologues, MAT and epitheliasin (90, 105). However the activity of these and other respiratory proteases is balanced by the presence of locally produced protease inhibitors (80). To assess the efficiency of reovirus uncoating in the respiratory tract, we used a murine respiratory model (135) to compare viral loads after infection with virions or ISVPs. Four week-old CBA/J mice were inoculated intranasally (13, 153) with T1L virions or ISVPs. Organs were harvested at various times post-inoculation, and viral titers were determined by plaque assay on L929 cells. We observed equivalent lung titers at early times (12 h) following infection with virions or ISVPs (Fig. 4.2A), likely reflecting the inoculum. However, by 24 h post-inoculation, we recovered significantly higher titers in the lungs of ISVP-infected animals. Titers from the lungs of virion-infected animals increased more slowly. Peak lung titers in ISVP-infected animals were over a log greater than peak lung titers in virion-infected animals. Immunohistochemistry of lung samples taken at 24 h post-inoculation from both virion- and ISVP-infected animals revealed type-1 alveolar pneumocytes and monocytes expressing the reovirus nonstructural protein μNS (evidence of viral replication), although we observed many more μNS positive cells in the lungs of ISVP-infected animals

Fig. 4.2. Comparative analysis of reovirus infection in the respiratory tract after intranasal inoculation with virions or ISVPs. CBA/J mice (4 weeks-old) were inoculated intranasally with 1 x 10^7 PFU T1L virions or CHT-ISVPs. Organs were resected at indicated times post-inoculation, and viral titers in the lungs (A) and spleen (C) were determined by plaque assay on L929 cells. Results are expressed as a mean of viral titers for 6 to 12 mice per time point. Error bars indicate standard errors of the means (SEM). *, $P < 0.05$ (as determined by the Mann Whitney test). (B) At 24 h post-inoculation, lungs were isolated, sectioned and stained with antiserum directed against the reovirus nonstructural protein μNS. Viral antigen was detected using a horseradish peroxidase linked secondary antibody and diaminobenzidine, and slides were counterstained with hematoxcylin. Representative sections are shown and arrows point to some of the antigen-positive cells in the virion infected sample. Specificity of the staining was determined from control slides, which included infected lung sections incubated with pre-immune serum and uninfected lung sections incubated with μNS-specific antiserum (data not shown).

Fig. 4.2

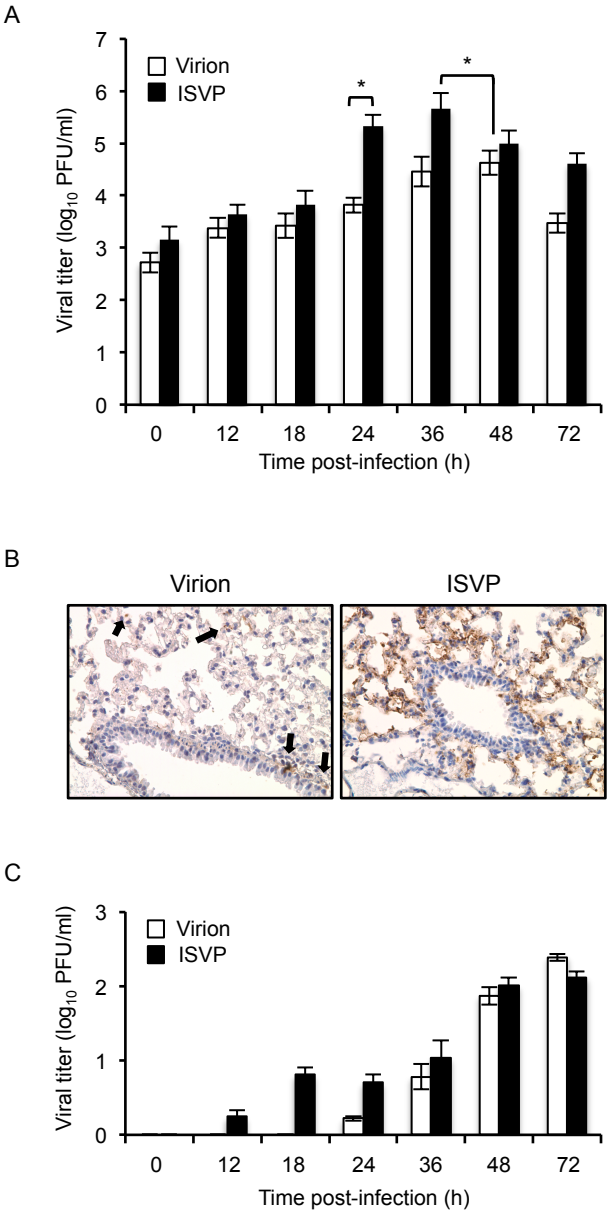
A
Virion
ISVP
*
*
Viral titer (log10 PFU/ml)
0
1
2
3
4
5
6
7
0
12
18
24
36
48
72
Time post-infection (h)
B
Virion
ISVP
C
Virion
ISVP
Viral titer (log10 PFU/ml)
0
1
2
3
0
12
18
24
36
48
72
Time post-infection (h)

(Fig. 4.2B). These data suggest that while endogenous respiratory proteases can productively uncoat reovirus virions *in vitro*, they do not do so efficiently in the murine respiratory tract.

To determine how the kinetics of replication in the respiratory tract impact dissemination, we analyzed viral titers in spleen after intranasal infection with virions or ISVPs (Fig. 4.2C). Virus was detected as early as 12 h post-inoculation in spleen samples from the ISVP-infected animals. At 24 h post-inoculation, virion-infected animals began to show evidence of viral spread and by 36 h post-inoculation there was no significant difference between the samples. We considered the possibility that early spread in the ISVP-infected animals reflected more rapid drainage of the inoculum, but the virus recovered in the spleen samples was E-64 sensitive, arguing that it represents progeny virions (data not shown). Because mice infected intranasally can swallow some of the inoculum, we measured virus in the intestines at early time points. Recovered titers varied broadly between animals (data not shown). While this virus could contribute to the observed spread in our intranasally infected animals, Kauffman and colleagues detected less than half a log of spread to the spleen 24 h after direct intragastric inoculation of 10^8 PFU T1L virions in similarly aged mice (110). Together, these data suggest that efficient replication of ISVPs in the lung leads to more rapid dissemination.

While studies in the murine enteric tract have shown that reovirus virions are converted to ISVPs within minutes after oral inoculation (20), our data suggest that the endogenous respiratory proteases in the lung do not rapidly convert virions to ISVPs. However, the balance of proteases and protease inhibitors in the respiratory tract can be impacted by inflammation (2, 52, 151, 174, 184, 238). Inflammatory cells, recruited to sites of infection or pathology, release a variety of microbicidal products (51, 57, 127). Serine proteases are expressed as components of this response (80), and our laboratory has previously shown that one such protease, NE, can promote reovirus infection in cell culture (86). Using the *in vitro* uncoating assay, we investigated the capacity of two other inflammatory proteases, Cat G (expressed by neutrophils) and mast cell chymase, to uncoat reovirus virions. We found that chymase mediated rapid virion disassembly, with almost all σ3 disappearing after 0.5 h (Fig. 4.3A). The kinetics of σ3 removal from virions treated with Cat G (Fig. 4.3B) was not as rapid, but by 5 h, particles had lost 70% of σ3, and the underlying μ1C protein had been cleaved to the characteristic δ fragment. When we used the chymase- and Cat G-SVPs particles in single cycle growth experiments in E-64-treated L929 cells, we found that they were infectious in the absence of cysteine protease activity (Fig. 4.3C). The finding that HAT- and chymase-SVPs with uncleaved μ1C replicate to high yields in E-64-treated cells supports other published work which suggests that cleavage of μ1C to yield the δ and φ fragments is not essential for reovirus infection in cell culture (36).

Fig. 4.3. Analysis of the effects of inflammatory proteases on reovirus virions and pathogenesis in the murine respiratory model. (A, B, and C) Reovirus T1L virions (5×10^{10}) were incubated with 50 μg/mL purified (A) chymase (Calbiochem) or 25 μg/mL purified (B) Cat G (Calbiochem) in VDB for the indicated times. Reactions were stopped with 5 mM benzamidine. The mock sample (M) consisted of virions held in reaction buffer in the absence of protease for 5 h. Treated particles were analyzed by SDS-12% polyacrylamide gels and proteins were visualized by Coomassie staining. The positions of reovirus capsid proteins are labeled. (C) L929 cells were untreated (white bars) or pretreated for 3 h with 300 μM E-64 (black bars) and infected with T1L virions, CHT-ISVPs, Cat G-SVPs or chymase-SVPs at an MOI of 5 PFU/cell. Infections were carried out in the presence or absence of E-64 and terminated at 1 day post-infection. Viral yields were determined by plaque assay on L929 cells. Values represent the mean (+/- SE) of triplicate samples.

Fig. 4.3

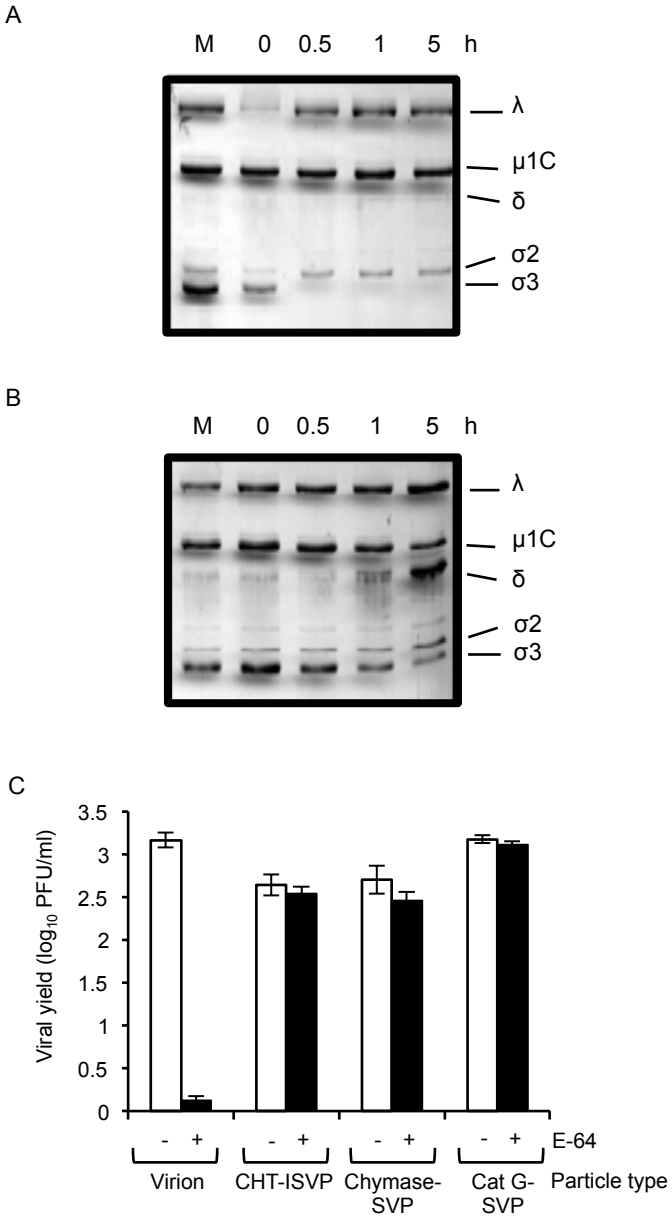
A
M 0 0.5 1 5 h
λ
μ1C
δ
σ2
σ3
B
M 0 0.5 1 5 h
λ
μ1C
δ
σ2
σ3
C
Viral yield (log10 PFU/ml)
3.5
3
2.5
2
1.5
1
0.5
0
- + - + - + - + E-64
Virion
CHT-ISVP
Chymase-SVP
Cat G-SVP
Particle type

Since our results demonstrated that inflammatory proteases NE (86), Cat G and chymase mediated productive reovirus uncoating, we hypothesized that lung injury or induction of inflammation would potentiate reovirus infection in the lungs by promoting virion uncoating. To test this we pretreated mice intranasally with lipopolysaccharide (LPS) or UV-inactivated T3D reovirus for 24 h to induce inflammation (68, 115, 118, 192). Treated and control mice were then inoculated with T1L reovirus virions and virus was quantified from lung tissue 24 h after infection. In animals pretreated with UV-inactivated virus and LPS, we recovered significantly more virus at 24 h post-inoculation than we did from untreated animals (Fig. 4.4A). To determine if pre-existing inflammation promoted extracellular conversion of virions to ISVPs, we harvested bronchoalveolar lavage fluid (BALF) from untreated or pretreated and infected animals and used these as inocula in single cycle yield experiments in E64-treated and untreated L929 cells. In mice that had been pretreated with LPS or UV-inactivated virus, the BALF samples contained significantly more E-64-resistant (uncoated) virus (Fig. 4.4B), consistent with our hypothesis. To determine the extent to which the pretreatments caused infiltration of inflammatory cells that might also serve as target cells, we quantified the influx of neutrophils and monocytes using Cytospin preparations of the BALF collected 8 h after treatment (Fig. 4.4C). Pretreatment with LPS resulted in the greatest increase in neutrophils; significant numbers of monocytes were recruited to the lungs after treatment with either LPS or UV-inactivated virus. It was notable that the control treatment (saline) also resulted in

Fig. 4.4. Analysis of the effects of pre-existing inflammation on reovirus virions and pathogenesis in the murine respiratory model. (A) Four week-old CBA/J mice were untreated or treated intranasally with 1.5 mg LPS, 1.7 x 10^9 UV-inactivated T3D virions or saline 24 h prior to intranasal infection with 1 x 10^7 PFU reovirus T1L virions. One day post-inoculation, lungs were harvested and viral titers determined by plaque assay on L929 cells. (B and C) Four week-old CBA/J mice were untreated or treated and infected as described for panel D. Eight h post-inoculation, BALF was harvested from infected mice. (B) Virus was released from half of the BALF sample by three cycles of freezing and thawing. The presence of uncoated particles and the relative levels of virus were assessed by using the BALF in single cycle growth experiments. L929 cells were pretreated or not with E-64 for 3 h and then infected with 100 µl of BALF. Viral yields were determined by plaque assay on L929 cells 1 day post-infection. (C) Neutrophils and monocytes in the BALF were quantified by cytospin analysis and hemotoxylin and eosin staining. Error bars indicate SEM. *, $P < 0.05$; ** $P < 0.01$; *** $P < 0.001$ (as determined by the Mann Whitney test).

Fig. 4.4

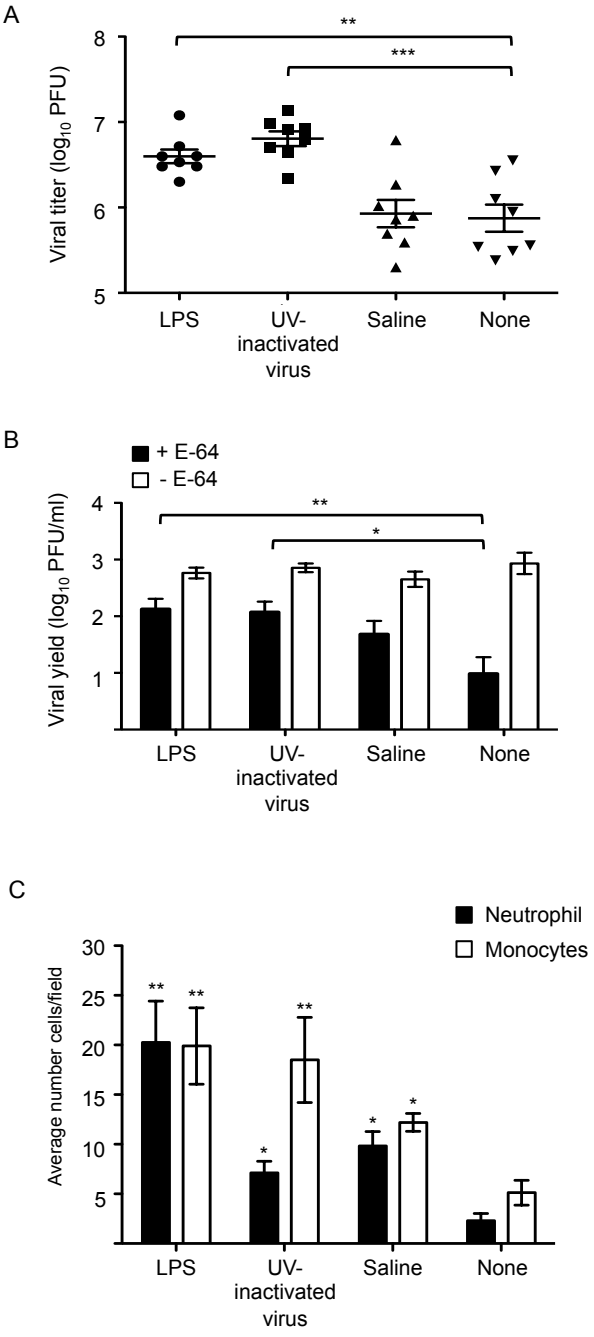
A
Viral titer (log_{10} PFU)
8
7
6
5
**
***
LPS
UV-inactivated virus
Saline
None
B
+ E-64
- E-64
Viral yield (log_{10} PFU/ml)
4
3
2
1
**
*
LPS
UV-inactivated virus
Saline
None
C
Neutrophil
Monocytes
Average number cells/field
30
25
20
15
10
5
**
**
*
**
*
*
LPS
UV-inactivated virus
Saline
None

an influx of inflammatory cells relative to untreated animals, however levels were significantly lower than in mice pretreated with LPS or UV-inactivated virus, and they did not correlate with a significant increase in ISVPs in the BALF. Together, our findings reveal that pre-existing inflammation in the lungs promotes reovirus uncoating in the respiratory lumen and results in the infiltration of potential target cells. These factors likely contribute to the increases in viral load in mice with pre-existing inflammation.

III. Discussion

The results of experiments described in this chapter reveal that TTSPs can uncoat reovirus virions and promote infection in cell culture (Fig. 4.1). Whether reovirus uncoating in HAT or TMPRSS2 transfected cells occurs extracellularly, at the cell membrane or intracellularly remains unknown. Böttcher-Friebertshäuser and colleagues demonstrated that influenza HA cleavage occurs at the cell membrane in HAT-expressing MDCK cells, and in intracellular compartments in TMPRSS2-expressing cells (29). Interestingly, TMPRSS2 overexpression has been associated with prostate cancer (216). Since protease-mediated uncoating is a major determinant of reovirus oncolysis (1), our results suggest that reovirus might selectively target prostate tumors that overexpress and secrete TMPRSS2.

In enteric reovirus infections, pancreatic serine proteases in the intestinal lumen rapidly convert virions to ISVPs (8). In contrast, in healthy lungs, there are few active proteases in the extracellular environment of the respiratory tract and this may impact reovirus infection. Consistent with this, we found that inoculation with uncoated particles resulted in more rapid viral replication in the lungs and systemic dissemination. We explored the capacity of inflammatory serine proteases to promote infection and found that, in addition to NE (86), Cat G and chymase were capable of mediating productive reovirus disassembly *in vitro* (Fig. 4.3).

To probe the role of specific proteases *in vivo*, we attempted to inhibit protease activity in the respiratory tract by prior intranasal inoculation of protease inhibitors (Text S4.1, Fig. S4.1). Preliminary studies suggested that the pretreatment protocol itself induced gross inflammation and slightly increased viral titers from the lung. Analysis of the cytokine response in the lungs confirmed that virions, ISVPs and UV-inactivated ISVPs induce inflammation upon inoculation in the respiratory tract (Text S4.2, Table S4.1). When we modified the model of respiratory infection to specifically induce inflammation prior to reovirus infection (by inoculation with LPS or UV-inactivated virus), we recovered a higher percentage of ISVPs in the BALF, as well as a significant infiltration of monocytes (Fig. 4.4). These animals also had significantly higher viral yields in the lungs. In contrast, prior inflammation did not promote infection when animals were

inoculated with ISVPs (data not shown). Together, these results are consistent with a model in which inflammation promotes reovirus infection through multiple mechanisms, including increased access to target cells and the presence of inflammatory proteases. Our findings may have broader implications for chronic pulmonary disease. Inflammation induced by a variety of chronic conditions, including asthma, emphysema, chronic obstructive pulmonary disease and acute respiratory distress syndrome (107, 113) may further compromise human health by providing an environment that is conducive to viral infection. Further work will be needed to address the possibility that other respiratory viruses (including influenza virus and SARS coronavirus) can also be activated by inflammatory proteases.

IV. Supplementary text

Text S4.1

Several studies in the literature report that the aerosolized pretreatment of mice with the protease inhibitor aprotinin can decrease viral titers of influenza infection (244, 245). We adapted this model and used it to try to understand the role of serine proteases in respiratory reovirus infection. We quantified viral titers after T1L inoculation of mice that had been pre-treated with aprotinin or saline intranasally (Fig. S4.1). Mice were treated at -1, 0 and +1 days relative to inoculation. As a control, we infected mice with two particle types, virions and

Fig. S4.1. Effect of serine protease inhibitor aprotinin on reovirus replication and systemic dissemination. Four week-old CBA/J mice were treated intranasally with 20 µl of saline or aprotinin (250 U) (Sigma-Aldrich) in 20 µl total volume -1 day, -20 min and +1 day post-infection. Mice were inoculated with 1 x 10^7 PFU of T1L. (A) Lungs, (B) MLN and (C) spleen were resected and organ titers were determined by plaque assay on L929 cells. Graphs represent data from a pilot experiment with 3 mice per treatment per time point.

Fig. S4.1

A

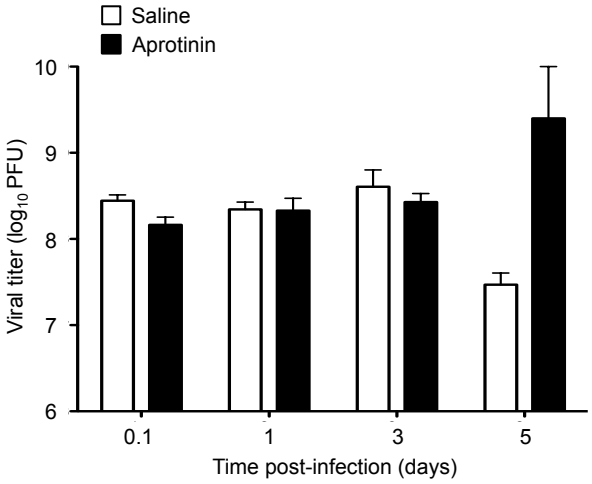
Saline
Aprotinin
Viral titer (log_{10} PFU)
10
9
8
7
6
0.1
1
3
5
Time post-infection (days)

B


Saline
Aprotinin
Viral titer (log_{10} PFU)
5
4
3
2
1
1
3
5
Time post-infection (days)

C

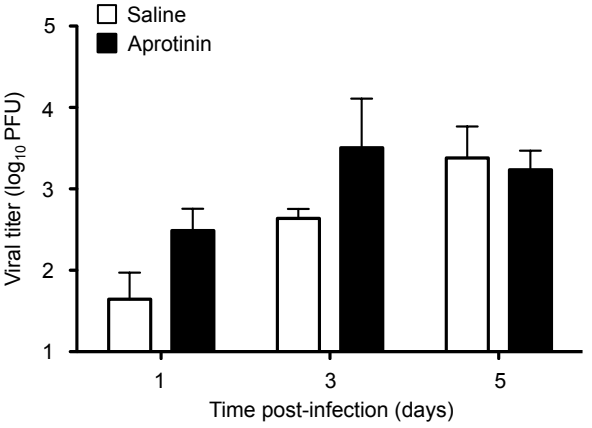
Saline
Aprotinin
Viral titer (log_{10} PFU)
5
4
3
2
1
1
3
5
Time post-infection (days)

ISVPs; ISVPs do not require active proteases for replication, and therefore we predicted that their primary replication would not be impacted by protease inhibitor treatment. As expected, treatment with aprotinin or saline resulted in little difference in viral loads in the lungs after control ISVP infection (data not shown). At early times, saline and aprotinin treatment did not significantly impact viral growth in the lungs compared to virion infection (S4.1A). Interestingly, titers recovered after virion infection in treated mice (S4.1A) were more than 5 logs greater than virion infection in untreated mice (Fig. 4.2A) at early times post-inoculation. These unexpected results suggested to us that the pretreatment protocol itself might induce inflammation that could increase extracellular conversion of virions to ISVPs and contribute to increased viral loads observed in the lungs.

We next assessed the impact of protease inhibitor treatment on viral dissemination after intranasal inoculation with reovirus virions. Protease inhibitor treatment did not significantly impact viral load in the draining lymph nodes (Fig. S4.1B), however titers in the MLN of treated mice were significantly higher than MLN titers in untreated mice (unpublished results). The increased viral load in the MLN likely reflects increased drainage due to higher viral loads in the lungs of treated mice. Viral loads in the spleen were modestly higher in mice treated with aprotinin at 1 and 3 days post-inoculation (Fig. S4.1C). Viral titers recovered in the spleen of treated mice (Fig. 4.1C) were more than a log greater than titers

recovered after virion inoculation of untreated mice at all time points examined (Fig. 4.2A). The enhanced viral load the spleen may be a result of increased access to hematogenous routes for systemic dissemination, as titers in the blood were significantly higher after infection of treated mice compared to blood titers in untreated mice (data not shown). These results are consistent with a model in which intranasal treatment with saline or aprotinin induces respiratory inflammation that promotes systemic viral dissemination.

Text S4.2

We observed significant differences in gross pathology after infection with different particle types. Gross observation of the lungs of mice inoculated with virions, ISVPs and UV-inactivated ISVPs showed dramatically increased areas of hemorrhage compared to saline control (Fig. S4.2A). Infection with replication-competent virions and ISVPs (Fig. S4.2B,C) elicited an abundance of hemorrhage while infection with replication-deficient UV-inactivated ISVPs (Fig. S4.2D) resulted in spotty hemorrhage. These results indicate that although infection with replication-competent particles induces the most severe pathology, viral replication is not required to induce hemorrhage in the lungs.

Since mice infected with virions, ISVPs and UV-inactivated ISVPs differed in gross pathology, we assessed the types of cytokines induced in our intranasal model of infection. We inoculated mice with T1L virions, ISVPs, UV-inactivated

Fig. S4.2. Analysis of gross pathology induced after intranasal inoculation of reovirus particles. Gross pathology of murine lungs 2 days after inoculation with (A) saline, (B) T1L virions, (C) T1L ISVPs, or (D) T1L UV-inactivated ISVPs.

Fig. S4.2

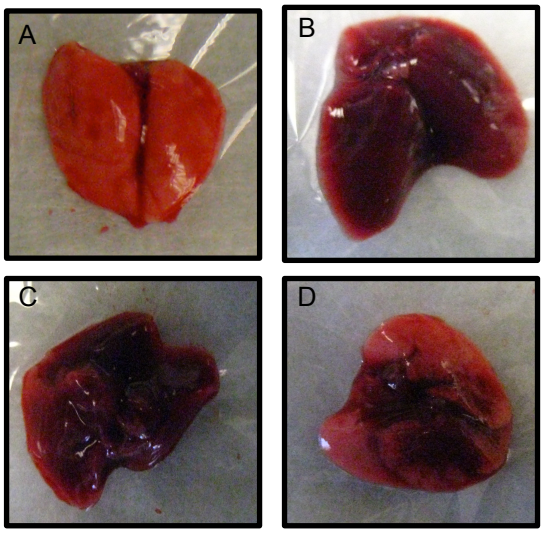

ISVPs or saline and harvested lungs at 2 days post-inoculation. Lung samples from treated mice were homogenized in gel saline and R&D systems murine proteome profiler kit was used to determine cytokine concentrations in lung samples. Inoculation with virion, ISVP or UV-inactivated ISVPs resulted in significant increases in expression of a majority of cytokines tested [IL-1ra, IL-4, IL-6, IL-7, IL-13, IL-16, IFN-gamma, M-CSF, GM-CSF, TNF-alpha, CCL1-5, CCL12, CXCL9-11, CXCL13, MIP-2, KC, C5a, TIMP-1, sICAM-1 (CD54) and TREM-1] when compared to saline treated controls (Table S4.1). These same treatments had no significant impact on the expression of IL-2, IL-3, IL-5, IL-10, IL-12, CCL11 (eotaxin) or CXCL12 (SDF-1), which are involved in activation of the adaptive immune response and may be induced at a later time point (Table S4.1). These results indicate that inoculation with virions, ISVPs or UV-inactivated ISVPs induces inflammation in the murine lungs.

Our results reveal that the structure of the infecting reovirus particle and its replication capacity influence the cytokine expression profile in the lungs after intranasal inoculation. Overall, inoculation with ISVPs resulted in the induction of a higher level of cytokines than inoculation with either virions or UV-inactivated ISVPs (data not shown). Levels of IL-1β, IL-17, IL-23 and IL-27 in the lungs were significantly increased after inoculation with ISVPs and UV-inactivated ISVPs but not when mice were inoculated with virions (Table S4.1). These cytokines are involved in the highly inflammatory Th17 response and recruitment of PMNs

Table S4.1. Effect of intranasal inoculation of reovirus particles on cytokine expression profile. Four week-old CBA/J mice were treated intranasally with 1 x 10^7 PFU T1L virions, 1 x 10^7 PFU T1L ISVPs or 1.7 x 10^9 UV-inactivated T1L ISVP particles in 20 µl total volume or 20 µl of saline. Two days post-treatment, lungs were resected and cytokine expression was detected using the Proteome Profiler Array panel A (R&D Systems) according to published protocol. Cytokine expression was quantified by Image J analysis. (A) Table represents statistical significance of cytokine induction compared to saline inoculated control. *, $P < 0.05$; ** $P < 0.01$; *** $P < 0.001$ (as determined by two-way ANOVA).

Table S4.1

	Virion	ISVP	UV-inactivated ISVP
IL-1ra	***	***	***
IL-4	*	***	**
IL-6	***	***	*
IL-7	***	***	***
IL-13	***	***	***
IL-16	***	***	***
IFN-y	***	***	***
M-CSF	***	***	***
GM-CSF	***	***	***
TNF-a	***	***	***
CCL1	***	***	***
CCL2/MCP-1	***	***	***
MIP-1a (CCL3)	***	***	***
MIP-1b (CCL4)	***	***	***
RANTES (CCL5)	***	***	***
MCP-5 (CCL12	***	***	***
MIG (CXCL9)	***	***	***
CXCL10	***	***	***
CXCL11	***	***	***
CXCL13	***	***	***
MIP-2	***	***	***
KC	***	***	***
C5a	***	***	***
TIMP-1	***	***	***
sICAM-1 (CD54)	***	***	***
TREM-1	***	***	***
IL-2	ns	ns	ns
IL-3	ns	ns	ns
IL-5	ns	ns	ns
IL-10	ns	ns	ns
IL-12 p70	ns	ns	ns
CCL11 (eotaxin)	ns	ns	ns
CXCL12 (SDF-1)	ns	ns	ns
IL-1b	ns	***	**
IL-17	ns	***	*
IL-23	ns	***	***
IL-27	ns	***	***
CCL17 (TARC)	**	ns	ns
G-CSF	***	***	ns
IL-1a	***	***	ns

(175). Virion inoculation resulted in significant induction of CCL17, while inoculation with ISVPs or UV-inactivated ISVPs did not induce significant levels of CCL17 in the lungs (Table S4.1). Interestingly, two cytokines (G-CSF and IL-1α), which are secreted by activated macrophages and PMNS (138), were only induced to significant levels when mice were inoculated with replication-competent virus (Table S4.1). This, coupled with lower overall induction of cytokines after treatment with UV-inactivated ISVPs, suggests that viral replication must occur to induce peak cytokine levels in the respiratory model of reovirus infection.

CHAPTER 5

Genetic Determinants of Reovirus Pathogenesis in a Murine Model of Respiratory Infection

I. Introduction

Many viruses enter host organisms by invading mucosal surfaces, including those that line the respiratory tract. Infection by some pneumotropic viruses is restricted to the respiratory tract, whereas others replicate in the lung and then disseminate to sites of secondary infection. Most influenza virus infections remain localized to the respiratory tract, despite the capacity of the virus to bind broadly-expressed cellular receptors (48). One factor that limits influenza virus infection is the requirement for host proteases to activate the hemagglutinin (HA) protein to allow membrane penetration (96, 227). While most influenza viruses are activated by secreted or membrane-associated proteases in the respiratory tract, highly pathogenic strains, such as avian H5N1 influenza virus, express HA molecules that can be cleaved by furin during virion maturation (112). These viruses have the potential to disseminate systemically (40, 96, 227).

Mammalian orthoreoviruses (reoviruses) naturally infect both the respiratory and gastrointestinal tracts (191). Like influenza virus, reovirus strains differ in the capacity to replicate at mucosal sites and disseminate systemically. Studies of strain-specific differences in reovirus mucosal infection and systemic

dissemination have enhanced an understanding of viral determinants and molecular mechanisms that regulate reovirus pathogenesis. For example, after peroral or intratracheal inoculation, reovirus serotype 1 Lang (T1L) replicates to higher titers than does serotype 3 Dearing (T3D) (153). This difference in replication efficiency at the site of primary replication segregates with the reovirus S1 gene segment (67, 153). Reassortant viruses with nine gene segments from T3D and an S1 gene from T1L (3HA1) replicate to high titers, similar to T1L (153). In contrast, reassortant viruses with nine gene segments from T1L and an S1 gene from T3D (1HA3) fail to replicate to high titers, similar to T3D (153). Genetic determinants of viral systemic dissemination from the murine lung are not known. However, the S1 gene is associated with the capacity of reovirus to spread systemically from the enteric tract (22, 110). After gastrointestinal infection, 3HA1, like T1L, spreads to sites of secondary replication, whereas 1HA3, like T3D, does not (110).

The S1 gene encodes two proteins, viral attachment protein σ1 and nonstructural protein, σ1s. The σ1 protein forms filamentous trimers with tail, body, and head domains (185). Genetic studies link σ1 to serotype-specific differences in reovirus replication in the gastrointestinal tract (37, 72, 110, 229). These differences are influenced by the sensitivity of some σ1 proteins (including that of strain T3D) to cleavage by pancreatic serine proteases (37, 160). Differences in sensitivity to protease-mediated cleavage are determined by a

single amino acid polymorphism (isoleucine or threonine at position 249) in the body domain of σ1 (37). Proteolysis of sensitive strains by CHT or trypsin leads to cleavage of σ1 and diminished infectivity in cultured cells. In contrast to the gastrointestinal tract, protease expression in the respiratory tract is limited in the absence of inflammation. It is not known if the limited replication of T3D in the murine lung is due to cleavage of σ1 by respiratory proteases.

Nonstructural protein σ1s also influences reovirus dissemination from sites of primary replication to visceral tissues in the host. Protein σ1s is a 14 kDa nonstructural protein encoded in an open-reading frame (ORF) that completely overlaps the σ1 coding sequence (65, 104, 193). Other than a cluster of positively charged amino acids near the amino terminus, little amino acid sequence identity exists in the σ1s proteins from different reovirus serotypes (32). The σ1s protein of strain T3D is implicated in reovirus-induced cell cycle arrest at the G2/M boundary (179, 181). Viruses in which either the T1L (22) or T3D (21) σ1s ORF has been ablated produce yields of viral progeny comparable to the corresponding wildtype viruses following replication in cell culture. However, σ1s-null viruses dissemination by hematogenous routes is limited in mice following either peroral (22) or intramuscular (21) inoculation. However, σ1s does not impact dissemination from the CNS (21). It is not known whether σ1s influences viral dissemination following infection in the murine lung.

In this study, we defined genetic and molecular determinants that regulate reovirus-induced pathology after respiratory inoculation. We report that two laboratory isolates of T3D, T3D-Cashdollar ($T3D^C$) and T3D-Fields ($T3D^F$), differ in their capacity to replicate in the respiratory tract and spread systemically. Two nucleotide polymorphisms in the S1 gene regulate these differences, and both S1 gene products are involved. Amino acid polymorphisms in both the tail and head domains of σ1 protein influence the sensitivity of virions to protease-mediated loss of infectivity and the polymorphism in the tail enhances the capacity of reovirus to disseminate in the host. Recombinant viruses that express the $T3D^C$ σ1 protein are less sensitive to proteolysis and disseminate systemically from the respiratory tract. Additionally, a recombinant virus that fails to express the σ1s protein produces lower titers in the lung and disseminates less efficiently to sites of secondary replication. These findings provide new insights into mechanisms underlying reovirus replication in the respiratory tract and systemic spread from the lung.

II. RESULTS

Strain-specific differences in reovirus infection in the murine respiratory tract. To determine whether serotype 1 and serotype 3 reovirus strains differ in the capacity to replicate in the murine respiratory tract, we inoculated CBA/J mice intranasally with 10^7 PFU of T1L, $T3D^F$, and $T3D^C$ and quantified viral titers in the lungs at days 1, 3, and 5 post-inoculation. Since the

$T3D^F$ and $T3D^C$ isolates of prototype reovirus strain T3D display a variety of distinct *in vitro* phenotypes (47, 234, 239), both isolates were used in our study. We found that T1L produced significantly higher titers in the lungs than did $T3D^F$ (Fig. 5.1A), similar to results obtained in previous experiments using a rat model (154). Interestingly, unlike $T3D^F$, the $T3D^C$ isolate produced high titers in the lungs, similar to those achieved by T1L (Fig. 5.1A). At days 3 and 5 post-inoculation, titers of T1L and $T3D^C$ reached 10^7 PFU or greater in the lungs of infected mice. These titers were 10- to 100-fold higher than those in the lungs of animals inoculated with $T3D^F$. Therefore, different laboratory isolates of T3D vary in the capacity to replicate in the murine lung.

Isolates of T3D differ in the capacity to disseminate from the respiratory tract. To determine whether the two T3D isolates also differ in the capacity to spread systemically from the respiratory tract, we quantified viral titers at sites of secondary replication following intranasal inoculation. Within a few hours of inoculation, we recovered similar titers of T1L, $T3D^C$, and $T3D^F$ in the draining mediastinal lymph nodes (MLN) (data not shown). However, by day 1 post-inoculation, titers of $T3D^C$ in the MLN were significantly higher than those of $T3D^F$ (Fig. 5.1B). By day 3, both T1L and $T3D^C$ reached titers 30- to 100-fold higher than those of $T3D^F$ and, by day 5, $T3D^F$ was not detected in the MLN, but titers of T1L and $T3D^C$ remained high. Differences in titers produced by these strains in the spleen were even more striking. T1L and $T3D^C$ were recovered

Fig. 5.1. Reovirus strains differ in the capacity to replicate in the respiratory tract and spread systemically. CBA/J mice were inoculated intranasally with 10^7 PFU of reovirus strains T1L, $T3D^C$, or $T3D^F$. Organs were resected at the indicated times post-inoculation, and viral titers in the (A) lungs, (B) MLN, and (C) spleen were quantified by plaque assay using L929 cells. Results are expressed as mean viral titers for 6 to 9 mice per time point. Error bars indicate SEM. *, $P < 0.05$; **, $P < 0.01$ and ***, $P < 0.001$ (Mann-Whitney test) relative to $T3D^F$.

Fig. 5.1

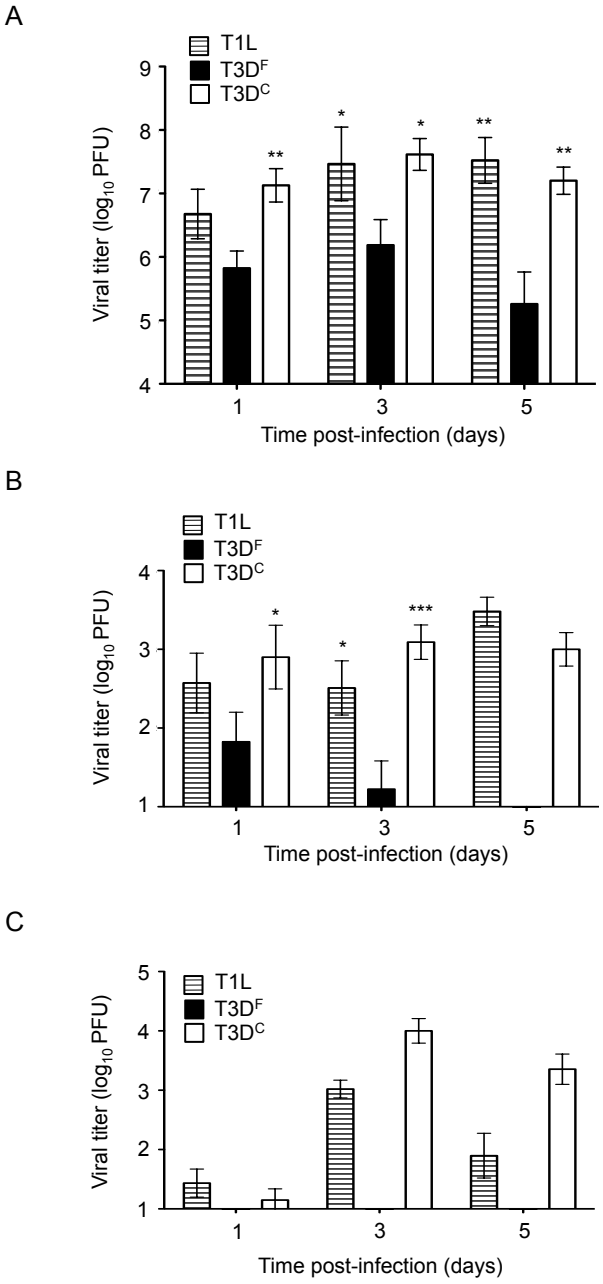
A
T1L
T3D^F
T3D^C
Viral titer (log10 PFU)
Time post-infection (days)
B
T1L
T3D^F
T3D^C
Viral titer (log10 PFU)
Time post-infection (days)
C
T1L
T3D^F
T3D^C
Viral titer (log10 PFU)
Time post-infection (days)

from the spleen at days 1, 3, and 5 post-inoculation, but $T3D^F$ was not (Fig. 5.1C). Thus, reovirus strains that differ in replication in the murine lung also differ in the capacity to disseminate systemically.

We considered the possibility that $T3D^F$ might not spread efficiently to the spleen because it fails to reach a threshold titer in the lungs. To test this hypothesis, we inoculated mice with 30 times more $T3D^F$ than used in the experiments shown in Fig. 1 and quantified viral titers in the lungs and spleen. The higher inoculum of $T3D^F$ resulted in titers in the lung approaching 10^8 PFU at days 1 and 3 post-inoculation, which were slightly higher than titers in the lung of mice inoculated with $T3D^C$ (Fig. 5.2A). However, despite producing high titers in lung tissue, $T3D^F$ did not spread efficiently to the spleen (Fig. 5.2B). Titers of $T3D^C$ in the spleen were in excess of 100-fold higher than those in mice inoculated with the higher dose of $T3D^F$. These results indicate that the $T3D^C$ and $T3D^F$ laboratory isolates of T3D differ in the capacity to disseminate from the respiratory tract, even when titers in the lung are equivalent.

After peroral inoculation, reovirus is thought to spread from Peyer patches through lymphatics to regional lymph nodes and the bloodstream (110, 219, 232). From the bloodstream, virus gains access to sites of secondary replication (155). To determine whether reovirus disseminates from the respiratory tract by the hematogenous route, we quantified virus in the blood on days 1, 2, 3, and 5

Fig. 5.2. Reovirus systemic dissemination is not dependent on respiratory viral load. CBA/J mice (4 weeks-old) were inoculated intranasally with 10^7 PFU $T3D^C$, 10^7 PFU $T3D^F$, or 3 x 10^8 PFU $T3D^F$. Organs were resected at the indicated times post-inoculation, and viral titers in the (A) lungs and (B) spleen were determined by plaque assay using L929 cells. Results are shown from a representative experiment of two performed with 3 mice per time point. Error bars indicate SEM. *, $P < 0.05$ (Student's t-test) relative to $T3D^F$.

Fig. 5.2

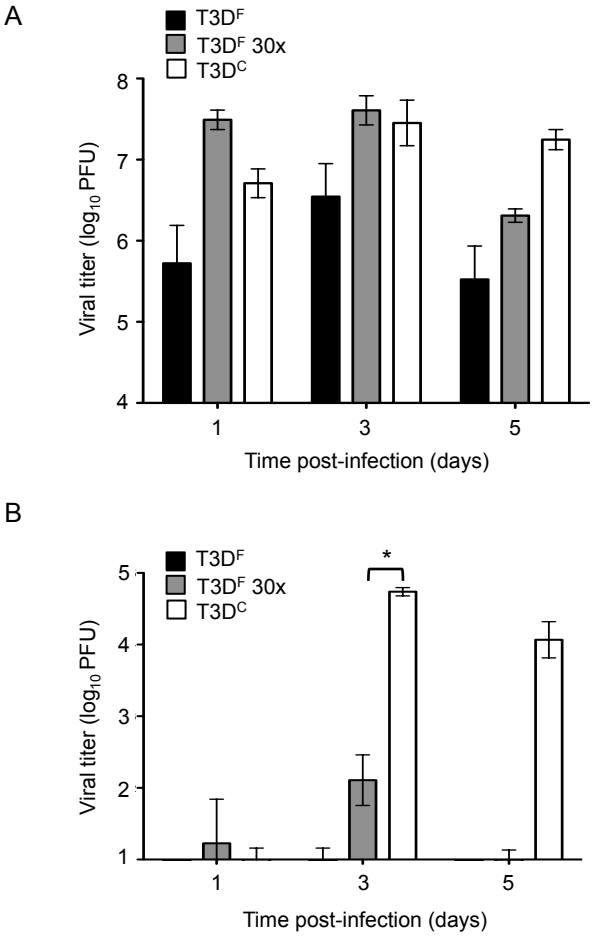
A
T3D^F
T3D^F 30x
T3D^C
Viral titer (log10 PFU)
8
7
6
5
4
1
3
5
Time post-infection (days)
B
T3D^F
T3D^F 30x
T3D^C
*
Viral titer (log10 PFU)
5
4
3
2
1
1
3
5
Time post-infection (days)

after intranasal inoculation with 10^7 PFU of T1L, $T3D^C$, or $T3D^F$. In this experiment, we recovered infectious virus from animals inoculated with either strain at 3 of 4 time points tested (Table 5.1). At those time points, over 40% of the animals were viremic, as determined by plaque assay. In contrast, infectious virus was not detected in the blood of mice inoculated with $T3D^F$. These results suggest that the capacity of strains T1L and $T3D^C$ to disseminate systemically from the respiratory tract is attributable to enhanced access to the bloodstream.

Construction and characterization of recombinant viruses containing $T3D^C$ S1 gene sequences. The S1 gene is a major determinant of reovirus dissemination from the gastrointestinal tract (21, 23, 219, 232). To determine whether the $T3D^C$ S1 gene contributed to the differences in dissemination efficiency displayed by T3D laboratory isolates, we used plasmid-based reverse genetics (119, 120) to engineer a recombinant $T3D^F$ virus with the $T3D^C$ coding sequences in the S1 gene (Fig. 5.3A). To determine whether the $T3D^C$ S1 gene influence viral growth in cell culture, we conducted single-cycle replication experiments with the recombinant viruses using mouse L929 fibroblasts. Cells were adsorbed with $T3D^F$ or rs$T3D^F$/$T3D^C$S1 at a MOI of 5 PFU per cell, and viral titers were determined by plaque assay over a 48 h time course. The recombinant virus with $T3D^C$ S1 gene produced yields comparable to $T3D^F$ and did so with similar kinetics (Fig. 5.3B). Thus, the $T3D^C$ S1 gene does not appear to alter the replication of $T3D^F$ in cell culture.

Table 5.1. Reovirus strains differ in the capacity to establish viremia after intranasal inoculation. CBA/J mice were inoculated intranasally with 10^7 PFU of T1L, $T3D^C$, or $T3D^F$. Blood was collected by heart puncture at the indicated times post-inoculation, and viral titers were determined by plaque assay using L929 cells.

Table 5.1

Viral strain	Time post-infection (days)	Viremia (positive mice/total mice)
T1L	1	0/3
	2	2/6
	3	1/3
	5	2/3
$T3D^C$	1	1/3
	2	1/3
	3	2/3
	5	0/3
$T3D^F$	1	0/3
	2	0/3
	3	0/3
	5	0/3

Fig. 5.3. Construction and characterization of $T3D^F$ viruses with $T3D^C$ sequences in the S1 gene. (A) Schematic of the reovirus $rsT3D^F/T3D^C$ S1 gene segment. The σ1 ORF is shown in gray, the σ1s ORF is shown in black, and the 5' and 3' UTRs are represented by white rectangles. Each $T3D^C$ nucleotide change in $T3D^F$ S1 is represented by a light gray bar. (B) Replication of recombinant viruses. L929 cells were adsorbed with $T3D^F$ or $rsT3D^F/T3D^C$S1 at an MOI of 5 PFU/cell. Viral titers were determined at the indicated times post-adsorption by plaque assay using L929 cells. The results are expressed as viral yields for triplicate samples. Error bars indicate SD.

Fig. 5.3

A

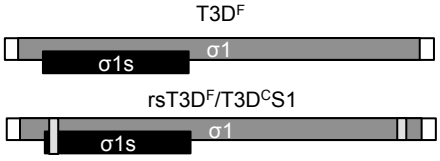
T3D^F
σ1
σ1s
rsT3D^F/T3D^{C}S1
σ1
σ1s

B

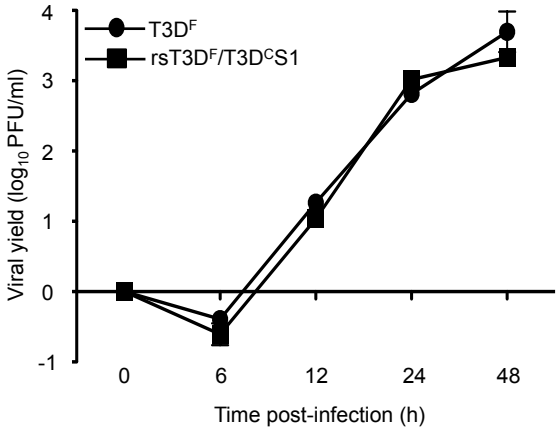
T3D^F
rsT3D^F/T3D^{C}S1
Viral yield (log_{10} PFU/ml)
4
3
2
1
0
-1
0
6
12
24
48
Time post-infection (h)

The role of T3D^C S1 gene sequences in reovirus respiratory infection. To determine whether the T3D^C S1 gene sequences promote reovirus replication in the murine lung, we inoculated mice intranasally with 10^7 PFU of T3D^F or recombinant T3D^F with the S1 gene coding sequences of T3D^C (rsT3D^F/T3D^{C}S1). We recovered similar titers (~ 10^7 PFU) in the lungs of mice inoculated with T3D^F or rsT3D^F/T3D^{C}S1 at day 1 post-inoculation (Fig. 5.4A). However, at days 2 and 4, titers of rsT3D^F/T3D^{C}S1 in the lungs were ~ 10-fold higher than those in animals infected with T3D^F. We observed similar trends in viral titers in the MLN, suggesting that viruses in the respiratory tract efficiently gained access to the lymphatic system (Fig. 5.4B). In contrast, we recovered rsT3D^F/T3D^{C}S1 but not T3D^F in the spleens of infected mice (Fig. 5.4C). These results suggest that coding sequences in the T3D^C S1 gene influences systemic dissemination from the lungs.

Role of T3D^C S1 gene products in reovirus replication and dissemination. The reovirus S1 gene encodes viral attachment protein σ1 and nonstructural protein σ1s. Both σ1 and σ1s proteins have been found to influence reovirus pathogenesis *in vivo* (21, 22, 110, 219, 220), however none of the studies to date involved the T3D^c isolate, and none of them used a respiratory model of pathogenesis. To determine whether the σ1s protein influences viral replication and dissemination from the murine respiratory tract, we used plasmid-based reverse genetics (119, 120) to engineer a recombinant rsT3D^F/T3D^{C}S1

Fig. 5.4. The $T3D^C$ S1 gene enhances respiratory infection and systemic dissemination. CBA/J mice were inoculated intranasally with 10^7 PFU of $T3D^F$ or $rsT3D^F/T3D^C$S1. Organs were harvested at the indicated times post-inoculation, and viral titers in the (A) lungs, (B) MLN, and (C) spleen were determined by plaque assay using L929 cells. Results are expressed as mean viral titers for 6 mice per time point. Error bars indicate SEM.

Fig. 5.4

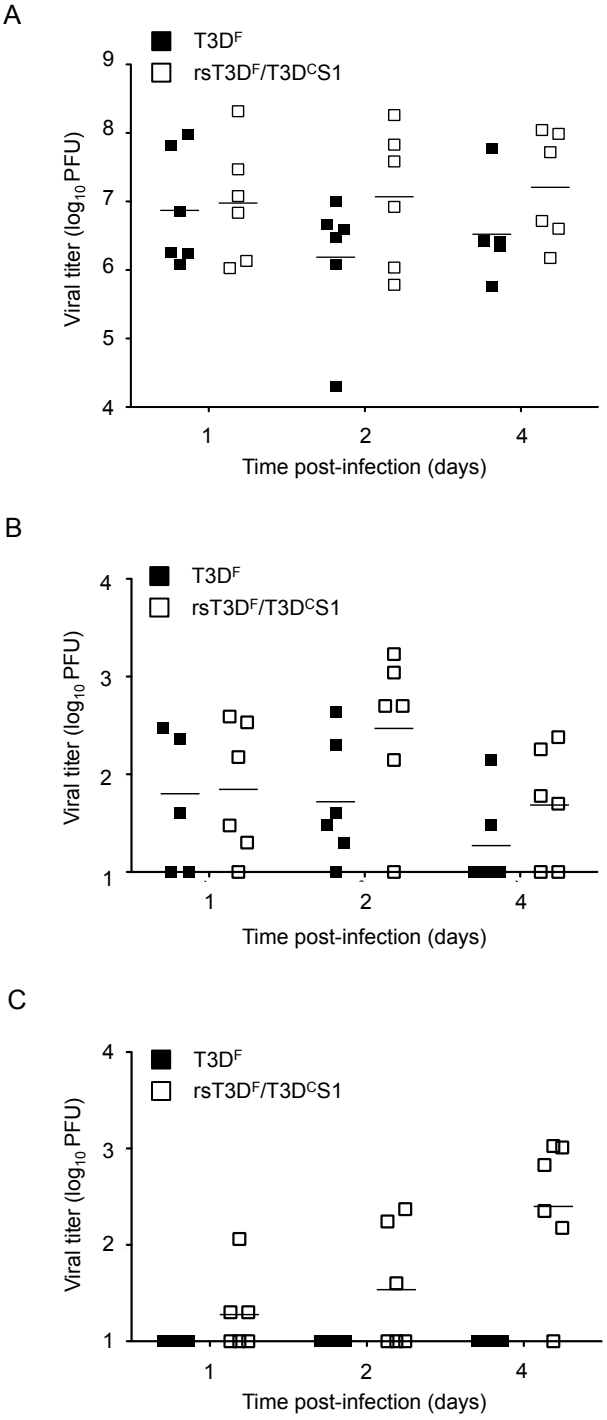
A
T3D^F
rsT3D^F/T3D^CS1
Viral titer (log10 PFU)
9
8
7
6
5
4
1
2
4
Time post-infection (days)
B
T3D^F
rsT3D^F/T3D^CS1
Viral titer (log10 PFU)
4
3
2
1
1
2
4
Time post-infection (days)
C
T3D^F
rsT3D^F/T3D^CS1
Viral titer (log10 PFU)
4
3
2
1
1
2
4
Time post-infection (days)

σ1s-null virus (Fig. 5.5A). We confirmed that the σ1s-null virus does not express σ1s by infecting L929 cells with rsT3D^F/T3D^{C}S1 σ1s-null and probing cell lysates with a σ1s-specific antibody (data not shown). We also assessed the capacity of rsT3D^F/T3D^{C}S1 σ1s-null to replicate in cell culture. As anticipated (22, 188), rsT3D^F/T3D^{C}S1 σ1s-null produced yields of viral progeny comparable to T3D^F and rsT3D^F/T3D^{C}S1 following replication in L929 cells (Fig. 5.5B).

The role of the T3D^C σ1s protein in reovirus replication in the murine lungs and systemic dissemination. To determine whether the σ1s protein functions in reovirus infection in the lung and dissemination from that site, we inoculated mice intranasally with 10^7 PFU of rsT3D^F/T3D^{C}S1 or rsT3D^F/T3D^{C}S1 σ1s-null, resected organs at days 1, 2, and 4 post-inoculation, and determined viral titers by plaque assay. We found that titers of T3D^F, rsT3D^F/T3D^{C}S1, and rsT3D^F/T3D^{C}S1 σ1s-null were equivalent in the lungs at day 1 post-inoculation and, as expected, titers of rsT3D^F/T3D^{C}S1 were significantly higher than those of T3D^F in the lungs at day 2 post-inoculation (Fig. 5.6A). In contrast, titers of rsT3D^F/T3D^{C}S1 σ1s-null were significantly lower in the lung than those of either T3D^F or rsT3D^F/T3D^{C}S1 at days 2 and 4 post-inoculation. All viruses gained access to the draining lymph and reached similar titers in the MLN (Fig. 5.6B). These results suggest that the σ1s protein contributes to reovirus replication in the respiratory tract but is dispensable for access to draining lymph nodes.

Fig. 5.5. Construction and characterization of σ1s-null viruses. (A) Schematic of the reovirus rsT3D^F/T3D^C S1 gene segment. The σ1 ORF is shown in gray, the σ1s ORF is shown in black, and the 5' and 3' UTRs are represented by white rectangles. Each T3D^C nucleotide change in T3D^F S1 is represented by a light gray bar. (B) Replication of recombinant viruses. L929 cells were adsorbed with T3D^F, rsT3D^F/T3D^{C}S1, or rsT3D^F/T3D^{C}S1 σ1s-null at an MOI of 5 PFU/cell. Viral titers were determined at the indicated times post-adsorption by plaque assay using L929 cells. The results are expressed as viral yields for triplicate samples. Error bars indicate SD.

Fig. 5.5

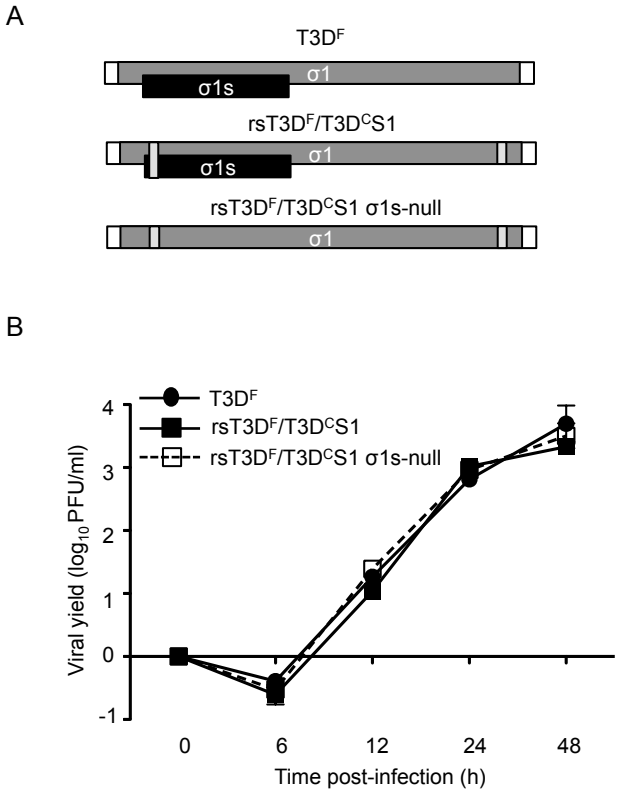
A
T3D^F
σ1s
σ1
rsT3D^F/T3D^CS1
σ1s
σ1
rsT3D^F/T3D^CS1 σ1s-null
σ1
B
T3D^F
rsT3D^F/T3D^CS1
rsT3D^F/T3D^CS1 σ1s-null
Viral yield (log10 PFU/ml)
4
3
2
1
0
-1
0
6
12
24
48
Time post-infection (h)

Fig. 5.6. The T3D^{C} σ1s protein promotes viral replication in the respiratory tract and enhances systemic dissemination. CBA/J mice were inoculated intranasally with 10^{7} PFU of T3D^{F}, rsT3D^{F}/T3D^{C}S1, or rsT3D^{F}/T3D^{C}S1 σ1s-null. Organs were harvested at the indicated times post-inoculation, and viral titers in the (A) lungs, (B) MLN, and (C) spleen were determined by plaque assay using L929 cells. Results are expressed as mean viral titers for 5-6 mice per time point. Error bars indicate SEM. **, $P < 0.01$ (Mann-Whitney test) relative to T3D^{F}.

Fig. 5.6

A

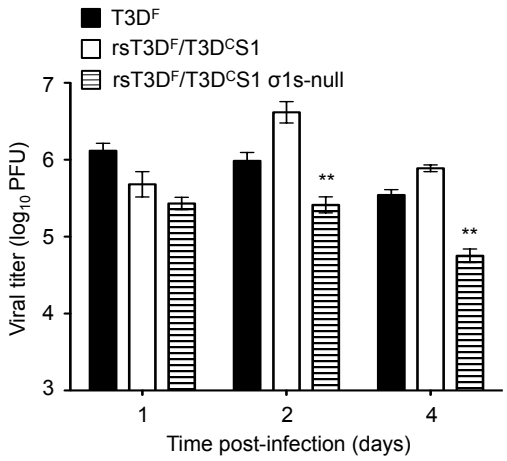
T3D^F
rsT3D^F/T3D^CS1
rsT3D^F/T3D^CS1 σ1s-null
Viral titer (log10 PFU)
7
6
5
4
3
**
**
1
2
4
Time post-infection (days)

B

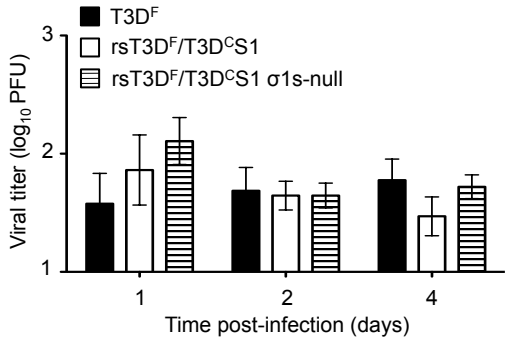
T3D^F
rsT3D^F/T3D^CS1
rsT3D^F/T3D^CS1 σ1s-null
Viral titer (log10 PFU)
3
2
1
1
2
4
Time post-infection (days)

C

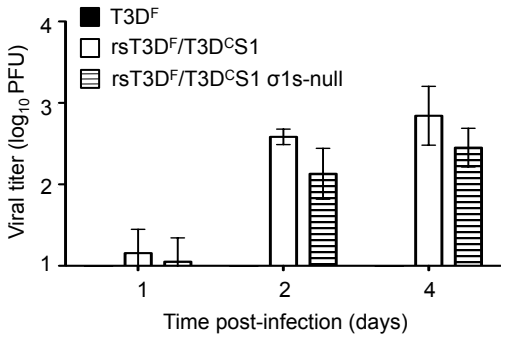
T3D^F
rsT3D^F/T3D^CS1
rsT3D^F/T3D^CS1 σ1s-null
Viral titer (log10 PFU)
4
3
2
1
1
2
4
Time post-infection (days)

To determine whether σ1s is required for hematogenous dissemination of reovirus from the respiratory tract, we quantified virus in the blood and spleen after intranasal inoculation with $T3D^F$, $rsT3D^F/T3D^CS1$, or $rsT3D^F/T3D^CS1$ σ1s-null viruses. We recovered virus in the blood in the majority of mice inoculated with $rsT3D^F/T3D^CS1$, but viremia was detected in only a single animal inoculated with $T3D^F$ (Table 5.2). Fewer mice inoculated with the $rsT3D^F/T3D^CS1$ σ1s-null virus developed viremia, suggesting that σ1s enhances $rsT3D^F/T3D^CS1$ access to the bloodstream. Interestingly, titers of $rsT3D^F/T3D^CS1$ σ1s-null in the spleen were only slightly lower than those in animals inoculated with $rsT3D^F/T3D^CS1$ (Fig. 5.6C). These results suggest that the $T3D^C$ σ1s protein enhances reovirus access to the bloodstream but is not absolutely required for systemic spread.

Effect of $T3D^C$ S1 gene coding changes on T3D lung replication and systemic dissemination. The $T3D^C$ and $T3D^F$ S1 genes differ at two nucleotides that result in amino acid changes, nucleotide 77 and nucleotide 1234. Nucleotide 77 alters amino acid 22 from valine to alanine in the σ1 tail and amino acid 3 from glutamine to histidine near the amino-terminus of nonstructural protein σ1s, whereas nucleotide 1234 alters amino acid 408 from threonine to alanine in the σ1 head. To determine how the individual sequence polymorphisms in the S1 gene contribute to the differences in dissemination efficiency displayed by T3D laboratory isolates, we engineered $T3D^F$ viruses that contain each of the individual $T3D^C$ coding changes in the S1 gene

Table 5.2. Role of rsT3DF/T3D^{C} S1 gene products in reovirus-induced viremia. CBA/J mice were inoculated intranasally with 10^{7} PFU T3D^{F}, rsT3D^{F}/T3D^{C}S1, or rsT3D^{F}/T3D^{C}S1 σ1s-null. Blood was collected by heart puncture at the indicated times post-inoculation, and viral titers were determined by plaque assay using L929 cells. Results are expressed as the number of mice with detectable virus in the blood (limit of detection 1 PFU/ml).

Table 5.2

Viral strain	Time post-infection (days)	Viremia	
		positive mice/ total mice	% mice positive
$T3D^F$	1	1/5	20
	2	0/5	0
	4	0/5	0
$rsT3D^F/T3D^CS1$	1	7/8	88
	2	6/8	75
	4	4/8	50
$rsT3D^F/T3D^CS1$ σ1s-null	1	3/5	60
	2	3/5	60
	4	1/5	20

(rsT3D^F/T3D^{C}S1-77 and rsT3D^F/T3D^{C}S1-1234) (Fig. 5.7A). Both of the recombinant viruses with single T3D^C S1 gene sequences produced yields in L929 cells comparable to T3D^F and did so with similar kinetics (Fig. 5.7B). Thus, the two changes in in the S1 gene at nucleotide 77 (σ1: valine to alanine at 22/σ1s: glutamine to histidine at 3) and nucleotide 1234 (σ1: threonine to alanine at 408) do not appear to alter the replication of T3D^F in cell culture.

To identify the T3D^C S1 gene coding polymorphisms that promote viral replication in the lung and dissemination from that site, we infected mice intranasally with T3D^F, rsT3D^F/T3D^{C}S1-77, or rsT3D^F/T3D^{C}S1-1234, resected organs at various times post-inoculation, and determined viral titers by plaque assay. We found that animals inoculated with T3D^F had titers in the lungs of approximately 10^6 PFU over the time course, whereas titers in the lungs of animals inoculated with rsT3D^F/T3D^{C}S1-1234 were significantly lower (Fig. 5.8A). In contrast, strain rsT3D^F/T3D^{C}S1-77, which contains amino acid polymorphisms in both the σ1 and σ1s proteins, replicated to higher titers than did either T3D^F or rsT3D^F/T3D^{C}S1-1234 at all times analyzed (Fig. 5.8A).

To determine whether one or both of the T3D^C S1 gene coding polymorphisms contribute to the capacity of T3D^C to disseminate systemically from the respiratory tract, we quantified viral titers in the spleen following

FIG 5.7 Construction and characterization of $T3D^F$ viruses with single $T3D^C$ sequences in the S1 gene. (A) Schematic of the reovirus S1 gene segment. The σ1 ORF is shown in gray, the σ1s ORF is shown in black, and the 5' and 3' UTRs are represented by white rectangles. Each $T3D^C$ nucleotide change in $T3D^F$ S1 is represented by a light gray bar. (B) Replication of recombinant viruses. L929 cells were adsorbed with $T3D^F$, rs$T3D^F$/$T3D^C$S1-77, or rs$T3D^F$/$T3D^C$S1-1234 at an MOI of 5 PFU/cell. Viral titers were determined at the indicated times post-adsorption by plaque assay using L929 cells. The results are expressed as viral yields for triplicate samples. Error bars indicate SD.

Fig. 5.7

A

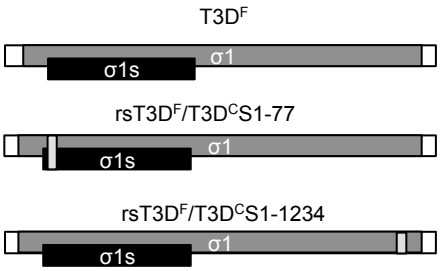
T3D^F
σ1
σ1s
rsT3D^F/T3D^{C}S1-77
σ1
σ1s
rsT3D^F/T3D^{C}S1-1234
σ1
σ1s

B

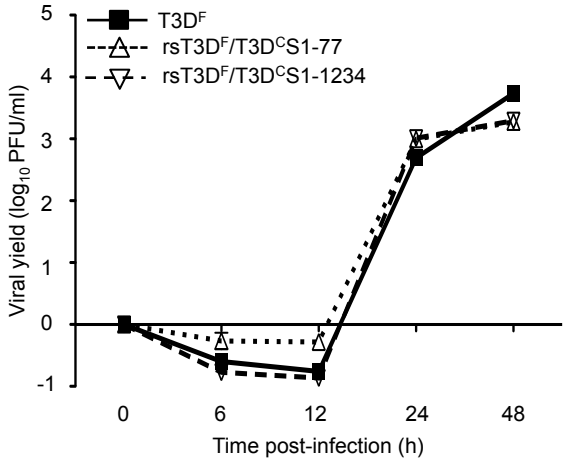
T3D^F
rsT3D^F/T3D^{C}S1-77
rsT3D^F/T3D^{C}S1-1234
Viral yield (log_{10} PFU/ml)
5
4
3
2
1
0
-1
0
6
12
24
48
Time post-infection (h)

intranasal inoculation (Fig. 5.8B). While both recombinant viruses with $T3D^C$ S1 gene sequences were capable of disseminating to the spleen, a greater number of animals inoculated with $rsT3D^F/T3D^C$S1-77 had evidence of viral spread, and the viral loads in these animals were higher than those in animals inoculated with $rsT3D^F/T3D^C$S1-1234. These results suggest that each of the $T3D^C$ coding polymorphisms in the S1 gene contributes to systemic viral dissemination from the respiratory tract, with the change at nucleotide 77, which impacts both the σ1 and the σ1s proteins, being the more influential of the two.

Effect of $T3D^C$ S1 gene coding changes on protease-mediated loss of infectivity. The S1 gene is the primary determinant of the capacity of reovirus to replicate in and spread from the gastrointestinal tract. $T3D^F$ does not replicate to high titers in the small intestine and it fails to spread after peroral inoculation (110). This phenotype has been associated with the susceptibility of the $T3D^F$ S1 gene-encoded σ1 protein to cleavage by the pancreatic serine proteases chymotrypsin and trypsin (37, 160). Although the respiratory tract contains comparably less protease activity than that in the gastrointestinal tract in the absence of infection or pathology (80), inflammation in the respiratory tract may promote infection through recruitment of leukocytes and increased expression of inflammatory proteases capable of mediating extracellular reovirus disassembly (167).

Fig 5.8. Each of the polymorphic coding sequences in the T3D S1 gene affects respiratory infection and dissemination. CBA/J mice were inoculated intranasally with 10^7 PFU of $T3D^F$, $rsT3D^F/T3D^C$S1-77, or $rsT3D^F/T3D^C$S1-1234. Organs were harvested at the indicated times post-inoculation, and viral titers in the (A) lungs, (B) MLN, and (C) spleen were determined by plaque assay using L929 cells. Results are expressed as mean viral titers for 6-8 mice per time point. Error bars indicate SEM. *, $P < 0.05$; **, $P < 0.01$ and ***, $P < 0.001$ (Mann-Whitney test) relative to $T3D^F$.

Fig. 5.8

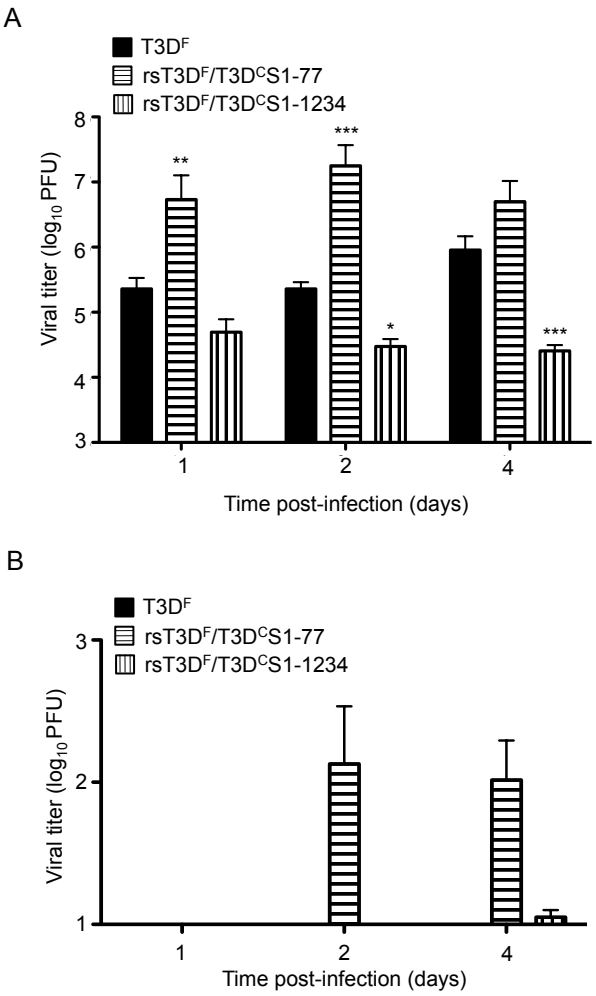
A
T3D^F
rsT3D^F/T3D^CS1-77
rsT3D^F/T3D^CS1-1234
Viral titer (log10 PFU)
8
7
6
5
4
3
**
***
*
***
1
2
4
Time post-infection (days)
B
T3D^F
rsT3D^F/T3D^CS1-77
rsT3D^F/T3D^CS1-1234
Viral titer (log10 PFU)
3
2
1
1
2
4
Time post-infection (days)

To explore the possibility that differences in protease sensitivity contribute to differences in the capacity of the two T3D isolates to spread from the respiratory tract, we first compared the effects of CHT on the infectivity of $T3D^F$ and the recombinant viruses with the individual and both $T3D^C$ S1 gene coding polymorphisms (Fig. 5.9A). We assessed changes in infectivity over time by comparing the titer of protease-treated samples and mock-treated samples. As anticipated (160), $T3D^F$ virions lost infectivity after 30 min of incubation with chymotrypsin. In contrast, recombinant virions with $T3D^C$ S1 gene coding changes retained infectivity after 30 and 60 min of chymotrypsin treatment. To test whether the $T3D^C$ S1 gene coding changes also affect sensitivity to an inflammatory protease, we performed similar experiments using neutrophil elastase. While $T3D^F$ virions lost infectivity within 5 min of treatment with neutrophil elastase (Fig. 5.9B), recombinant viruses with $T3D^C$ S1 gene coding changes retained infectivity through 15 min of protease treatment. Because $T3D^C$ and $T3D^F$ share sequences in the known protease-sensitive region of σ1, these results indicate that sequences outside of this region affect the sensitivity of virions to inactivation by serine proteases.

III. DISCUSSION

In this chapter, we present results of experiments that revealed strain specific differences in reovirus pathogenesis after respiratory inoculation. Prior to my thesis work, nothing was known about the genetic determinants that regulate

Fig. 5.9. $T3D^C$ S1 coding sequences segregate with resistance to protease-mediated loss of infectivity. Purified virions of $T3D^F$, $rsT3D^F/T3D^C$S1-77, $rsT3D^F/T3D^C$S1-1234, and $rsT3D^F/T3D^C$S1 at a concentration of 5×10^{10} particles were treated with either (A) chymotrypsin or (B) neutrophil elastase at 37°C. Viral titers before and after treatment were determined by plaque assay using L929 cells. Changes in viral infectivity are expressed as the ratio of $\log_{10}$ viral titer at each treatment time relative to mock treatment. Results are shown from representative experiment of 3 performed.

Fig. 5.9

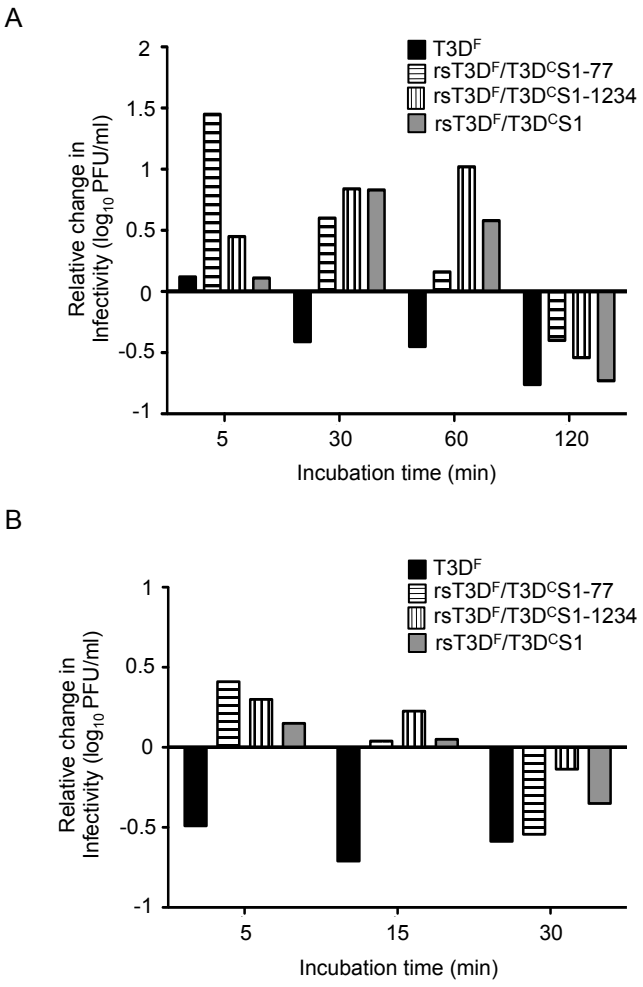
A
T3D^F
rsT3D^F/T3D^CS1-77
rsT3D^F/T3D^CS1-1234
rsT3D^F/T3D^CS1
Relative change in Infectivity (log10 PFU/ml)
2
1.5
1
0.5
0
-0.5
-1
5
30
60
120
Incubation time (min)
B
T3D^F
rsT3D^F/T3D^CS1-77
rsT3D^F/T3D^CS1-1234
rsT3D^F/T3D^CS1
Relative change in Infectivity (log10 PFU/ml)
1
0.5
0
-0.5
-1
5
15
30
Incubation time (min)

reovirus replication and dissemination in a murine model of respiratory infection. We used a reverse genetic approach to identify determinants of reovirus replication in the respiratory tract and systemic dissemination from the respiratory tract. By identifying viral determinants that regulate dissemination, one could improve the safety and efficacy of reovirus as a cancer therapeutic.

As discussed in more detail in chapter 3, we found that reovirus $T3D^F$ replicated to lower titers in the respiratory tract and fail to disseminate systemically. Interestingly, another isolate of strain Dearing, $T3D^C$, replicated to high titers in the lungs and spread systemically, similar to T1L (Fig. 1). Since $T3D^C$ shows a variety of distinct phenotypes *in vitro*, including enhanced virion disassembly, we examined the role of genes that encode outer capsid proteins (M2, S4 and S1) in reovirus replication in the lungs and dissemination from the respiratory tract. We found that the $T3D^C$ S4 and M2 genes did not increase either reovirus titers in the lungs or systemic dissemination (Fig. S5.1), however the $T3D^C$ S1 gene significantly increased both replication in the lungs and systemic dissemination (Fig. 5.4).

The $T3D^C$ S1 gene has two nucleotide changes relative to the $T3D^F$ S1 gene that affect protein coding. The $T3D^C$ change at nucleotide 77 alters an amino acid in the σ1 tail and an amino acid near the amino-terminus of σ1s, whereas nucleotide 1234 alters an amino acid in the σ1 head. These residues

are not associated with any known epitope recognition, receptor binding or protease sensitive region (31, 37, 38, 88, 91, 116, 123, 157, 159, 161, 185, 221, 240). However, our data demonstrates that both $T3D^C$ sequences decrease protease-mediated inactivation (Fig. 5.8), but only the $T3D^C$ change at nucleotide 77 increases viral titers in the lungs and systemic dissemination (Fig. 5.7). Based on this, we conclude that the alanine 22 alteration in σ1, the glutamine 3 alteration in σ1s or a combination of the two may be responsible for $T3D^C$ replication and spread phenotype.

Exciting preliminary studies suggest that $T3D^F$ particles contain fewer virion-associated σ1 and this may lead to more rapid loss of infectivity in the presence of proteases. Some type 3 reovirus strains, including $T3D^F$, rapidly lose infectivity in the gastrointestinal tract due to a polymorphism in the neck of the σ1 protein (160). $T3D^F$ and $T3D^C$ share the polymorphism in σ1 at amino acid 249 that confers susceptibility to protease-mediated cleavage (37). Yet, our results reveal that $T3D^C$ virions and particles with the $T3D^C$ S1 gene do not lose infectivity in the presence of serine proteases like the $T3D^F$ virions do. In addition, preliminary work reveals that $T3D^C$, unlike $T3D^F$, is recovered at high titers in the spleen after peroral inoculation (Fig. S5.2). This suggests that $T3D^C$ may not lose infectivity as rapidly as $T3D^F$ *in vivo*. Early results also suggest that $T3D^C$ and $T3D^F$ virions treated with the respiratory serine protease HAT have similar rates of σ1 cleavage, but differ significantly in the amount of virion-associated σ1

trimers before treatment with protease (Fig. S5.3). This suggests that the $T3D^C$ change associated with the extreme N-terminus may stabilizes σ1 in the virion. The role of each $T3D^C$ coding polymorphism on the quantity of encapsidated σ1 and stability of σ1 trimers is the subject of current studies.

Until recently, the cell attachment protein σ1 was considered the primary determinant of reovirus pathogenesis (110, 219, 228, 229, 232). It is clear, however, that the σ1s protein is required for peak growth in the gastrointestinal tract (22) and hematogenous spread after peroral (22) or intramuscular (21) inoculation. Consistent with a role for σ1s in viral replication at mucosal sites, our results demonstrate that the $T3D^C$ σ1s protein significantly increases viral replication in the respiratory tract and hematogenous dissemination (Fig. 5.5, Table 5.2). Interestingly, the $T3D^C$ σ1s protein did not significantly impact viral titers in the spleen (Fig 5.5C). This suggests that the $T3D^C$ σ1s protein enhances access to the blood but is not required for replication at secondary sites of infection. The importance of σ1s for pathogenesis was highlighted when it was determined that, after intramuscular or peroral inoculation, the majority of disseminated σ1s-null virus had reverted to wildtype expression of σ1s (21, 22). We have analyzed the S1 gene sequences of 5 virus isolates from organs resected from mice inoculated intranasally with $rsT3D^F/T3D^C$S1 σ1s-null virus. Our results revealed that over half had reverted to wildtype σ1s expression,

which emphasizes the importance of the T3D^C σ1s protein in dissemination from the respiratory tract.

The mechanisms by which σ1s promotes reovirus dissemination are currently unknown. One possible mechanism behind this is the role of σ1s in reovirus-induced apoptosis (97). Type 1 σ1s is not required for induction of apoptosis in cell culture (22), however type 3 σ1s is required for reovirus-induced apoptosis in cells of the heart and CNS (97). The process of reovirus release from target cells is not well understood, however some viruses, including some orthoreoviruses, induce apoptosis for efficient reovirus release (143). Our lab has recently found that T3D^C induces higher levels of apoptosis in cell culture than T3D^F (data not shown). Failure to induce apoptosis and inefficient release from cells may explain the lower viral yields in the lungs of mice inoculated with type 3 σ1s-null viruses. Due to time constraints, we were not able to dissect the individual roles of the σ1 and σ1s proteins in a rsT3D^F/T3D^{C}S1-77 virus, and this will be a future goal for the lab.

IV. Supplementary text

Text S5.1

As discussed in more detail in chapter 3, we found that reovirus T3D^F and T1L differ in capacity to replicate in the murine respiratory tract. T1L replicated to

Fig. S5.1. The $T3D^C$ S4 and M2 genes do not enhance viral replication or dissemination after intranasal reovirus inoculation. CBA/J mice were inoculated intranasally with 10^7 PFU of $T3D^C$, $T3D^F$, $rsT3D^F/T3D^C$S4M2 or $rsT3D^F/T3D^C$S4. Organs were harvested 2 days post-inoculation, and viral titers in the (A) lungs, (B) MLN, and (C) spleen were determined by plaque assay using L929 cells. Results are expressed as viral titer per mouse.

Fig. S5.1

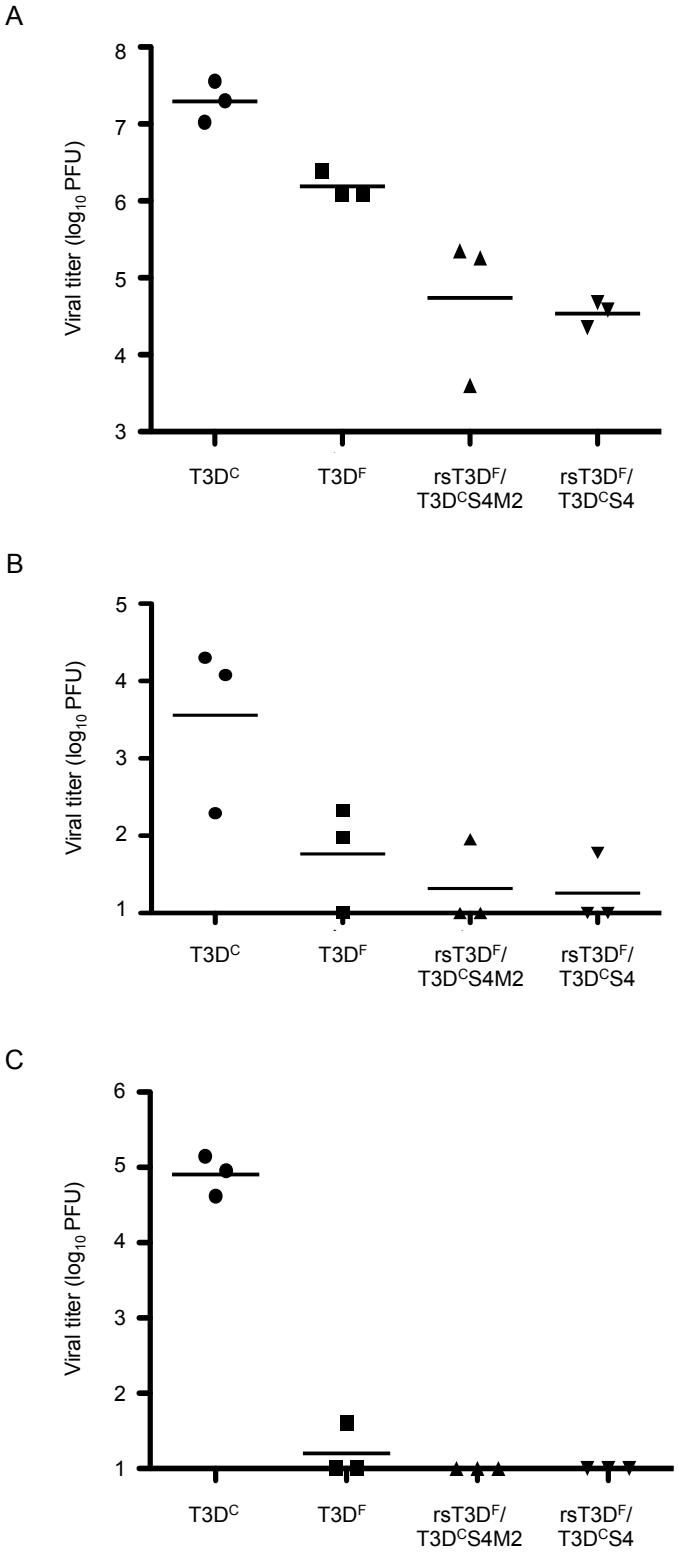
A
B
C
Viral titer (log_{10} PFU)
8
7
6
5
4
3
2
1
T3D^C
T3D^F
rsT3D^F/ T3D^{C}S4M2
rsT3D^F/ T3D^{C}S4

significantly higher titers than T3D (Fig. 1A). Interestingly, another T3D isolate, $T3D^C$, replicated to similar titers as T1L in the lungs (Fig. 1A). $T3D^C$ also shows a variety of distinct phenotypes *in vitro*, including enhanced virion disassembly. The S4 gene encodes the outer capsid protein σ3 and the M2 gene encodes the membrane penetration protein μ1, both proteins are involved in virion disassembly (95, 162, 194, 197). We considered that the reovirus S4 or M2 genes may promote reovirus replication in the respiratory tract. To test this, we generated recombinant $T3D^F$ viruses with $T3D^C$ S4 ($rsT3D^F/T3D^CS4$) or $T3D^C$ S4 and M2 ($rsT3D^F/T3D^CS4M2$) genes. Both recombinant viruses display enhanced uncoating *in vitro* similar to wildtype $T3D^C$ (data not shown). Intranasal inoculation of $rsT3D^F/T3D^CS4$ or $rsT3D^F/T3D^CS4M2$ did not result in increased replication in the respiratory tract (Fig. S5.1A). Titers of recombinant viruses in the lungs were nearly a log lower than wildtype $T3D^F$. In addition, intranasal inoculation of viruses with enhanced uncoating phenotypes did not result in increased titers in the MLN or spleen (Fig. S5.1B,C). These preliminary results suggest that viruses that enhanced uncoating does not promote reovirus replication in the respiratory tract or access to secondary sites of replication.

Text S5.2

$T3D^F$ fails to replicate in the gastrointestinal tract due to a polymorphism that confers susceptibility to protease-mediated cleavage of σ1. The σ1 polymorphism at amino acid 249 is shared by both isolates of T3D. However,

$T3D^C$ is more resistant to protease-mediated cleavage (Fig. 5.8), replicates to high titers in the respiratory tract, and disseminates systemically after intranasal inoculation (Fig. 5.1). There are no reports examining $T3D^C$ capacity to replicate in or disseminate from the gastrointestinal tract. To determine if $T3D^C$ can replicate in the gastrointestinal tract, we inoculated newly weaned mice with 10^8 PFU of T1L, $T3D^F$ or $T3D^C$ and quantified viral titers by plaque assay on L929 cells (Fig. S5.2). As expected (110), T1L replicated to high titers, while $T3D^F$ was not recovered in the gastrointestinal tract (Fig. S5.2A). In addition, $T3D^C$ was not recovered in the gastrointestinal tract at any time point examined (Fig. S5.2A). These results suggest that $T3D^C$, like $T3D^F$, fails to replicate in the gastrointestinal tract, which is likely due to protease-mediated cleavage of the cell attachment protein σ1.

While $T3D^C$ is not recovered in the gastrointestinal tract after peroral inoculation, virus may enter cells and access secondary sites for replication. $T3D^C$ and $T3D^F$ gained access the mesenteric lymph nodes, although at lower titers and less frequency compared to titers in the lymph nodes after T1L inoculation (Fig. S5.2B). Our results also demonstrate that both $T3D^F$ and $T3D^C$ gain access to the spleen, although at varying titers (Fig. S5.2C). Interestingly, titers of $T3D^C$ in the spleen are even higher than titers of T1L in the spleen. These results imply that capacity to disseminate from the gastrointestinal tract is

Fig. S5.2. Analysis of viral replication in the gastrointestinal tract and systemic dissemination of murine reoviruses T1L, T3D^{F} and T3D^{C}. CBA/J mice (3 weeks-old) were inoculated intragastrically with 1 x 10^{8} PFU of T1L, T3D^{F} or T3D^{C} virions. Organs were resected at indicated times post-inoculation. Viral titers in the (A) intestine, (B) MLN, and (C) spleen were determined by plaque assay on L929 cells. Results are expressed as viral titer for each mouse examined.

Fig. S5.2

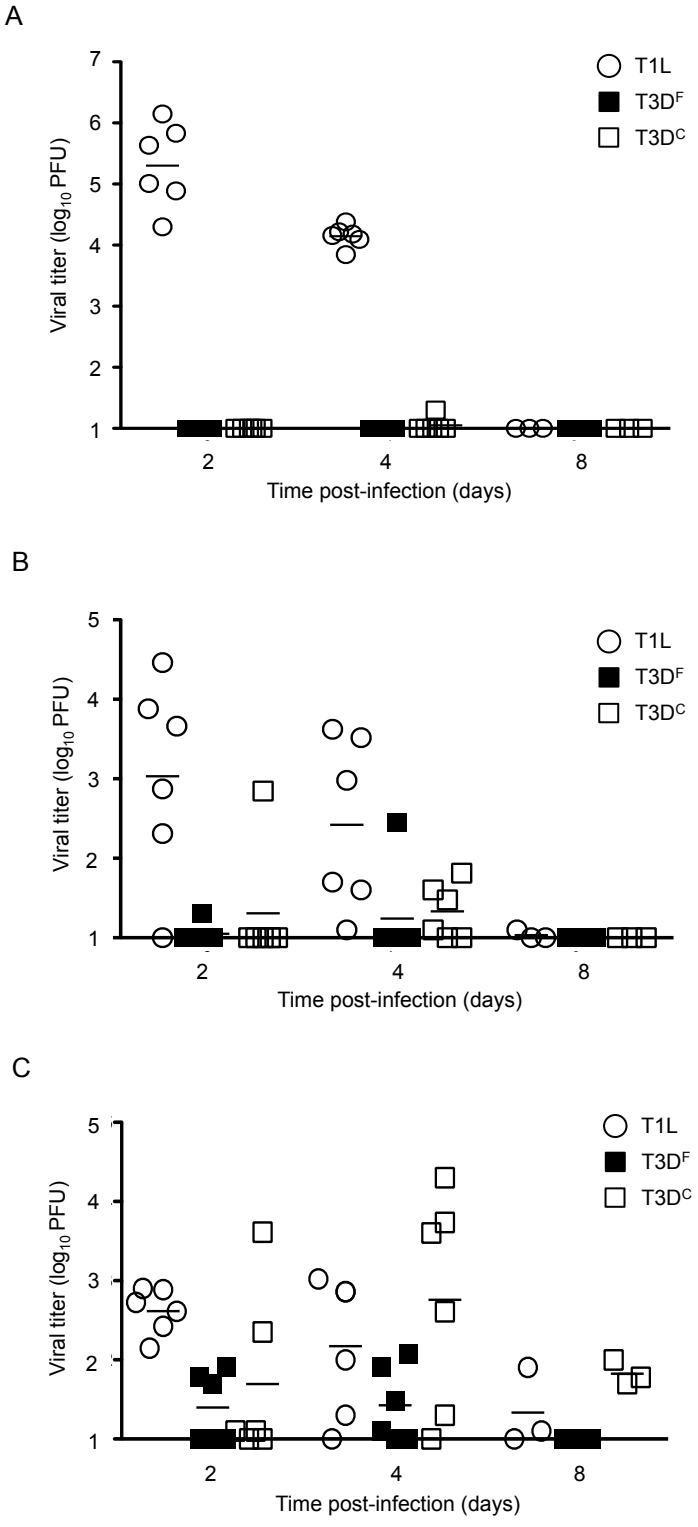
A
B
C
T1L
T3D^F
T3D^C
Viral titer (log_{10} PFU)
Time post-infection (days)
1
2
3
4
5
6
7
2
4
8

not solely based upon sensitivity of the cell attachment protein to cleavage as previously thought. This is consistent with our respiratory infection model in that $T3D^C$ polymorphisms in S1 lesson protease-mediated cleavage of σ1 and promote systemic dissemination.

Text S5.3

To determine if polymorphisms in $T3D^C$ altered protease mediated cleavage of σ1, virions of $T3D^F$ and $T3D^C$ were digested *in vitro* with a serine protease HAT. Digestion was stopped and viral proteins were resolved by SDS-PAGE and visualized by Coomassie blue staining (Fig. S4.3A). There is no significant difference in λ band intensity, which demonstrates that equivalent numbers of $T3D^F$ and $T3D^C$ particles were analyzed in each treatment group. Prior to staining, gels were transferred to a nitrocellulose filter and probed with a polyclonal anti-reovirus antibody. Consistent with our previous results, we observed that HAT cleaves σ3, as demonstrated by decreased σ3 band intensity after protease treatment (Fig. S5.3B). The polymorphism in σ1 at amino acid 249 results in trypsin and CHT (serine protease) cleavage products with a molecular weight of around 25 kDa (37). A band at the expected weight is resolved after HAT (32.5 ng/ml) treatment of $T3D^F$ and $T3D^C$ (Fig. S53B, arrow). These results demonstrate that HAT treatment of $T3D^F$ and $T3D^C$ results in cleavage of the cell attachment protein σ1.

To further characterize $T3D^F$ and $T3D^C$ σ1 after treatment with HAT, the membrane was reprobed with a polyclonal anti-reovirus antibody directed against the head portion of σ1 (22). We observed 3 distinct forms of σ1 after HAT treatment of $T3D^C$ virions, but only 2 of 3 forms in HAT treated $T3D^F$ particles (Fig. S5.3C). HAT (32.5 ng/ml) treatment of $T3D^F$ and $T3D^C$ virions resulted in near equivalent ratios of cleaved to intact σ1. This suggests that $T3D^F$ and $T3D^C$ do not significantly differ in their sensitivity to protease-mediated cleavage of σ1 after treatment with HAT. Interestingly, we observed significantly higher intensity of σ1 monomers and trimers associated with $T3D^C$ particles. Regions in the N-terminal portion of σ1 are known to be responsible for σ1 encapsidation (141). Interestingly, the $T3D^C$ S1 sequence at nucleotide 77 is within this region. These preliminary results suggest that $T3D^C$ sequences in S1 may promote σ1 encapsidation and trimerization.

Fig. S5.3. Digestion of reovirus strains $T3D^F$ and $T3D^C$ with the endogenous respiratory protease HAT. Purified virions were untreated or treated with indicated concentrations of HAT for 2 h. Reactions were stopped with PMSF (1mM). Treated virus was loaded into wells of 4-20% gradient polyacrylamide gels. After electrophoresis, the gels were transferred to a nitrocellulose filter and the gel was stained with (A) Coomassie blue. The filter was incubated with polyclonal antibodies directed against (B) reovirus particles or the (C) σ1 head (22). (A and B) Viral proteins λ, μ1C, δ, σ1, σ2, and σ3 are labeled at the right. An arrow marks the expected σ1 cleavage product (37). (C) σ1 trimer, monomer and fragment are labeled at the right. We quantified the σ1 fragment and monomer bands by Image J analysis and found that the monomer to fragment ratio of $T3D^C$ was 1:1.5 while $T3D^F$ was 1:1.2. The experiments shown are preliminary results.

Fig. S5.3

A

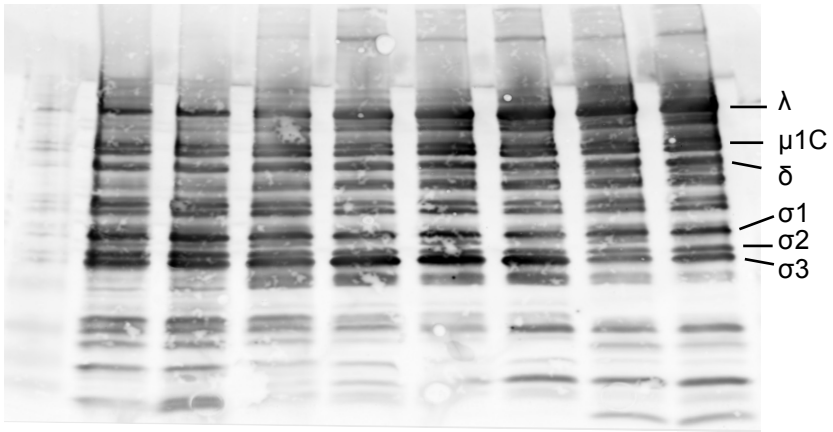

Reovirus strain:	$T3D^C$	$T3D^F$	$T3D^C$	$T3D^F$	$T3D^C$	$T3D^F$	$T3D^C$	$T3D^F$
HAT concentration:	Untreated		0.325 ng/μl		3.25 ng/μl		32.5 ng/μl	

B

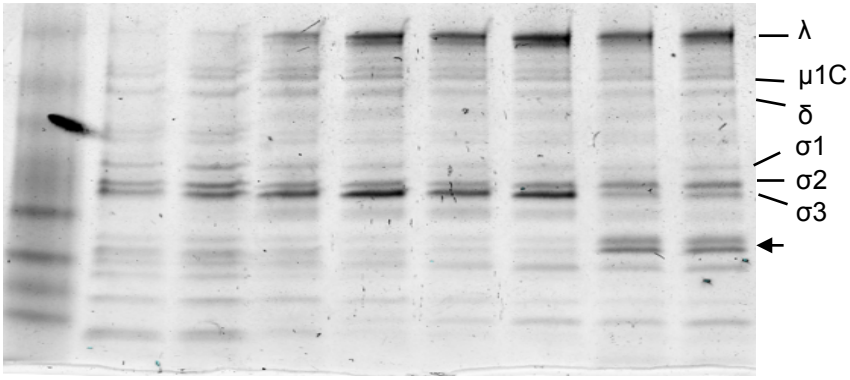

Reovirus strain:	$T3D^C$	$T3D^F$	$T3D^C$	$T3D^F$	$T3D^C$	$T3D^F$	$T3D^C$	$T3D^F$
HAT concentration:	Untreated		0.325 ng/μl		3.25 ng/μl		32.5 ng/μl	

C

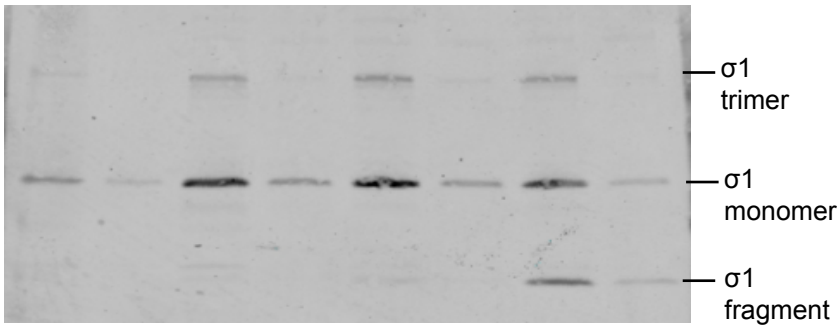

Reovirus strain:	$T3D^C$	$T3D^F$	$T3D^C$	$T3D^F$	$T3D^C$	$T3D^F$	$T3D^C$	$T3D^F$
HAT concentration:	Untreated		0.325 ng/μl		3.25 ng/μl		32.5 ng/μl	

CHAPTER 6

Major Conclusions and Outstanding Questions

Viral and host determinants that regulate reovirus infection of the intestine, CNS and heart are well established (110, 144, 199, 218, 219, 229, 232). However prior to the work described in this thesis, relatively little was known about reovirus infection in the respiratory tract. We sought to characterize reovirus pathogenesis after respiratory infection. To accomplish this goal, we developed a murine model of respiratory reovirus infection and our results suggest that reovirus disassembly in the respiratory tract was not as efficient or rapid as virion disassembly after gastrointestinal infection (20). In addition, we discovered that respiratory inflammation promotes viral replication in the respiratory tract (167). Through the course of this work, we found that two isolates of the prototypic strain T3D differed significantly in their capacity to replicate and disseminate after respiratory infection. Using the recently developed reovirus reverse genetics system (119, 120), we found that the $T3D^C$ S1 coding polymorphism at nucleotide 77 increased viral growth and dissemination. The work presented in this thesis has significantly contributed to the understanding of reovirus induced pathology, replication and dissemination after respiratory infection. It also raises many questions that remain to be answered and will be discussed in this chapter.

I. Endogenous and inflammatory respiratory proteases promote reovirus disassembly *in vitro*.

Results discussed in Chapter 4 demonstrate that both endogenous respiratory and inflammatory proteases can mediate reovirus disassembly (167). We examined two endogenous respiratory proteases, HAT and TMPRSS2, which have been shown to activate influenza and SARS coronavirus membrane fusion (15, 16, 27, 28, 83, 196, 204), for their capacity to initiate reovirus disassembly. Both HAT and TMPRSS2 promoted reovirus infection in a restrictive cell line (85) and *in vitro* treatment with HAT triggered reovirus uncoating and generated ISVPs. These are the first known respiratory proteases that have been shown to mediate productive reovirus disassembly. As mentioned in Chapter 4, although we were not able to identify conditions that promoted TMPRSS2-mediated reovirus disassembly *in vitro,* we did show that TMPRSS2 promotes reovirus infection in cell culture. TMPRSS2 overexpression is common in prostate cancers (130, 216). Since reovirus uncoating is key to reovirus' oncolytic potential (1), identifying proteases and the mechanisms of reovirus disassembly is critical to optimally generate oncolytic reoviruses that match a specific tumor protease profile.

Prior work from our laboratory had established that the inflammatory proteases NE and Cat S can mediate reovirus uncoating (84, 86). We assessed reovirus uncoating in the presence of mast cell chymase and another PMN-

associated protease, Cat G. Both of these inflammatory proteases promoted reovirus disassembly and generation of ISVPs. Thus, the experiments described in Chapter 4 led to the identification of four new proteases that can initiate reovirus disassembly, however the efficiency of *in vitro* virion disassembly differed, depending on the protease. This may be an artifact of suboptimal treatment conditions, but could be related to differences in protease specificity. A wide range of proteases can cleave the protease sensitive region of σ3, however the capacity of different proteases to initiate σ3 cleavage varies between reovirus strains and can be influenced by residues near the protease sensitive region on σ3 (62, 106, 148, 197, 233).

The apparent universal and, possibly, redundant nature of host proteases that can mediate σ3 cleavage suggests that, in order to optimize reovirus use as an oncolytic agent, a library of σ3 sequences paired with optimal protease cleavage partners should be generated. Specific residues that influence CHT-mediated reovirus uncoating, including those that slow disassembly kinetics, have recently been identified (59). These can function as a starting point for further study into host proteases that mediate reovirus disassembly. Studies should begin with proteases discussed in Chapter 4 and include proteases (MMP9, MMP2, and TMPRSS4) which are associated with increased expression in tumors (183, 235). Once protease - σ3 sequence pairs have been identified

and tested in tumor cell culture lines, murine xenograft models could be used to test reovirus oncolytic efficacy *in vivo*.

II. Respiratory inflammation promotes reovirus replication in the respiratory tract.

Viral and bacterial infections often exacerbate chronic inflammatory respiratory diseases (173). Inflammation, in turn, can influence viral infection. For example, influenza virus replicates to higher titers and infection is resolved more slowly in chronically inflamed lungs (87). One possible mechanism for this effect involves changes in protease expression in inflamed tissue. Inflammation increases protease expression that can promote viral infection of respiratory viruses that require host protease activity to establish infection (173). The inflammatory protease NE has been shown to promote SARS coronavirus and reovirus infection in cell culture (14, 86, 146). In Chapter 4, we presented evidence that respiratory inflammation promotes reovirus infection in murine lungs. The mechanism behind the increased viral loads observed in inflamed lungs is unknown. However, we found that inflammation led to a significant influx of inflammatory cells and significantly increased reovirus uncoating in the respiratory lumen. Enhanced protease expression and an increase in target cells may account for the increased titers observed in the murine respiratory tract.

With the emergence of new respiratory viruses and drug-resistant influenza viruses, there is a critical need to develop new therapies to combat viral respiratory infections. Host proteases that are critical for infection represent potential targets for antiviral development (244). Protease inhibitor treatment has shown promise against RSV (166) and influenza (171, 245) in mouse models. This approach could be pursued in the reovirus infection models, which are more tractable than models of more pathogenic viruses. An aerosolized delivery mechanism for protease inhibitor studies in the murine model of respiratory infection would be ideal to characterize the efficacy of specific protease inhibitors on viral replication.

III. The $T3D^C$ σ1 polymorphisms impact reovirus capacity to replicate and disseminate after respiratory tract infection.

In the course of our studies, we discovered that two isolates of type 3 strain Dearing differ in their capacity to replicate in the respiratory tract and disseminate systemically. Results of our genetic analysis reveal that the $T3D^C$ S1 gene promotes viral replication and systemic dissemination. The $T3D^C$ and $T3D^F$ S1 genes differ in two nucleotides that result in amino acid polymorphisms. Each $T3D^C$ polymorphism influences viral replication in the lungs. The polymorphism at nucleotide 77 enhances viral replication in the lungs while the $T3D^C$ polymorphism at nucleotide 1234 dampens viral replication relative to wildtype

$T3D^F$. Several questions regarding the role of $T3D^C$ polymorphisms in σ1 have arisen from the studies detailed in Chapter 5 and will be outlined here.

Our studies reveal that reovirus uncoating in the respiratory tract is less efficient than uncoating in the gastrointestinal tract, where uncoating occurs within 5 min (20). While the proteases that mediate reovirus uncoating in the respiratory tract are unknown, the lungs maintain a protease:antiprotease balance in the absence of pathology (52, 151, 238). In this environment, reovirus strains that rapidly disassemble or can utilize a wider range of proteases for disassembly would have an advantage in establishing respiratory tract infection. A number of different studies demonstrate that reovirus strains can differ in capacity be uncoated by host proteases (4, 45, 233). Unpublished work from our lab reveals that a wider range of cellular proteases can mediate $T3D^C$ uncoating compared to $T3D^F$. The capacity to use a wider range of cellular proteases may increase host cell range and replication, which may account for $T3D^C$'s enhanced replication and dissemination compared to $T3D^F$ in the respiratory model. Recent work demonstrates that mutations in the S4 protein show enhanced pathogenesis (unpublished). Our lab is currently working to characterize differences in protease-mediated disassembly of T3D isolates.

The failure of T3D to replicate in the gastrointestinal tract is due to protease-mediated cleavage of the cell attachment protein. Both $T3D^F$ and $T3D^C$

share the sequence at amino acid 249, which confers this sensitivity to protease-mediated cleavage of σ1. However, the $T3D^C$ σ1 protein contains two alanine substitutions at amino acids 22 and 408 that promote resistance to protease-mediated cleavage. This result indicates that sequences outside the known protease sensitive site in σ1 function to stabilize σ1 in the presence of protease. We analyzed the published sequences of the σ1 protein of isolates resistant to cleavage, and while they all share the polymorphism at amino acid 249, we found that they all contain an additional polymorphism at amino acid 22 and a majority of the clones also contained polymorphisms at amino acid 408 (Table 6.1) (37, 55, 160). These amino acids coincide with the changes in the $T3D^C$ S1 gene that reduce protease-mediated inactivity. Thus, while amino acid 249 may be the primary determinant for CHT-mediated cleavage of σ1, $T3D^C$ residues at amino acids 22 and 408 likely contribute to σ1 stability. We are currently examining the impact of $T3D^C$ residues in S1 on the rate of σ1 cleavage.

Interestingly, our preliminary results suggest that the T3D isolates do not differ in sensitivity to protease-mediated cleavage of σ1. Protease treatment of $T3D^C$ or $T3D^F$ virions results in near equivalent ratios of full-length σ1 to the σ1 fragment. Interestingly, we noticed that $T3D^C$ virions have significantly more virion-associated σ1 than $T3D^F$ virions even prior to protease treatment. This suggests that the increased rate at which $T3D^F$ loses infectivity in the presence of protease, relative to $T3D^C$, may not be due to the sensitivity of σ1 to cleavage but

Table 6.1. Comparison of σ1 polymorphisms in type 3 reovirus clones. Sequences and sensitivity to protease-mediated cleavage were obtained from published reports and confirmed experimentally in the case of $T3D^F$ (37). *Preliminary results suggest that $T3D^C$ is susceptible to protease-mediated cleavage.

Table 6.1

Virus	Sensitive to protease-mediated cleavage	Amino acid		
		249	22	408
$T3D^F$	Y	T	V	T
$T3D^C$	Y*	T	A	A
T3C9	N	I	A	T
T3C18	N	I	A	T
T3C43	N	I	I	A
T3C44	N	I	I	A
T3C45	N	I	I	A
T3C84	N	I	I	A
T3C93	N	I	I	A

in the quantity of encapsidated σ1. Mechanisms of σ1 trimerization and encapsidation are not well understood. However, the structure between amino acids 3 and 34 is known to be important for virion anchoring (125, 142). The $T3D^C$ alanine change at amino acid 22 in σ1 is within this region (50, 62). This suggests that $T3D^C$ alanine 22 may increase σ1 encapsidation.

Our results show that both $T3D^C$ sequences in σ1 have a stabilizing effect on virion infectivity in the presence of protease, however these changes have distinct effects on viral replication *in vivo*. The $T3D^C$ sequence at amino acid 22 promotes dissemination while the sequence at amino acid 408 appears to promote viral clearance. However, these residues are not associated with any known epitope recognition, receptor binding or protease sensitive region (31, 37, 38, 88, 91, 116, 123, 157, 159, 161, 185, 221, 240). Hydrophobic residues in the tail and base of the head are thought to be responsible for σ1 trimer stabilization (39, 185), however numerous acid residues in the head of σ1 are proposed to increase σ1 trimer instability (39). The $T3D^C$ 408 polymorphism impacts the head of σ1. We currently do not understand how this change leads to lower viral titers in the lungs of animals inoculated with rs$T3D^F$/$T3D^C$S1-1234. We are currently collaborating with Dr. Terry Dermody to characterize the impact of alanine 22 and alanine 408 on the quantity of virion-associated σ1, changes in protease-mediated cleavage patterns, and changes in σ1 trimer stability. It will be

important to also determine how or if these polymorphisms impact σ1 association cellular receptors.

IV. The T3D^C σ1s protein enhances viral replication in the lungs and hematogenous dissemination.

My work revealed that T3D isolates differ in capacity to replicate in the lungs and spread systemically. The T3D^C S1 polymorphism at nucleotide 77 significantly enhanced viral replication and dissemination after intranasal inoculation. As discussed above, the T3D^C polymorphism at nucleotide 77 impacts the cell attachment protein σ1. As the S1 gene expresses two viral proteins in overlapping reading frames, the T3D^C change at nucleotide 77 also creates a glutamine to histidine change at amino acid 3 in the nonstructural protein σ1s. The importance of σ1s in viral replication and dissemination has recently been established (21, 22). The σ1s protein is required to reach peak titers in the gastrointestinal tract after oral inoculation and promotes hematogenous reovirus dissemination after peroral and muscular inoculation (21, 22). Our results demonstrate that T3D^C σ1s promotes reovirus replication in the respiratory tract and hematogenous dissemination. Several questions regarding the role of the T3D^C polymorphism in σ1s have arisen from the studies detailed in Chapter 5 and will be outlined here.

The mechanism by which σ1s promotes replication *in vivo* remains unknown. The σ1s protein is required to induce apoptosis *in vivo* and reovirus-induced apoptosis increases progeny release from infected cells (97, 143). One possible mechanism by which σ1s may promote viral replication is by inducing cellular apoptosis, which, in turn, could increase release of reovirus progeny. Recent work from our lab demonstrates that $T3D^C$ induces significantly higher levels of apoptosis than $T3D^F$ in cell culture. In addition, progeny release is significantly more efficient after $T3D^C$ infection compared to $T3D^F$ infection in cell culture (unpublished observation). Decreased progeny release may explain the lower viral yields in lungs we observed after inoculation with $T3D^C$ σ1s-null viruses. Future experiments will be aimed at characterizing the role of σ1s in reovirus induced apoptosis and release.

Many viruses encode nonstructural proteins that disrupt innate and adaptive immune response mechanisms to evade detection and delay viral clearance. For example, rotavirus NSP1 antagonizes innate immune responses by mediating degradation of IFN-regulatory factors (198). It is possible that σ1s disrupts innate or adaptive immune mechanisms and the absence of σ1s leads to more rapid reovirus clearance. A $rsT3D^F/T3D^C$S1 virus lacking σ1s does not replicate to high titers and appears to clear more rapidly from the lungs. Future studies should characterize the host immune response to the panel of viruses we

generated and described in Chapter 5, this will help identify any role of σ1s in immune disruption.

After peroral or intramuscular inoculation of σ1s-null viruses, viral replication in secondary sites is delayed but peak titers do not significantly differ (21, 22). This delay is due to a block in access to hematogenous routes for dissemination. Our results also show that σ1s promotes hematogenous access after intranasal inoculation, but does not significantly influence dissemination to the spleen. However, the majority of σ1s-null viruses recovered after systemic dissemination were revertant viruses which express $T3D^C$ σ1s. This suggests that the $T3D^C$ σ1s protein is important for access to and replication at secondary sites. The mechanisms by which σ1s promotes reovirus dissemination are currently unknown. As discussed above, the reovirus σ1s protein may influence reovirus replication by mediating apoptosis or immune modulation (97, 180, 181). These same mechanisms may be important for hematogenous dissemination. Histological studies following inoculation with σ1s-null viruses will help characterize the role of σ1s in reovirus infection of the respiratory tract and if it is required for replication in specific cell types. To determine if reovirus spreads through hematogenous routes by cell-free, cell-associated or a combination, blood components could be separated and reovirus positive cells could be detected by flow cytometry. In addition, virus present in the serum could be

quantified by plaque assay. These experiments will help determine the mechanism by which $T3D^C$ σ1s protein promotes reovirus dissemination.

V. What other genetic polymorphisms contribute to $T3D^C$ enhanced replication and dissemination *in vivo*?

Virion disassembly is an important determinant for reovirus-mediated apoptosis and viral replication *in vivo* (1, 20). We considered that virion disassembly, which are regulated by the reovirus S4 and M2 genes, may influence viral replication in the respiratory tract (4, 194, 197). Based on this, we examined the role of the $T3D^C$ S4 and M2 genes in reovirus replication in the respiratory tract. Upon intranasal inoculation, we found that titers of $T3D^F$ viruses with $T3D^C$ S4 or $T3D^C$ S4 and M2 genes are recovered at lower titers in the lungs than titers of wildtype $T3D^F$. These results suggest that the $T3D^C$ polymorphisms in the S4 and M2 genes do not significantly influence reovirus replication in the murine respiratory tract.

Interesting recent work demonstrates that the reovirus M1 gene modulates the host immune response. Irvin and colleagues found that the reovirus M1 gene, which expresses the μ2 protein, regulates the IFN response in cardiac myocytes and fibroblasts (93, 102, 128, 246). Reovirus capacity to block IFN production depends upon a proline to serine polymorphism in the μ2 protein at amino acid 208 (102). T1L, which encodes serine 208, inhibits IFN production while infection

with $T3D^F$, which lacks this polymorphism, does not (102). Interestingly, the $T3D^C$ M1 gene also encodes the serine 208 polymorphism. This suggests that the capacity of T1L and $T3D^C$ to replicate to high titers in the respiratory tract and disseminate may be influenced by modulation of the host immune response. Future studies will examine the role of the $T3D^C$ polymorphisms in the M1 gene on viral replication in the respiratory tract and systemic reovirus dissemination.

In conclusion, the work contained within this thesis has demonstrated for the first time that endogenous respiratory and inflammatory proteases that can mediate reovirus disassembly and that respiratory inflammation promotes reovirus replication in the lungs. In addition, we described genetic polymorphisms in prototypic T3D isolates that regulate reovirus infection and dissemination in a murine model of respiratory infection. In conclusion, the capacity of $T3D^C$ to replicate and disseminate systemically is likely influenced by multiple mechanisms including increased σ1 encapsidation, resistance to protease-mediated inactivation and a property of the nonstructural protein σ1s, such as efficient induction of apoptosis. It is my hope that the work in this thesis has laid the foundation for future research examining mechanisms of reovirus replication and dissemination *in vivo*.

References

1. **Alain, T., T. S. Kim, X. Lun, A. Liacini, L. A. Schiff, D. L. Senger, and P. A. Forsyth.** 2007. Proteolytic disassembly is a critical determinant for reovirus oncolysis. Mol. Ther. **15:**1512-1521.
2. **Altiok, O., R. Yasumatsu, G. Bingol-Karakoc, R. J. Riese, M. T. Stahlman, W. Dwyer, R. A. Pierce, D. Bromme, E. Weber, and S. Cataltepe.** 2006. Imbalance between cysteine proteases and inhibitors in a baboon model of bronchopulmonary dysplasia. Am. J. Respir. Crit. Care Med. **173:**318-326.
3. **Amerongen, H. M., G. A. Wilson, B. N. Fields, and M. R. Neutra.** 1994. Proteolytic processing of reovirus is required for adherence to intestinal M cells. J. Virol. **68:**8428-8432.
4. **Baer, G. S., and T. S. Dermody.** 1997. Mutations in reovirus outer-capsid protein sigma3 selected during persistent infections of L cells confer resistance to protease inhibitor E64. J. Virol. **71:**4921-4928.
5. **Baer, G. S., D. H. Ebert, C. J. Chung, A. H. Erickson, and T. S. Dermody.** 1999. Mutant cells selected during persistent reovirus infection do not express mature cathepsin L and do not support reovirus disassembly. J. Virol. **73:**9532-9543.
6. **Bando, Y., E. Kominami, and N. Katunuma.** 1986. Purification and tissue distribution of rat cathepsin L. Journal of Biochemistry (Tokyo) **100:**35-42.
7. **Barrett, A. J., and H. Kirschke.** 1981. Cathepsin B, Cathepsin H, and cathepsin L. Methods Enzymol. **80 Pt C:**535-561.
8. **Barton, E. S., J. L. Connolly, J. C. Forrest, J. D. Chappell, and T. S. Dermody.** 2001. Utilization of sialic acid as a coreceptor enhances reovirus attachment by multistep adhesion strengthening. J. Biol. Chem. **276:**2200-2211.
9. **Barton, E. S., J. C. Forrest, J. L. Connolly, J. D. Chappell, Y. Liu, F. J. Schnell, A. Nusrat, C. A. Parkos, and T. S. Dermody.** 2001. Junction adhesion molecule is a receptor for reovirus. Cell **104:**441-451.
10. **Bass, D. M., D. Bodkin, R. Dambrauskas, J. S. Trier, B. N. Fields, and J. L. Wolf.** 1990. Intraluminal proteolytic activation plays an important role in replication of type 1 reovirus in the intestines of neonatal mice. J. Virol. **64:**1830-1833.
11. **Bastian, T. W., and S. A. Rice.** 2009. Identification of sequences in herpes simplex virus type 1 ICP22 that influence RNA polymerase II modification and viral late gene expression. J. Virol. **83:**128-139.
12. **Beckham, J. D., K. D. Tuttle, and K. L. Tyler.** 2010. Caspase-3 activation is required for reovirus-induced encephalitis in vivo. J. Neurovirol. **16:**306-317.
13. **Bellum, S. C., D. Dove, R. A. Harley, W. B. Greene, M. A. Judson, L. London, and S. D. London.** 1997. Respiratory reovirus 1/L induction of

intraluminal fibrosis: A model for the study of bronchiolitis obliterans organizing pneumonia. Am. J. Pathol. **150:**2243-2254.

14. **Belouzard, S., I. Madu, and G. R. Whittaker.** 2010. Elastase-mediated activation of the severe acute respiratory syndrome coronavirus spike protein at discrete sites within the S2 domain. J. Biol. Chem. **285:**22758-22763.
15. **Bertram, S., I. Glowacka, P. Blazejewska, E. Soilleux, P. Allen, S. Danisch, I. Steffen, S.-Y. Choi, Y. Park, H. Schneider, K. Schughart, and S. Pöhlmann.** 2010. TMPRSS2 and TMPRSS4 facilitate trypsin-independent influenza virus spread in Caco-2 cells. J. Virol. **84:**10016-10025.
16. **Bertram, S., I. Glowacka, M. a. Müller, H. Lavender, K. Gnirß, I. Nehlmeier, D. Niemeyer, Y. He, G. Simmons, C. Drosten, E. J. Soilleux, O. Jahn, I. Steffen, and S. Pöhlmann.** 2011. Cleavage and activation of the SARS-coronavirus spike-protein by human airway trypsin-like protease (HAT). J. Virol.
17. **Bertram, S., I. Glowacka, and I. Steffen.** 2010. Novel insights into proteolytic cleavage of influenza virus hemagglutinin. Reviews in Medical Virology**:**298-310.
18. **Bharhani, M. S., J. S. Grewal, R. Peppler, C. Enockson, L. London, and S. D. London.** 2007. Comprehensive phenotypic analysis of the gut intra-epithelial lymphocyte compartment: perturbations induced by acute reovirus 1/L infection of the gastrointestinal tract. Int. Immunol. **19:**567-579.
19. **Bodkin, D. K., and B. N. Fields.** 1989. Growth and survival of reovirus in intestinal tissue: role of the L2 and S1 genes. J. Virol. **63:**1188-1193.
20. **Bodkin, D. K., M. L. Nibert, and B. N. Fields.** 1989. Proteolytic Digestion of Reovirus in the intestinal lumens of neonatal mice. J. Virol. **63:**4676-4681.
21. **Boehme, K. W., J. M. Frierson, J. L. Konopka, T. Kobayashi, and T. S. Dermody.** 2011. The Reovirus {sigma}1s Protein Is a Determinant of Hematogenous but Not Neural Viral Dissemination in Mice. J. Virol.
22. **Boehme, K. W., K. M. Guglielmi, and T. S. Dermody.** 2009. Reovirus nonstructural protein sigma1s is required for establishment of viremia and systemic dissemination. Proc. Natl. Acad. Sci. U. S. A. **106:**19986-19991.
23. **Boehme, K. W., M. Ikizler, T. Kobayashi, and T. S. Dermody.** 2011. Reverse genetics for mammalian reovirus. Methods (San Diego, Calif.)**:**1-5.
24. **Borsa, J., T. P. Copps, M. D. Sargent, D. G. Long, and J. D. Chapman.** 1973. New intermediate subviral particles in the in vitro uncoating of reovirus virions by chymotrypsin. J. Virol. **11:**552-564.
25. **Borsa, J., and A. F. Graham.** 1968. Reovirus: RNA polymerase activity in purified virions. Biochem. Biophys. Res. Commun. **33:**895-901.

26. **Borsa, J., B. D. Morash, M. D. Sargent, T. P. Copps, P. A. Lievaart, and J. G. Szekely.** 1979. Two modes of entry of reovirus particles into L cells. J. Gen. Virol. **45:**161-170.
27. **Böttcher, E., C. Freuer, T. Steinmetzer, H.-D. Klenk, and W. Garten.** 2009. MDCK cells that express proteases TMPRSS2 and HAT provide a cell system to propagate influenza viruses in the absence of trypsin and to study cleavage of HA and its inhibition. Vaccine **27:**6324-6329.
28. **Böttcher, E., T. Matrosovich, M. Beyerle, H.-D. Klenk, W. Garten, and M. Matrosovich.** 2006. Proteolytic activation of influenza viruses by serine proteases TMPRSS2 and HAT from human airway epithelium. J. Virol. **80:**9896-9898.
29. **Böttcher-Friebertshäuser, E., C. Freuer, F. Sielaff, S. Schmidt, M. Eickmann, J. Uhlendorff, T. Steinmetzer, H.-D. Klenk, and W. Garten.** 2010. Cleavage of influenza virus hemagglutinin by airway proteases TMPRSS2 and HAT differs in subcellular localization and susceptibility to protease inhibitors. J. Virol. **84:**5605-5614.
30. **Buchholz, U. J., S. Finke, and K. K. Conzelmann.** 1999. Generation of bovine respiratory syncytial virus (BRSV) from cDNA: BRSV NS2 is not essential for virus replication in tissue culture, and the human RSV leader region acts as a functional BRSV genome promoter. J. Virol. **73:**251-259.
31. **Campbell, J. A., P. Schelling, J. D. Wetzel, E. M. Johnson, J. C. Forrest, G. A. Wilson, M. Aurrand-Lions, B. A. Imhof, T. Stehle, and T. S. Dermody.** 2005. Junctional adhesion molecule a serves as a receptor for prototype and field-isolate strains of mammalian reovirus. J. Virol. **79:**7967-7978.
32. **Cashdollar, L. W., R. A. Chmelo, J. R. Wiener, and W. K. Joklik.** 1985. Sequences of the S1 genes of the three serotypes of reovirus. Proc. Natl. Acad. Sci. U. S. A. **82:**24-28.
33. **Chaipan, C., D. Kobasa, S. Bertram, I. Glowacka, I. Steffen, T. S. Tsegaye, M. Takeda, T. H. Bugge, S. Kim, Y. Park, A. Marzi, and S. Pöhlmann.** 2009. Proteolytic activation of the 1918 influenza virus hemagglutinin. J. Virol. **83:**3200-3211.
34. **Chandran, K., and M. L. Nibert.** 1998. Protease cleavage of reovirus capsid protein mu1/mu1C is blocked by alkyl sulfate detergents, yielding a new type of infectious subvirion particle. J. Virol. **72:**467-475.
35. **Chandran, K., J. S. Parker, M. Ehrlich, T. Kirchhausen, and M. L. Nibert.** 2003. The delta region of outer-capsid protein micro 1 undergoes conformational change and release from reovirus particles during cell entry. J. Virol. **77:**13361-13375.
36. **Chandran, K., J. S. L. Parker, M. Ehrlich, T. Kirchhausen, and M. L. Nibert.** 2003. The δ region of outer-capsid protein μ 1 undergoes conformational change and release from reovirus particles during cell entry. J. Virol. **77:**13361-13375.

37. **Chappell, J. D., E. S. Barton, T. H. Smith, G. S. Baer, D. T. Duong, M. L. Nibert, and T. S. Dermody.** 1998. Cleavage susceptibility of reovirus attachment protein sigma1 during proteolytic disassembly of virions is determined by a sequence polymorphism in the sigma1 neck. J. Virol. **72:**8205-8213.
38. **Chappell, J. D., J. L. Duong, B. W. Wright, and T. S. Dermody.** 2000. Identification of carbohydrate-binding domains in the attachment proteins of type 1 and type 3 reoviruses. J. Virol. **74:**8472-8479.
39. **Chappell, J. D., A. E. Prota, T. S. Dermody, and T. Stehle.** 2002. Crystal structure of reovirus attachment protein sigma1 reveals evolutionary relationship to adenovirus fiber. EMBO J. **21:**1-11.
40. **Chen, J., K. Lee, D. Steinhauer, D. Stevens, J. Skehel, and D. Wiley.** 1998. Structure of the hemagglutinin precursor cleavage site, a determinant of influenza pathogenicity and the origin of the labile conformation. Cell **95:**409-417.
41. **Chokki, M., S. Yamamura, H. Eguchi, T. Masegi, H. Horiuchi, H. Tanabe, T. Kamimura, and S. Yasuoka.** 2004. Human airway trypsin-like protease increases mucin gene expression in airway epithelial cells. Am. J. Respir. Cell Mol. Biol. **30:**470-478.
42. **Chow, N.-L., and A. J. Shatkin.** 1975. Blocked and unblocked 5 termini in reovirus genome RNA. J. Virol. **15:**1057-1064.
43. **Chua, K. B., G. Crameri, A. Hyatt, M. Yu, M. R. Tompang, J. Rosli, J. McEachern, S. Crameri, V. Kumarasamy, B. T. Eaton, and L.-F. Wang.** 2007. A previously unknown reovirus of bat origin is associated with an acute respiratory disease in humans. Proc. Natl. Acad. Sci. U. S. A. **104:**11424-11429.
44. **Chua, K. B., K. Voon, G. Crameri, H. S. Tan, J. Rosli, J. A. McEachern, S. Suluraju, M. Yu, and L.-F. Wang.** 2008. Identification and characterization of a new orthoreovirus from patients with acute respiratory infections. PloS one **3:**e3803-e3803.
45. **Clark, K. M., J. D. Wetzel, Y. Gu, D. H. Ebert, S. A. McAbee, E. K. Stoneman, G. S. Baer, Y. Zhu, G. J. Wilson, B. V. Prasad, and T. S. Dermody.** 2006. Reovirus variants selected for resistance to ammonium chloride have mutations in viral outer-capsid protein sigma3. J. Virol. **80:**671-681.
46. **Clarke, P., J. D. Beckham, J. S. Leser, C. C. Hoyt, and K. L. Tyler.** 2009. Fas-mediated apoptotic signaling in the mouse brain following reovirus infection. J. Virol. **83:**6161-6170.
47. **Coffey, C. M., A. Sheh, I. S. Kim, K. Chandran, M. L. Nibert, and J. S. L. Parker.** 2006. Reovirus outer capsid protein micro1 induces apoptosis and associates with lipid droplets, endoplasmic reticulum, and mitochondria. J. Virol. **80:**8422-8438.

48. **Connor, R., Y. Kawaoka, R. Webster, and J. Paulson.** 1994. Receptor specificity in human, avian, and equine H2 and H3 influenza virus isolates. Virology **205:**17-23.
49. **Cook, D. N., and K. Bottomly.** 2007. Innate immune control of pulmonary dendritic cell trafficking. Proceedings of the American Thoracic Society **4:**234-239.
50. **Coombs, K. M., B. N. Fields, and S. C. Harrison.** 1990. Crystallization of the reovirus type 3 Dearing core. Crystal packing is determined by the lambda 2 protein. J. Mol. Biol. **215:**1-5.
51. **Crosby, L. M., and C. M. Waters.** 2010. Epithelial repair mechanisms in the lung. Am. J. Physiol. Lung Cell Mol. Physiol. **298:**715-731.
52. **Davies, P. L., O. B. Spiller, M. L. Beeton, N. C. Maxwell, E. Remold-O'Donnell, and S. Kotecha.** 2010. Relationship of proteinases and proteinase inhibitors with microbial presence in chronic lung disease of prematurity. Thorax **65:**246-251.
53. **Debiasi, R. L., B. A. Robinson, B. Sherry, R. Bouchard, R. D. Brown, M. Rizeq, C. Long, K. L. Tyler, and N. Carolina.** 2004. Caspase Inhibition Protects against Reovirus-Induced Myocardial Injury In Vitro and In Vivo. J. Virol. **78:**11040-11050.
54. **Dechert, R.** 2003. The pathophysiology of acute respiratory distress syndrome. Respiratory Care Clinics **9:**283-296.
55. **Dermody, T. S., M. L. Nibert, R. Bassel-Duby, and B. N. Fields.** 1990. Sequence diversity in S1 genes and S1 translation products of 11 serotype 3 reovirus strains. J. Virol. **64:**4842-4850.
56. **Dermody, T. S., M. L. Nibert, J. D. Wetzel, X. Tong, and B. N. Fields.** 1993. Cells and viruses with mutations affecting viral entry are selected during persistent infections of L cells with mammalian reoviruses. J. Virol. **67:**2055-2063.
57. **Doerschuk, C. M.** 2000. Leukocyte trafficking in alveoli and airway passages. Respir. Res. **1:**136-140.
58. **Donaldson, S. H., A. Hirsh, D. C. Li, G. Holloway, J. Chao, R. C. Boucher, and S. E. Gabriel.** 2002. Regulation of the epithelial sodium channel by serine proteases in human airways. J. Biol. Chem. **277:**8338-8345.
59. **Doyle, J. D., P. Danthi, E. A. Kendall, L. S. Ooms, J. D. Wetzel, and T. S. Dermody.** 2012. Molecular determinants of proteolytic disassembly of the reovirus outer capsid. J. Biol. Chem.
60. **Drayna, D., and B. N. Fields.** 1982. Biochemical studies on the mechanism of chemical and physical inactivation of reovirus. J. Gen. Virol. **63:**161-170.
61. **Driessen, C., R. A. Bryant, A. M. Lennon-Dumenil, J. A. Villadangos, P. W. Bryant, G. P. Shi, H. A. Chapman, and H. L. Ploegh.** 1999. Cathepsin S controls the trafficking and maturation of MHC class II molecules in dendritic cells. J. Cell Biol. **147:**775-790.

62. **Dryden, K. A., G. Wang, M. Yeager, M. L. Nibert, K. M. Coombs, D. B. Furlong, B. N. Fields, and T. S. Baker.** 1993. Early steps in reovirus infection are associated with dramatic changes in supramolecular structure and protein conformation: analysis of virions and subviral particles by cryoelectron microscopy and image reconstruction. J. Cell Biol. **122:**1023-1041.
63. **Ebert, D. H., J. Deussing, C. Peters, and T. S. Dermody.** 2002. Cathepsin L and cathepsin B mediate reovirus disassembly in murine fibroblast cells. J. Biol. Chem. **277:**24609-24617.
64. **Ehrlich, M., W. Boll, A. Van Oijen, R. Hariharan, K. Chandran, M. L. Nibert, and T. Kirchhausen.** 2004. Endocytosis by random initiation and stabilization of clathrin-coated pits. Cell **118:**591-605.
65. **Ernst, H., and A. J. Shatkin.** 1985. Reovirus hemagglutinin mRNA codes for two polypeptides in overlapping reading frames. Proc. Natl. Acad. Sci. USA **82:**48-52.
66. **Fan, J. Y., C. S. Boyce, and C. F. Cuff.** 1998. T-Helper 1 and T-helper 2 cytokine responses in gut-associated lymphoid tissue following enteric reovirus infection. Cell. Immunol. **188:**55-63.
67. **Farone, a. L., C. W. Frevert, M. B. Farone, M. J. Morin, B. N. Fields, J. D. Paulauskis, and L. Kobzik.** 1996. Serotype-dependent induction of pulmonary neutrophilia and inflammatory cytokine gene expression by reovirus. J. Virol. **70:**7079-7084.
68. **Farone, A. L., S. M. O'Donnell, C. S. Brooks, K. M. Young, J. M. Pierce, J. D. Wetzel, T. S. Dermody, and M. B. Farone.** 2006. Reovirus strain-dependent inflammatory cytokine responses and replication patterns in a human monocyte cell line. Viral Immunol. **19:**546-557.
69. **Fields, B. N.** 1971. Temperature-sensitive mutants of reovirus type 3 features of genetic recombination. Virology **46:**142-148.
70. **Fields, B. N., and M. I. Greene.** 1982. Genetic and molecular mechanisms of viral pathogenesis: implications for prevention and treatment. Nature **300:**19-23.
71. **Fields, B. N., and W. K. Joklik.** 1969. Isolation and preliminary genetic and biochemical characterization of temperature-sensitive mutants of reovirus. Virology **37:**335-342.
72. **Fields, B. N., H. L. Weiner, D. T. Drayna, and A. H. Sharpe.** 1980. The role of Reovirus hemagglutinin in viral virulence. Annals New York Academy of Sciences.
73. **Flamand, A., J. P. Gagner, L. A. Morrison, and B. N. Fields.** 1991. Penetration of the nervous systems of suckling mice by mammalian reoviruses. J. Virol. **65:**123-131.
74. **Forrest, J. C., J. A. Campbell, P. Schelling, T. Stehle, and T. S. Dermody.** 2003. Structure-function analysis of reovirus binding to junctional adhesion molecule 1: Implications for the mechanism of reovirus attachment. J. Biol. Chem. **278:**48434-48444.

75. **Furlong, D. B., M. L. Nibert, and B. N. Fields.** 1988. Sigma 1 protein of mammalian reoviruses extends from the surfaces of viral particles. J. Virol. **62:**246-256.
76. **Furuichi, Y., M. Morgan, S. Muthukrishnan, and A. J. Shatkin.** 1975. Reovirus messenger RNA contains a methylated, blocked 5'-terminal structure: m-7G(5')ppp(5')G-MpCp-. Proc. Natl. Acad. Sci. U. S. A. **72:**362-366.
77. **Furuichi, Y., M. A. Morgan, and A. J. Shatkin.** 1979. Synthesis and translation of mRNA containing 5'-terminal 7-ethylguanosine cap. J. Biol. Chem. **254:**6732-6738.
78. **Furuichi, Y., S. Muthukrishnan, and A. J. Shatkin.** 1975. 5'-Terminal m-7G(5')ppp(5')G-m-p in vivo: identification in reovirus genome RNA. Proc. Natl. Acad. Sci. U. S. A. **72:**742-745.
79. **Gadek, J. E., and E. R. Pacht.** 1990. The protease-antiprotease balance within the human lung: implications for the pathogenesis of emphysema. Lung **168:**552-564.
80. **Garcia-Verdugo, I., D. Descamps, M. Chignard, L. Touqui, and J.-M. Sallenave.** 2010. Lung protease/anti-protease network and modulation of mucus production and surfactant activity. Biochimie **92:**1608-1617.
81. **Gentsch, J. R., and A. F. Pacitti.** 1985. Effect of neuraminidase treatment of cells and effect of soluble glycoproteins on type 3 reovirus attachment to murine L cells. J. Virol. **56:**356-364.
82. **George, A., S. Kost, C. L. Witzleben, J. J. Cebra, and D. H. Rubint.** 1990. Reovirus-induced liver disease in severe combined immunodeficient (SCID) mice. J. Exp. Med. **171:**929-934.
83. **Glowacka, I., S. Bertram, M. A. Müller, P. Allen, E. Soilleux, S. Pfefferle, I. Steffen, T. S. Tsegaye, Y. He, K. Gnirss, D. Niemeyer, H. Schneider, C. Drosten, and S. Pöhlmann.** 2011. Evidence that TMPRSS2 activates the SARS-coronavirus spike-protein for membrane fusion and reduces viral control by the humoral immune response. J. Virol. **85:**4122-4134.
84. **Golden, J. W., J. A. Bahe, W. T. Lucas, M. L. Nibert, and L. A. Schiff.** 2004. Cathepsin S supports acid-independent infection by some reoviruses. J. Biol. Chem. **279:**8547-8557.
85. **Golden, J. W., J. Linke, S. Schmechel, K. Thoemke, and L. A. Schiff.** 2002. Addition of exogenous protease facilitates reovirus infection in many restrictive cells. J. Virol. **76:**7430-7443.
86. **Golden, J. W., and L. A. Schiff.** 2005. Neutrophil elastase, an acid-independent serine protease, facilitates reovirus uncoating and infection in U937 promonocyte cells. Virol J. **2:**http://www.virologyj.com/content/2/1/48.
87. **Gualano, R. C., M. J. Hansen, R. Vlahos, J. E. Jones, R. a. Park-Jones, G. Deliyannis, S. J. Turner, K. a. Duca, and G. P. Anderson.**

2008. Cigarette smoke worsens lung inflammation and impairs resolution of influenza infection in mice. Respir. Res. **9:**53-70.

88. **Guglielmi, K. M., E. Kirchner, G. H. Holm, T. Stehle, and T. S. Dermody.** 2007. Reovirus binding determinants in junctional adhesion molecule-A. J. Biol. Chem. **282:**17930-17940.
89. **Haller, B. L., M. L. Barkon, X. Y. Li, W. M. Hu, J. D. Wetzel, T. S. Dermody, and H. W. Virgin.** 1995. Brain- and intestine-specific variants of reovirus serotype 3 strain dearing are selected during chronic infection of severe combined immunodeficient mice. J. Virol. **69:**3933-3937.
90. **Hansen, I. A., M. Fassnacht, S. Hahner, F. Hammer, M. Schammann, S. R. Meyer, A. B. Bicknell, and B. Allolio.** 2004. The adrenal secretory serine protease AsP is a short secretory isoform of the transmembrane airway trypsin-like protease. Endocrinology **145:**1898-1905.
91. **Helander, A., K. J. Silvey, N. J. Mantis, A. B. Hutchings, K. Chandran, W. T. Lucas, M. L. Nibert, and M. R. Neutra.** 2003. The viral sigma1 protein and glycoconjugates containing alpha2-3-linked sialic acid are involved in type 1 reovirus adherence to M cell apical surfaces. J. Virol. **77:**7964-7977.
92. **Hingorani, P., W. Zhang, J. Lin, L. Liu, C. Guha, and E. A. Kolb.** 2011. Systemic administration of reovirus (Reolysin) inhibits growth of human sarcoma xenografts. Cancer **117:**1764-1774.
93. **Holm, G. H., A. J. Pruijssers, L. Li, P. Danthi, B. Sherry, and T. S. Dermody.** 2010. Interferon regulatory factor 3 attenuates reovirus myocarditis and contributes to viral clearance interferon regulatory factor 3 attenuates reovirus myocarditis and contributes to viral clearance. J. Virol. **84:**6900-6908.
94. **Honey, K., T. Nakagawa, C. Peters, and A. Rudensky.** 2002. Cathepsin L regulates CD4+ T cell selection independently of its effect on invariant chain: a role in the generation of positively selecting peptide ligands. J. Exp. Med. **195:**1349-1358.
95. **Hooper, J. W., and B. N. Fields.** 1996. Role of the μ1 protein in reovirus stability and capacity to cause chromium release from host cells. J. Virol. **70:**459-467.
96. **Horimoto, T., and Y. Kawaoka.** 1994. Reverse genetics provides direct evidence for a correlation of hemagglutinin cleavability and virulence of an avian influenza A virus. J. Virol. **68:**3120-3128.
97. **Hoyt, C. C., S. M. Richardson-Burns, and R. J. Goody.** 2005. Nonstructural protein sigma1s is a determinant of reovirus virulence and influences the kinetics and severity of apoptosis induction in the heart and central nervous system. J. Virol. **79:**2743-2753.
98. **Hrdy, D. B., D. H. Rubin, and B. N. Fields.** 1982. Molecular basis of reovirus neurovirulence: role of the M2 gene in avirulence. Proc. Natl. Acad. Sci. U. S. A. **79:**1298-1302.

99. **Huang, I. C., B. J. Bosch, F. Li, W. Li, K. H. Lee, S. Ghiran, N. Vasilieva, T. S. Dermody, S. C. Harrison, P. R. Dormitzer, M. Farzan, and P. J. M. Rottier.** 2006. SARS coronavirus , but not human coronavirus NL63 , utilizes cathepsin L to Infect ACE2-expressing cells J. Biol. Chem. **281:**3198-3203.
100. **Hutchings, A. B., A. Helander, K. J. Silvey, K. Chandran, W. T. Lucas, M. L. Nibert, and M. R. Neutra.** 2004. Secretory immunoglobulin A antibodies against the sigma-1 outer capsid protein of reovirus type 1 Lang prevent infection of mouse peyer patches. J. Virol. **78:**947-957.
101. **Ingbar, D. H.** 2000. Mechanisms of replair and remodeling flollowing acute lung injury Clin. Chest Med. **21:**589-616.
102. **Irvin, S. C., J. Zurney, L. S. Ooms, J. D. Chappell, T. S. Dermody, and B. Sherry.** 2011. A single amino acid polymorphism in reovirus protein mu2 determines repression of interferon signaling and modulates myocarditis. J. Virol.
103. **Ivanovic, T., M. A. Agosto, L. Zhang, K. Chandran, S. C. Harrison, and M. L. Nibert.** 2008. Peptides released from reovirus outer capsid form membrane pores that recruit virus particles. The EMBO journal **27:**1289-1298.
104. **Jacobs, B. L., and C. E. Samuel.** 1985. Biosynthesis of reovirus-specified polypeptides: the reovirus s1 mRNA encodes two primary translation products. Virology **143:**63-74.
105. **Jacquinet, E. R., N.V., Rao, G.V., and J.R. Hoidal.** 2000. Cloning, genomic organization, chromosomal assignment and expression of a novel mosaic serine proteinase: epitheliasin. FEBS Lett. **468:**93-100.
106. **Jane-Valbuena, J., L. A. Breun, L. A. Schiff, and M. L. Nibert.** 2002. Sites and determinants of early cleavages in the proteolytic processing pathway of reovirus surface protein sigma3. J. Virol. **76:**5184-5197.
107. **Jeffery, P. K.** 2001. Remodeling in Asthma and Chronic Obstructive Lung Disease. Crit. Care Med. **164:**S28-38.
108. **Johnson, E. M., J. D. Doyle, J. D. Wetzel, R. P. McClung, N. Katunuma, J. D. Chappell, M. K. Washington, and T. S. Dermody.** 2009. Genetic and pharmacologic alteration of cathepsin expression influences reovirus pathogenesis. J. Virol. **83:**9630-9640.
109. **Joklik, W. K.** 1972. Studies on the effect of chymotrypsin on reovirions. Virology **49:**700-715.
110. **Kauffman, R. S., J. L. Wolf, R. Finberg, J. S. Trier, and B. N. Fields.** 1983. The sigma 1 protein determines the extent of spread of reovirus from the gastrointestinal tract of mice. Virology **124:**403-410.
111. **Kawaguchi, K., T. Etoh, K. Suzuki, M. T. Mitui, A. Nishizono, N. Shiraishi, and S. Kitano.** 2010. Efficacy of oncolytic reovirus against human gastric cancer with peritoneal metastasis in experimental animal model.1433-1438.

112. **Kenk, H. D., and W. Garten.** 1994. Host cell proteases controlling virus pathogenicity. Trends Microbiol. **2:**39-43.
113. **Kim, E. Y., J. T. Battaile, A. C. Patel, Y. You, and E. Agapov.** 2008. Persistent activation of an innate immune axis translates respiratory viral infection into chronic lung disease. Nat. Med. **14:**633-640.
114. **Kim, M., K. A. Garant, N. I. zur Nieden, T. Alain, S. D. Loken, S. J. Urbanski, P. A. Forsyth, D. E. Rancourt, P. W. K. Lee, and R. N. Johnston.** 2011. Attenuated reovirus displays oncolysis with reduced host toxicity. Br. J. Cancer **104:**290-299.
115. **Kinniry, P., J. Pick, S. Stephens, D. Jain, C. C. Solomides, R. Niven, R. Segal, and M. Christofidou-Solomidou.** 2006. KL4-surfactant prevents hyperoxic and LPS-induced lung injury in mice. Pediatr. Pulmonol. **41:**916-928.
116. **Kirchner, E., K. M. Guglielmi, H. M. Strauss, T. S. Dermody, and T. Stehle.** 2008. Structure of reovirus sigma1 in complex with its receptor junctional adhesion molecule-A. PLoS pathogens **4:**e1000235-e1000235.
117. **Kirschke, H., B. Wiederanders, D. Bromme, and A. Rinne.** 1989. Cathepsin S from bovine spleen. Purification, distribution, intracellular localization and action on proteins. Biochem. J. **264:**467-473.
118. **Knapp, S., S. Florquin, D. T. Golenbock, and T. van der Poll.** 2006. Pulmonary lipopolysaccharide (LPS)-binding protein inhibits the LPS-induced lung inflammation in vivo. J. Immunol. **176:**3189-3195.
119. **Kobayashi, T., A. A. R. Antar, K. W. Boehme, P. Danthi, E. A. Eby, K. M. Guglielmi, G. H. Holm, M. Elizabeth, M. S. Maginnis, S. Naik, W. B. Skelton, J. Denise, G. J. Wilson, J. D. Chappell, and S. Terence.** 2008. Plasmid-Based Reverse Genetics for Animal Double-Stranded RNA Viruses: Manipulation of the viral genome and development of a novel gene-transduction system. Cell **1:**147-157.
120. **Kobayashi, T., L. S. Ooms, M. Ikizler, J. D. Chappell, and T. S. Dermody.** 2010. An improved reverse genetics system for mammalian orthoreoviruses. Virology **398:**194-200.
121. **Kothandaraman, S., M. Herbert, R. Raines, and M. L. Nibert.** 1998. No role for pepstatin-A-sensitive acidic proteinases in reovirus infection of L or MDCK cells. Virology **251:**264-272.
122. **Kozak, M., and A. J. Shatkin.** 1978. Identification of features in the 5' terminal fragments from reovirus mRNA which are important for ribosome binding. Cell **13:**201-212.
123. **Lee, P. W., E. C. Hayes, and W. K. Joklik.** 1981. Protein sigma 1 is the reovirus cell attachment protein. Virology **108:**156-163.
124. **Leone, G., R. Duncan, and P. W. Lee.** 1991. Trimerization of the reovirus cell attachment protein (sigma 1) induces conformational changes in sigma 1 necessary for its cell-binding function. Virology **184:**758-761.
125. **Leone, G., D. C. Mah, and P. W. Lee.** 1991. The incorporation of reovirus cell attachment protein sigma 1 into virions requires the N-terminal

hydrophobic tail and the adjacent heptad repeat region. Virology **182:**346-350.
126. **Letvin, N. L., R. S. Kauffman, and R. Finberg.** 1981. T lymphocyte immunity to reovirus: cellular requirements for generation and role in clearance of primary infections. J. Immunol. **127:**2334-2339.
127. **Ley, K.** 2004. Weird and weirder: how circulating chemokines coax neutrophils to the lung. Am. J. Physiol. Lung Cell Mol. Physiol. **286:**463-464.
128. **Li, L., and B. Sherry.** 2010. IFN-alpha expression and antiviral effects are subtype and cell type specific in the cardiac response to viral infection. Virology **396:**59-68.
129. **Liemann, S., K. Chandran, T. S. Baker, M. L. Nibert, and S. C. Harrison.** 2002. Structure of the reovirus membrane-penetration protein, Mu1, in a complex with is protector protein, Sigma3. Cell **108:**283-295.
130. **Lin, B., C. Ferguson, J. T. White, S. P. Tmprss, S. Wang, R. Vessella, L. D. True, L. Hood, and P. S. Nelson.** 1999. Prostate-localized and androgen-regulated expression of the membrane-bound serine protease TMPRSS2 prostate-localized and androgen-regulated expression of the membrane-bound. Cancer Res. **59:**4180-4184.
131. **Liuzzo, J. P., S. S. Petanceska, and L. A. Devi.** 1999. Neurotrophic factors regulate cathepsin S in macrophages and microglia: A role in the degradation of myelin basic protein and amyloid beta peptide. Mol. Med. **5:**334-343.
132. **Liuzzo, J. P., S. S. Petanceska, D. Moscatelli, and L. A. Devi.** 1999. Inflammatory mediators regulate cathepsin S in macrophages and microglia: A role in attenuating heparan sulfate interactions. Mol. Med. **5:**320-333.
133. **Lolkema, M. P., H.-T. Arkenau, K. Harrington, P. Roxburgh, R. Morrison, V. Roulstone, K. Twigger, M. Coffey, K. Mettinger, G. Gill, T. R. J. Evans, and J. S. de Bono.** 2011. A phase I study of the combination of intravenous reovirus type 3 Dearing and gemcitabine in patients with advanced cancer. Clinical cancer research : an official journal of the American Association for Cancer Research **17:**581-588.
134. **London, L., E. I. Majeski, S. Altman-Hamamdzic, C. Enockson, M. K. Paintlia, R. a. Harley, and S. D. London.** 2002. Respiratory Reovirus 1/L Induction of Diffuse Alveolar Damage: Pulmonary Fibrosis Is Not Modulated by Corticosteroids in Acute Respiratory Distress Syndrome in Mice. Clin. Immunol. **103:**284-295.
135. **London, L., E. I. Majeski, M. K. Paintlia, R. A. Harley, and S. D. London.** 2002. Respiratory reovirus 1/L induction of diffuse alveolar damage: a model of acute respiratory distress syndrome. Exp. Mol. Pathol. **72:**24-36.

136. **Lucia-Jandris, P., J. W. Hooper, and B. N. Fields.** 1993. Reovirus M2 gene is associated with chromium release from mouse L cells. J. Virol. **67:**5339-5345.
137. **Luh, S.-P., and C.-H. Chiang.** 2007. Acute lung injury/acute respiratory distress syndrome (ALI/ARDS): the mechanism, present strategies and future perspectives of therapies. Journal of Zhejiang University. Science. B **8:**60-69.
138. **Ma, J., T. Chen, J. Mandelin, A. Ceponis, N. E. Miller, M. Hukkanen, G. F. Ma, and Y. T. Konttinen.** 2003. Regulation of macrophage activation. Cell. Mol. Life Sci. **60:**2334-2346.
139. **Maginnis, M. S., J. C. Forrest, S. A. Kopecky-bromberg, S. K. Dickeson, S. A. Santoro, M. M. Zutter, G. R. Nemerow, J. M. Bergelson, and T. S. Dermody.** 2006. Beta1 integrin mediates internalization of mammalian reovirus. J. Virol. **80:**2760-2770.
140. **Maginnis, M. S., B. A. Mainou, A. Derdowski, E. M. Johnson, R. Zent, and T. S. Dermody.** 2008. NPXY motifs in the beta1 integrin cytoplasmic tail are required for functional reovirus entry. J. Virol. **82:**3181-3191.
141. **Mah, D. C., G. Leone, J. M. Jankowski, and P. W. Lee.** 1990. The N-terminal quarter of reovirus cell attachment protein sigma 1 possesses intrinsic virion-anchoring function. Virology **179:**95-103.
142. **Mah, D. C. W., G. Leone, J. M. Jankowski, and P. W. Lee.** 1990. The amino-terminal quarter of reovirus cell attachment protein sigma-1 possesses intrinsic virion-anchoring function. Virology **179:**95-103.
143. **Marcato, P., M. Shmulevitz, D. Pan, D. Stoltz, and P. W. Lee.** 2007. Ras transformation mediates reovirus oncolysis by enhancing virus uncoating, particle infectivity, and apoptosis-dependent release. Mol. Ther. **15:**1522-1530.
144. **Matoba, Y., B. Sherry, B. N. Fields, and T. W. Smith.** 1991. Identification of the viral genes responsible for growth of strains of reovirus in cultured mouse heart cells. J. Clin. Invest. **87:**1628-1633.
145. **Matsushima, R., A. Takahashi, Y. Nakaya, H. Maezawa, M. Miki, Y. Nakamura, F. Ohgushi, and S. Yasuoka.** 2006. Human airway trypsin-like protease stimulates human bronchial fibroblast proliferation in a protease-activated receptor-2-dependent pathway. Am. J. Physiol. Lung Cell Mol. Physiol. **290:**L385-395.
146. **Matsuyama, S., M. Ujike, S. Morikawa, M. Tashiro, and F. Taguchi.** 2005. Protease-mediated enhancement of severe acute respiratory syndrome coronavirus infection. Proc. Natl. Acad. Sci. U. S. A. **102:**12543-12547.
147. **Matute-Bello, G., C. W. Frevert, and T. R. Martin.** 2008. Animal models of acute lung injury. Am. J. Physiol. Lung Cell Mol. Physiol. **295:**L379-399.
148. **Mendez, II, Y. M. She, W. Ens, and K. M. Coombs.** 2003. Digestion pattern of reovirus outer capsid protein sigma3 determined by mass spectrometry. Virology **311:**289-304.

149. **Metcalf, P., M. Cyrklaff, and M. Adrian.** 1991. The three-dimensional structure of reovirus obtained by cryo-electron microscopy. EMBO J. **10:**3129-3136.
150. **Miyamoto, S. D., R. D. Brown, B. A. Robinson, K. L. Tyler, C. S. Long, and R. L. Debiasi.** 2009. Cardiac cell-specific apoptotic and cytokine responses to reovirus infection: determinants of myocarditic phenotype. J. Card. Fail. **15:**529-539.
151. **Moraes, T. J., C. W. Chow, and G. P. Downey.** 2003. Proteases and lung injury. Crit. Care Med. **31:**S189-194.
152. **Morin, B. M. J., A. Warner, and B. N. Fieldsw.** 1994. A Pathway for Entry of Reoviruses into the Host through M Cells of the Respiratory Tract J. Exp. Med. **180:**1523-1527.
153. **Morin, M. J., A. Warner, and B. N. Fields.** 1996. Reovirus infection in rat lungs as a model to study the pathogenesis of viral pneumonia. J. Virol. **70:**541-548.
154. **Morin, M. J., A. Warner, and B. N. Fields.** 1996. Reovirus infection in the rat lungs as a model to study the pathogenesis of viral pneumonia. J. Virol **70:**541-550.
155. **Morrison, L. A., R. L. Sidman, and B. N. Fields.** 1991. Direct spread of reovirus from the intestinal lumen to the central nervous system through vagal autonomic nerve fibers. Proc. Natl. Acad. Sci. USA **88:**3852-3856.
156. **Muthukrishnan, S., G. W. Both, Y. Furuichi, and A. J. Shatkin.** 1975. 5'-Terminal 7-methylguanosine in eukaryotic mRNA is required for translation. Nature **255:**33-37.
157. **Nagata, L., S. Masri, R. Pon, and P. Lee.** 1987. Analysis of functional domains on reovirus cell attachment protein sigma 1 using cloned S1 gene deletion mutants. Virology **160:**162-168.
158. **Nakagawa, T., W. Roth, P. Wong, A. Nelson, A. Farr, J. Deussing, J. A. Villadangos, H. Ploegh, C. Peters, and A. Y. Rudensky.** 1998. Cathepsin L: critical role in Ii degradation and CD4 T cell selection in the thymus. Science **280:**450-453.
159. **Nason, E. L., J. D. Wetzel, S. K. Mukherjee, E. S. Barton, B. V. Prasad, and T. S. Dermody.** 2001. A monoclonal antibody specific for reovirus outer-capsid protein sigma3 inhibits sigma1-mediated hemagglutination by steric hindrance. J. Virol. **75:**6625-6634.
160. **Nibert, M. L., J. D. Chappell, and T. S. Dermody.** 1995. Infectious subvirion particles of reovirus type 3 Dearing exhibit a loss in infectivity and contain a cleaved sigma 1 protein. J. Virol. **69:**5057-5067.
161. **Nibert, M. L., T. S. Dermody, and B. N. Fields.** 1990. Structure of the reovirus cell-attachment protein: a model for the domain organization of sigma 1. J. Virol. **64:**2976-2989.
162. **Nibert, M. L., and B. N. Fields.** 1992. A carboxy-terminal fragment of protein mu 1/mu 1C is present in infectious subvirion particles of

mammalian reoviruses and is proposed to have a role in penetration. J. Virol. **66:**6408-6418.
163. **Nibert, M. L., D. B. Furlong, and B. N. Fields.** 1991. Mechanisms of viral pathogenesis. Distinct forms of reoviruses and their roles during replication in cells and host. The Journal of clinical investigation **88:**727-734.
164. **Nibert, M. L., L. A. Schiff, and B. N. Fields.** 1991. Mammalian reoviruses contain a myristoylated structural protein. J. Virol. **65:**1960-1967.
165. **Niwa, Y., Y. Beppu, and T. Towatari.** 1996. Cellular proteases involved in the pathologenicity of enveloped animal immunodeficiency influenza virus and sendai Science **36:**325-341.
166. **Numata, M., H. W. Chu, A. Dakhama, and D. R. Voelker.** 2010. Pulmonary surfactant phosphatidylglycerol inhibits respiratory syncytial virus-induced inflammation and infection. Proc. Natl. Acad. Sci. U. S. A. **107:**320-325.
167. **Nygaard, R. M., J. W. Golden, and L. A. Schiff.** 2012. Impact of Host Proteases on Reovirus Infection in the Respiratory Tract. J. Virol. **86:**1238-1243.
168. **O'Donnell, S. M. O., M. W. Hansberger, J. L. Connolly, J. D. Chappell, M. J. Watson, J. M. Pierce, J. D. Wetzel, W. Han, E. S. Barton, J. C. Forrest, T. Valyi-nagy, F. E. Yull, T. S. Blackwell, J. N. Rottman, B. Sherry, and T. S. Dermody.** 2005. Organ-specific roles for transcription factor NF-ŒʃB in reovirus-induced apoptosis and disease. The Journal of clinical investigation **115:**2341-2350.
169. **Onishi, K., Y. Li, K. Ishii, H. Hisaeda, L. Tang, X. Duan, T. Dainichi, Y. Maekawa, N. Katunuma, and K. Himeno.** 2004. Cathepsin L is crucial for a Th1-type immune response during Leishmania major infection. Microbes and infection / Institut Pasteur **6:**468-474.
170. **Ouattara, L., F. Barin, M. A. Barthez, B. Bonnaud, P. Roingeard, A. Goudeau, P. Castelnau, G. Vernet, G. Paranhos-Baccala, and F. Komurian-Pradel.** 2011. Novel Human Reovirus Isolated from Children with Acute Necrotizing Encephalopathy. Emerg. Infect. Dis. **17**.
171. **Ovcharenko, A. V., and O. P. Zhirnov.** 1994. Aprotinin aerosol treatment of influenza and paramyxovirus bronchopneumonia of mice. Antiviral Res. **23:**107-118.
172. **Pacitti, A. F., and J. R. Gentsch.** 1987. Inhibition of reovirus type 3 binding to host cells by sialylated glycoproteins is mediated through the viral attachment protein. J. Virol. **61:**1407-1415.
173. **Papi, A., C. M. Bellettato, F. Braccioni, M. Romagnoli, P. Casolari, G. Caramori, L. M. Fabbri, and S. L. Johnston.** 2006. Infections and airway inflammation in chronic obstructive pulmonary disease severe exacerbations. Am. J. Respir. Crit. Care Med. **173:**1114-1121.
174. **Parks, W. C., and S. D. Shapiro.** 2001. Matrix metalloproteinases in lung biology. Respir. Res. **2:**10-19.

175. **Pelletier, M., L. Maggi, A. Micheletti, E. Lazzeri, N. Tamassia, C. Costantini, L. Cosmi, C. Lunardi, F. Annunziato, S. Romagnani, and M. Casseatella.** 2010. Evidence for a cross-talk between human neutrophils and Th17 cells. Blood **115:**335-343.
176. **Petanceska, S., S. Burke, S. J. Watson, and L. Devi.** 1994. Differential distribution of messenger RNAs for cathepsins B, L and S in adult rat brain: an in situ hybridization study. Neuroscience **59:**729-738.
177. **Petanceska, S., P. Canoll, and L. A. Devi.** 1996. Expression of rat cathepsin S in phagocytic cells. J. Biol. Chem. **271:**4403-4409.
178. **Petanceska, S., and L. Devi.** 1992. Sequence analysis, tissue distribution, and expression of rat cathepsin S. J. Biol. Chem. **267:**26038-26043.
179. **Poggioli, G. J., T. S. Dermody, and K. L. Tyler.** 2001. Reovirus-Induced 1s-Dependent G 2 / M Phase Cell Cycle Arrest Is Associated with Inhibition of p34 cdc2. J. Virol. **75:**7429-7434.
180. **Poggioli, G. J., T. S. Dermody, and K. L. Tyler.** 2001. Reovirus-induced sigma1s-dependent G(2)/M phase cell cycle arrest is associated with inhibition of p34(cdc2). J. Virol. **75:**7429-7434.
181. **Poggioli, G. J., C. Keefer, J. L. Connolly, T. S. Dermody, and K. L. Tyler.** 2000. Reovirus-induced G(2)/M cell cycle arrest requires sigma1s and occurs in the absence of apoptosis. J. Virol. **74:**9562-9570.
182. **Prestwich, R. J., E. J. Ilett, F. Errington, R. M. Diaz, L. P. Steele, T. Kottke, J. Thompson, F. Galivo, K. J. Harrington, H. S. Pandha, P. J. Selby, R. G. Vile, and A. a. Melcher.** 2009. Immune-mediated antitumor activity of reovirus is required for therapy and is independent of direct viral oncolysis and replication. Clinical cancer research : an official journal of the American Association for Cancer Research **15:**4374-4381.
183. **Qian, F., S. J. Chan, Q. M. Gong, A. S. Bajkowski, D. F. Steiner, and A. Frankfater.** 1991. The expression of cathepsin B and other lysosomal proteinases in normal tissues and in tumors. Biomed. Biochim. Acta **50:**531-540.
184. **Reid, P. T., and J.-M. Sallenave.** 2001. Neutrophil-derived elastases and their inhibitors : Potential role in the pathogenesis of lung disease. Curr. Opin. Investig. Drugs **2:**59-67.
185. **Reiter, D. M., J. M. Frierson, E. E. Halvorson, T. Kobayashi, T. S. Dermody, and T. Stehle.** 2011. Crystal Structure of Reovirus Attachment Protein Sigma1 in Complex with Sialylated Oligosaccharides. PLoS pathogens **7:**e1002166-e1002166.
186. **Richardson-Burns, S. M., D. J. Kominsky, and K. L. Tyler.** 2002. Reovirus-induced neuronal apoptosis is mediated by caspase 3 and is associated with the activation of death receptors. J. Neurovirol. **8:**365-380.
187. **Riese, R. J., R. N. Mitchell, J. A. Villadangos, G. P. Shi, J. T. Palmer, E. R. Karp, G. T. De Sanctis, H. L. Ploegh, and H. A. Chapman.** 1998.

Cathepsin S activity regulates antigen presentation and immunity. J. Clin. Invest. **101:**2351-2363.

188. **Rodgers, S. E., J. L. Connolly, J. D. Chappell, and T. S. Dermody.** 1998. Reovirus Growth in Cell Culture Does Not Require the Full Complement of Viral Proteins Journal of vi **72:**8597-8604.
189. **Roth, W., J. Deussing, V. A. Botchkarev, M. Pauly-Evers, P. Saftig, A. Hafner, P. Schmidt, W. Schmahl, J. Scherer, I. Anton-Lamprecht, K. Von Figura, R. Paus, and C. Peters.** 2000. Cathepsin L deficiency as molecular defect of furless: hyperproliferation of keratinocytes and pertubation of hair follicle cycling. FASEB J. **14:**2075-2086.
190. **Rubin, B. D. H., and B. N. Fields.** 1980. Molecular basis of revirus virulence: M2 gene. **152**.
191. **Sabin, A. B.** 1959. A new group of respiratory formerly classified as ECHO type 10 is described. Science **130:**1387-1389.
192. **Sajjan, U., S. Ganesan, A. T. Comstock, J. Shim, Q. Wang, D. R. Nagarkar, Y. Zhao, A. M. Goldsmith, J. Sonstein, M. J. Linn, J. L. Curtis, and M. B. Hershenson.** 2009. Elastase- and LPS-exposed mice display altered responses to rhinovirus infection. Am. J. Physiol. Lung Cell Mol. Physiol. **297:**L931-944.
193. **Sarkar, G., J. Pelletier, R. Bassel-Duby, A. Jayasuriya, B. N. Fields, and N. Sonenberg.** 1985. Identification of a new polypeptide coded by reovirus gene S1. J. Virol. **54:**720-725.
194. **Schiff, L. A.** 1998. Reovirus capsid proteins sigma 3 and mu 1: interactions that influence viral entry, assembly, and translational control. Curr. Top. Microbiol. Immunol. **233:**167-183.
195. **Schiff, L. A., M. L. Nibert, and K. L. Tyler.** 2007. Fields Virology Orthoreoviruses and Their Replication. Lippincott, Williams and Wilkins.
196. **Shatkin, A. J.** 1971. Viruses with segmented ribonucleic acid genomes: multiplication of influenza versus reovirus. Bacteriol. Rev. **35:**250-266.
197. **Shepard, D., J. Ehnstrom, and L. A. Schiff.** 1995. Association of reovirus outer capsid proteins sigma 3 and mu 1 causes a conformational change that renders sigma 3 protease sensitive. J. Virol. **69:**8180-8184.
198. **Sherry, B.** 2009. Rotavirus and reovirus modulation of the interferon response. Journal of interferon & cytokine research : the official journal of the International Society for Interferon and Cytokine Research **29:**559-567.
199. **Sherry, B., and B. N. Fields.** 1989. The reovirus M1 gene, encoding a viral core protein, is associated with the myocarditic phenotype of a reovirus variant. J. Virol. **63:**4850-4856.
200. **Shi, G. P., J. S. Munger, J. P. Meara, D. H. Rich, and H. A. Chapman.** 1992. Molecular cloning and expression of human alveolar macrophage cathepsin S, an elastinolytic cysteine protease. J. Biol. Chem. **267:**7258-7262.

201. **Shi, G. P., A. C. Webb, K. E. Foster, J. H. Knoll, C. A. Lemere, J. S. Munger, and H. A. Chapman.** 1994. Human cathepsin S:chromosomal localization, gene structure, and tissue distribution. J. Biol. Chem. **269:**11530-11536.
202. **Shirogane, Y., M. Takeda, M. Iwasaki, N. Ishiguro, H. Takeuchi, Y. Nakatsu, M. Tahara, H. Kikuta, and Y. Yanagi.** 2008. Efficient multiplication of human metapneumovirus in Vero cells expressing the transmembrane serine protease TMPRSS2. J. Virol. **82:**8942-8946.
203. **Shmulevitz, M., P. Marcato, and P. W. K. Lee.** 2005. Unshackling the links between reovirus oncolysis, Ras signaling, translational control and cancer. Oncogene **24:**7720-7728.
204. **Shulla, A., T. Heald-Sargent, G. Subramanya, J. Zhao, S. Perlman, and T. Gallagher.** 2011. A transmembrane serine protease is linked to the severe acute respiratory syndrome coronavirus receptor and activates virus entry. J. Virol. **85:**873-882.
205. **Silvey, K. J., A. M. Y. B. Hutchings, M. Vajdy, M. M. Petzke, and M. R. Neutra.** 2001. Role of immunoglobulin A in protection against reovirus entry into murine peyer patches. J. Virol. **75:**10870-10879.
206. **Simmons, G., S. Bertram, I. Glowacka, I. Steffen, C. Chaipan, J. Agudelo, K. Lu, A. J. Rennekamp, H. Hofmann, P. Bates, and S. Pöhlmann.** 2011. Different host cell proteases activate the SARS-coronavirus spike-protein for cell-cell and virus-cell fusion. Virology **413:**265-274.
207. **Simmons, G., D. N. Gosalia, A. J. Rennekamp, J. D. Reeves, S. L. Diamond, and P. Bates.** 2005. Inhibitors of cathepsin L prevent severe acute respiratory syndrome coronavirus entry. Proc. Natl. Acad. Sci. U. S. A. **102:**11876-11881.
208. **Skehel, J. J., and W. K. Joklik.** 1969. Studies on the in vitro transcription of reovirus RNA catalyzed by reovirus cores. Virology **39:**822-831.
209. **Smith, J. A., S. C. Schmechel, B. R. G. Williams, R. H. Silverman, and L. A. Schiff.** 2005. Involvement of the Interferon-Regulated Antiviral Proteins PKR and RNase L in Reovirus-Induced Shutoff of Cellular Translation. J. Virol. **79:**2240-2250.
210. **Spendlove, R. S., M. E. McClain, and E. H. Lennette.** 1970. Enhancement of reovirus infectivity by extracellular removal or alteration of the virus capsid by proteolytic enzymes. J. Gen. Virol. **8:**83-94.
211. **Strong, J. E., M. C. Coffey, D. Tang, P. Sabinin, and P. W. Lee.** 1998. The molecular basis of viral oncolysis: usurpation of the Ras signaling pathway by reovirus. The EMBO journal **17:**3351-3362.
212. **Sturzenbecker, L. J., M. L. Nibert, D. Furlong, and B. N. Fields.** 1987. Intracellular digestion of reovirus particles requires a low pH and is an essential step in the viral infectious cycle. J. Virol. **61:**2351-2361.
213. **Takahashi, M., T. Sano, K. Yamaoka, T. Kamimura, N. Umemoto, H. Nishitani, and S. Yasuoka.** 2001. Localization of human airway trypsin-

like protease in the airway : an immunohistochemical study. Histochem. Cell Biol. **115:**181-187.
214. **Taterka, J., J. J. Cebra, and D. H. Rubin.** 1995. Characterization of cytotoxic cells from reovirus-infected SCID mice: activated cells express natural killer- and lymphokine-activated killer-like activity but fail to clear infection. J. Virol. **69:**3910-3914.
215. **Tomashefski, J. F.** 2000. Pulmonary pathology of acute respiratory syndrome. Clin. Chest Med. **21:**435-466.
216. **Tomlins, S. A., D. R. Rhodes, S. Perner, S. M. Dhanasekaran, R. Mehra, X.-W. Sun, S. Varambally, X. Cao, J. Tchinda, R. Kuefer, C. Lee, J. E. Montie, R. B. Shah, K. J. Pienta, M. a. Rubin, and A. M. Chinnaiyan.** 2005. Recurrent fusion of TMPRSS2 and ETS transcription factor genes in prostate cancer. Science **310:**644-648.
217. **Tosteson, M. T., M. L. Nibert, and B. N. Fields.** 1993. Ion channels induced in lipid bilayers by subvirion particles of the nonenveloped mammalian reoviruses. Proc. Natl. Acad. Sci. U.S.A. **90:**10549-10552.
218. **Tyler, K. L., R. T. Bronson, K. B. Byers, and B. Fields.** 1985. Molecular basis of viral neurotropism: experimental reovirus infection. Neurology **35:**88-92.
219. **Tyler, K. L., D. A. McPhee, and B. N. Fields.** 1986. Distinct pathways of viral spread in the host determined by reovirus S1 gene segment. Science (New York, N.Y.) **233:**770-774.
220. **Tyler, K. L., M. K. Squier, S. E. Rodgers, B. E. Schneider, S. M. Oberhaus, T. A. Grdina, J. J. Cohen, and T. S. Dermody.** 1995. Differences in the capacity of reovirus strains to induce apoptosis are determined by the viral attachment protein sigma 1. J. Virol. **69:**6972-6979.
221. **Vedula, S. R. K., T. S. Lim, E. Kirchner, K. M. Guglielmi, T. S. Dermody, T. Stehle, W. Hunziker, and C. T. Lim.** 2008. A comparative molecular force spectroscopy study of homophilic JAM-A interactions and JAM-A interactions with reovirus attachment protein sigma1. Journal of molecular recognition : JMR **21:**210-216.
222. **Virgin, H., R. Bassel-duby, B. N. Fields, and K. L. Tyler.** 1988. Antibody Protects against Lethal Infection with the Neurally Spreading Reovirus Type 3 (Dearing). J. Virol. **62:**4594-4604.
223. **Virgin, H. W., and K. L. Tyler.** 1991. Role of immune cells in protection against and control of reovirus infection in neonatal mice. J. Virol. **65:**5157-5164.
224. **Ware, L. B., and M. A. Matthay.** 2000. The acute respiratory distress syndrome. N. Engl. J. Med. **342:**1334-1349.
225. **Wareing, M. D., A. B. Lyon, B. Lu, C. Gerard, and S. R. Sarawar.** 2004. Chemokine expression during the development and resolution of a pulmonary leukocyte response to influenza A virus infection in mice. J. Leukoc. Biol. **76:**886-895.

226. **Wark, P., S. Johnston, I. Moric, J. Simpson, M. Hensley, and P. Gibson.** 2002. Neutrophil degranulation and cell lysis is associated with clinical severity in virus-induced asthma. Eur. Respir. J. **19:**68-75.
227. **Webster, R., and R. Rott.** 1987. Influenza virus a pathogenicity: The pivital role of hemagglutinin. Cell **50:**665-666.
228. **Weiner, H. L., D. T. Drayna, D. R. Averill, and B. N. Fields.** 1977. Molecular basis of reovirus virulence. Role of the S1 gene. Proc. Natl. Acad. Sci. USA **74:**5744-5748.
229. **Weiner, H. L., M. L. Powers, and B. N. Fields.** 1980. Absolute linkage of virulence and central nervous system cell tropism of reoviruses to viral hemagglutinin. J. Infect. Dis **141:**609-616.
230. **Weltzin, R., P. Lucia-jandris, P. Michetti, B. N. Fields, J. P. Kraehenbuhl, and M. R. Neutra.** 1989. Binding and transepithelial transport of immunoglobulins by intestinal M cells: demonstration using monoclonal IgA antibodies against enteric viral proteins. J. Cell Biol **108:**1673-1685.
231. **Wetzel, J. D., G. J. Wilson, G. S. Baer, L. R. Dunnigan, J. P. Wright, D. S. Tang, and T. S. Dermody.** 1997. Reovirus variants selected during persistent infections of L cells contain mutations in the viral S1 and S4 genes and are altered in viral disassembly. J. Virol. **71:**1362-1369.
232. **Wilson, G. A., L. A. Morrison, and B. N. Fields.** 1994. Association of the reovirus S1 gene with serotype 3-induced biliary atresia in mice. J. Virol. **68:**6458-6465.
233. **Wilson, G. J., E. L. Nason, C. S. Hardy, D. H. Ebert, J. D. Wetzel, B. V. Venkataram Prasad, and T. S. Dermody.** 2002. A single mutation in the carboxy terminus of reovirus outer-capsid protein sigma 3 confers enhanced kinetics of sigma 3 proteolysis, resistance to inhibitors of viral disassembly, and alterations in sigma 3 structure. J. Virol. **76:**9832-9843.
234. **Wisniewski, M. L., B. G. Werner, L. G. Hom, L. J. Anguish, C. M. Coffey, and J. S. L. Parker.** 2011. Reovirus infection or ectopic expression of outer capsid protein micro1 induces apoptosis independently of the cellular proapoptotic proteins Bax and Bak. J. Virol. **85:**296-304.
235. **Wojton, J., and B. Kaur.** 2010. Impact of tumor microenvironment on oncolytic viral therapy. Cytokine Growth Factor Rev. **21:**127-134.
236. **Wolf, J. L., R. S. Kauffman, R. Finberg, R. Dambrauskas, B. N. Fields, and J. S. Trier.** 1983. Determinants of reovirus interaction with the intestinal M cells and absorptive cells of murine intestine. Gastroenterology **82:**291-300.
237. **Wolf, J. L., D. H. Rubin, R. Finberg, R. S. Kauffman, a. H. Sharpe, J. S. Trier, and B. N. Fields.** 1981. Intestinal M cells: a pathway for entry of reovirus into the host. Science (New York, N.Y.) **212:**471-472.
238. **Wolters, P. J., and H. A. Chapman.** 2000. Importance of lysosomal cysteine proteases in lung disease. Respir. Res. **1:**170-177.

239. **Yin, P., N. D. Keirstead, T. J. Broering, M. M. Arnold, J. S. L. Parker, M. L. Nibert, and K. M. Coombs.** 2004. Comparisons of the M1 genome segments and encoded mu2 proteins of different reovirus isolates. Virol J. **1:**6-6.
240. **Zhang, B., T. S. Lim, S. R. K. Vedula, A. Li, C. T. Lim, and V. B. C. Tan.** 2010. Investigation of the binding preference of reovirus sigma1 for junctional adhesion molecule A by classical and steered molecular dynamics. Biochemistry (Mosc). **49:**1776-1786.
241. **Zhang, L., M. a. Agosto, T. Ivanovic, D. S. King, M. L. Nibert, and S. C. Harrison.** 2009. Requirements for the formation of membrane pores by the reovirus myristoylated micro1N peptide. J. Virol. **83:**7004-7014.
242. **Zheng, T., Z. Zhu, Z. Wang, R. J. Homer, B. Ma, R. J. Riese, Jr., H. A. Chapman, Jr., S. D. Shapiro, and J. A. Elias.** 2000. Inducible targeting of IL-13 to the adult lung causes matrix metalloproteinase- and cathepsin-dependent emphysema. J. Clin. Invest. **106:**1081-1093.
243. **Zhirnov, O. P., M. R. Ikizler, and P. F. Wright.** 2002. Cleavage of influenza A virus hemagglutinin in human respiratory epithelium Is cell associated and sensitive to exogenous antiproteases. Society **76:**8682-8689.
244. **Zhirnov, O. P., H. D. Klenk, and P. F. Wright.** 2011. Aprotinin and similar protease inhibitors as drugs against influenza. Antiviral Res. **92:**27-36.
245. **Zhirnov, O. P., A. V. Ovcharenko, and A. G. Bukrinskaya.** 1984. Suppression of influenza virus replication in infected mice by protease inhibitors. J. Gen. Virol. **65 (Pt 1):**191-196.
246. **Zurney, J., T. Kobayashi, G. H. Holm, T. S. Dermody, and B. Sherry.** 2009. Reovirus mu2 protein inhibits interferon signaling through a novel mechanism involving nuclear accumulation of interferon regulatory factor 9. J. Virol. **83:**2178-2187.